D4.1 Report

Online Modelling Tools and Techniques for Early Warning Systems

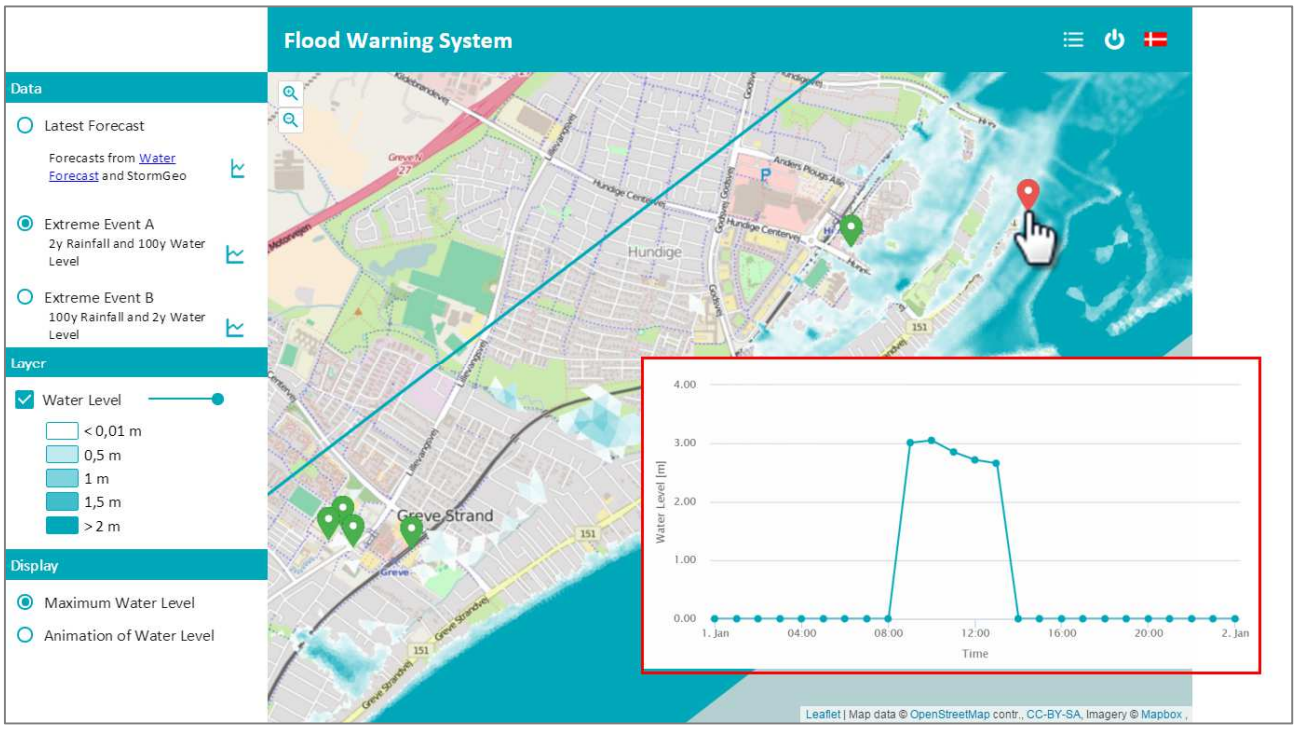

This project has received funding from the European Union´s Seventh Framework Programme for Research, Technological Development and Demonstration under Grant Agreement N° 603663 for the research project PEARL (Preparing for Extreme And Rare events in coastal regions).

D4.1 Report

Online Modelling Tools and Techniques for Early Warning Systems

Authors: *DHI, TUHH*

Contributors: *Hyds*

Dissemination level (select one):
PU = Public
PP = Restricted to other programme participants (including the Commission Services).
CO = Confidential, only for members of the consortium (including the Commission Services).

Document Information

Project Number	***603663***	Acronym	**PEARL**
Full Title	Preparing for Extreme and Rare events in coastaL regions		
Project URL	http://www.pearl-fp7.eu/		
Document URL			
EU Project Officer	Eleni Manoli		

Deliverable	Number	D.4.1	Title	Online Modelling Tools and Techniques for Early Warning Systems
Work Package	Number	WP4	Title	Flood forecasting and early warning systems for coastal regions

Date of Delivery	Contractual	MM.DD.YYYY	Actual	MM.DD.YYYY
Status	version x.x		final □	
Nature	prototype □ report □ dissemination □			
Dissemination level	public □ consortium □			

Abstract (for dissemination, 100 words)	This report on online tools and techniques for early warning systems (EWS) aims to assess and identify points of enhancement for methods used real-time flood forecasting and warning. It presents a review and analysis of methodologies for real-time coastal flood modelling. The various components of flood EWS's are identified, and possible enhancements for their use in fluvial, pluvial, and coastal flooding applications are discussed. In addition, state-of-the-art techniques for flood hazard mapping, which are widely used in EWS's, are identified and presented. The tools and techniques for real-time flood modelling and early warning discussed in the report are exemplified by a review of existing systems and demonstrated through detailed presentations of case study applications under the PEARL project.
Keywords	Real-time, flood modelling, forecasting, flood warning

Version Log				
Issue Date	Rev. No.	Author	Change	Approved by

Disclaimer

The research leading to these results has received funding from the European Union Seventh Framework Programme (FP7/2007-2013) under Grant agreement n° 603663 for the research project PEARL (Preparing for Extreme And Rare events in coastaL regions).

Summary

This report on online tools and techniques for early warning systems presents a review and analysis of methodologies for real-time coastal flood modelling for flood warning. The various modelling tools used in flood warning systems are identified, and possible enhancements for their use in fluvial, pluvial, and coastal flooding applications are discussed. In addition, state-of-the-art techniques for flood hazard mapping, which are also widely used in warning systems, are identified and presented. The tools and techniques for real-time flood modelling and early warning discussed in the report are exemplified by a review of existing systems, and demonstrated through detailed presentations of case study applications under the PEARL project. Analysis and evaluation of real-time flood early warning systems implemented in case cities in Europe (Germany, Denmark and Spain) and the Caribbean (Saint Lucia) are performed and presented. The review and evaluation of the operational performance of the various methodologies aim to assess and identify points of enhancement for these methods for real-time flood forecasting and warning applications.

Contents

List of figures

List of tables

Abbreviations/Acronyms

API	Application Programming Interface
BSH	Bundesamt für Seeschifffahrt und Hydrographie (German Federal Maritime and Hydrographic Agency)
CET	Central European Time
COST	European Cooperation in Science and Technology
CPU	Central Processing Unit
DTM	Digital Terrain Model
DVAAFS	Deterministic Venice *Acqua Alta* Forecast System
ECMWF	European Centre for Medium-range Weather Forecasts
EDXL	Emergency Data Exchange Language
EU	European Union
EWS	Early Warning Systems
GIS	Geographic Information System
GPU	Graphics Processing Unit
JMA	Japan Meteorological Agency
LAM	Limited-area Model
LNHE	*Laboratoire National d'Hydraulique et Environnement*
MLLW	Mean Lower Low Water
MOS	Model Output Statistics
MSL	Mean Sea Level
MSM	Meso-scale Models
NCEP	National Centers for Environmental Prediction
NOAA	National Oceanic and Atmospheric Administration
NWP	Numerical Weather Prediction
PEARL	Preparing for Extreme And Rare events in coastaL regions
PSWS	Public Storm Warning Signal
QPF	Quantitative Precipitation Forecast
RMSE	Root Mean Squared Error
STEPS	Short Term Ensemble Prediction System
SWAN	Simulating Waves Nearshore
TUHH	Technische Universität Hamburg-Harburg (Hamburg University of Technology)

WMO	World Meteorological Organization
WP4	Work Package 4
WRF	Weather Research and Forecasting

1 Introduction

Coastal areas are exposed to various types of water-related hazards including storm surges river floods, flash floods, urban floods, and tsunamis (Kron, 2015). But these areas are also highly attractive to human settlement, making them some of the most densely populated regions in the world (Neumann et al., 2015; Brown et al., 2013). These factors contribute to the high levels of flood risk in urban coasts. Rapid rates of urbanisation are also projected to continue in the future (Neumann et al., 2015), and combined with the impacts of climate change, significant increases in flood risks in urban coastal communities are expected (Vojinovic et al. 2014; Djordjevic et al., 2011).

Water services are under increasing pressures from rapid urbanization. Add to this the impacts of climate change and occurrence of extreme events, it is a challenge for the development of drainage systems to keep pace with the water management demands of the rapidly growing population and urban area (Parkinson & Mark, 2005). Drainage systems, as well as flood protection structures, are designed according to a 'design storm' (Butler & Davies, 2011) to meet a certain 'level of service'. This means they are only built to accommodate or withstand events with a particular likelihood of occurrence (return period). Thus, there will always be events with magnitudes exceeding design levels causing disasters such as flooding even when design standards are updated considering the impacts of climate change. Urban flooding is, therefore, inevitable as drainage systems are designed for a given return period (Djordjevic et al., 2011), and all urban drainage systems will reach the limit of their hydraulic capacity in their lifespan (Parkinson & Mark, 2005). This highlights the importance of flood disaster management strategies for urban areas.

The use of flood warning systems for flood mitigation and urban water management offers a solution not requiring expensive construction and yet allowing optimal use of existing infrastructure and reduction of flood impacts. Although structural measures, such as the use of reservoirs and levees, are some of the most commonly-used for flood mitigation (Linsley & Franzini, 1992), they cannot offer complete protection against floods due to their limited design capacities (Moore et al., 2005). Thus, strategies for when conditions exceed the design criteria and floods occur must be in place. The establishment of a real-time urban flood information system is an example of such a strategy (Djordjevic et al., 2011; Abebe & Price, 2005). A flood information and warning system promotes preparedness—for communities to reduce direct interaction with the flood, and for the authorities to prepare for the implementation of emergency plans, which subsequently reduces flood damages.

The flood mitigation cycle, shown in Figure 1, combines and organizes various approaches into a consistent strategy for reducing flood impacts (Parkinson & Mark, 2005). The issuance of warnings is an important component implemented before the flood. Its objective is to increase the preparedness of communities and the authorities to deal with the upcoming flood event. It enables timely evacuation, relocation of valuables, and management of potentially-affected infrastructure by the community (Moore et al., 2005).

Monitoring, identification of potential flood hazards, and release of flood warnings are involved in the process (Parkinson & Mark, 2005), and technological developments have made the use of information and communications technology and hydroinformatics in these components a standard. Hydroinformatics tools, such as computational flood models, are used in the identification of potential flood hazards. These can be physically-based, data-driven, conceptual, or combinations of different types, and are especially useful for risk assessment and flood forecasting in warning systems (Price & Vojinovic, 2008). Flood information from these modelling tools is used

in the decision-making process related to the issuance of flood warnings and deployment of emergency support services.

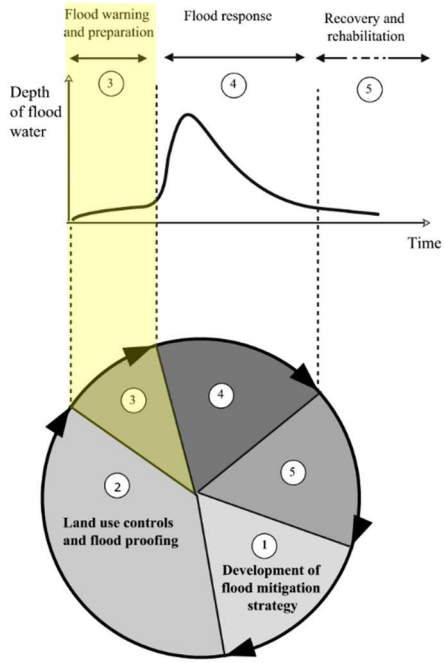

Figure 1 The flood mitigation cycle highlighting the 'Flood warning and preparation' stage. (Source: Parkinson & Mark, 2005)

In this report, a review and assessment of modelling tools and techniques used in early warning systems for urban coastal flooding are presented. The aim of the work package on 'Flood forecasting and early warning systems for coastal regions' (WP4) of which this study is a part, is to improve flood forecasting and modelling tools for early warning systems. The objectives of this study are:

- To assess and enhance existing methodologies and tools for real-time coastal flood modelling and flood hazard mapping, and
- To develop and implement real-time coastal flood modelling systems, which are accessible to end-users over the internet, in selected case studies.

A description of the general components of flood warning systems is given at the beginning of Chapter 2 of the report. Then, the succeeding sections focus on modelling tools used in the different components of flood warning systems. Existing methods and tools for real-time urban coastal flood modelling are reviewed, and considerations and possible enhancements for the methods are identified and discussed. State-of-the-art techniques for flood hazard mapping, which are widely used in warning systems, are also presented. Literature on existing flood early warning systems is used as examples and illustrations for the discussions. Descriptions of implemented real-time flood warning systems in the PEARL case cities of Hamburg (Germany), Greve (Denmark), and Castries (Saint Lucia) are presented in Chapter 3. The implemented systems are analysed and evaluated in terms of operational performance to assess and identify points of enhancement for these methods for real-time flood forecasting and warning applications. Finally, the last chapter presents a summary and suggested framework for real-time coastal flood warning, including recommendations regarding the use of modelling tools for coastal pluvial and fluvial flooding applications.

2 Tools and Techniques for Flood Warning Systems

Flood warning systems issue advance information about impending flooding, allowing people exposed to the hazard and the authorities to prepare, take action and reduce risks. The basic components of these systems are shown in Figure 2 and described below.

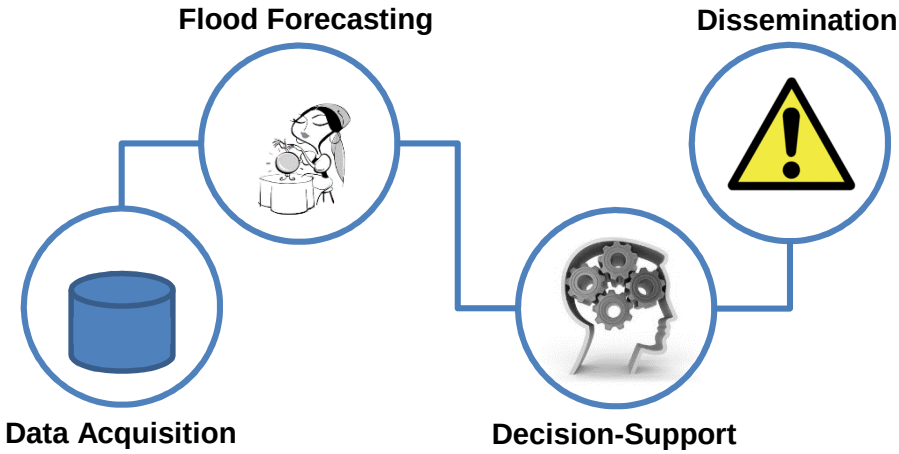

Figure 2 Typical components of an integrated flood forecasting and warning system.

Flood warning systems are subject to expectations regarding forecasting technique, accuracy, forecast lead time and service delivery. Good warning systems should be able to detect floods well before they occur, accurately interpret data and forecast the flooding in areas likely to be affected, efficiently disseminate the warning to the public and relevant authorities, and encourage appropriate response through preparedness (Jha et al., 2012). Several interconnected modules typically comprise these systems, which are described below.

Data acquisition. This involves the collection, measurement, and processing of data needed to assess existing and estimated future flood conditions in the system. Real-time measurements of water level and discharge at various key locations support flood forecasting activities by:

1) Providing an up-to-date overall picture of hydraulic conditions in the system
2) Serving as initial conditions to the flood forecast model, if one is being used
3) Serving as calibration or assimilation data for the forecast model

In addition, this module would also involve the derivation of forecasts for the various major drivers to flooding in the system (see Chapters 2.1.1 and 2.1.2).

Flood forecasting. The occurrence of potential flooding in the system is computed based on acquired data. Some systems issue warnings using estimates that are only based on past event experience and indicative threshold measurements at key points in the system, such as water levels at network outlets, sea levels at the harbour, accumulated rainfall amounts over a time period, and the like. However, forecasts upon which warnings are based should be as accurate as possible (Parkinson & Mark, 2005), and computational models are useful for this purpose (Price & Vojinovic, 2008). Models are used for flood forecasting in real-time modelling and/or offline analyses of the performance of the forecast system. They can be physically-based, data-driven, conceptual, or combinations of different model types. Selection of the modelling tool for forecasting largely depends on the flood type, dominant processes involved, data availability, desired level of

accuracy and intended forecast time (Parkinson & Mark, 2005; Abebe & Price, 2005). Real-time modelling tools, which are widely used in the 'forecasting' component of warning systems, are the focus of this report and discussed in succeeding sections.

Decision-support. This module integrates, processes and analyses information from the other components of the system for advanced planning and action regarding the forecasted hazard. The analysis of the data and modelling results, including consideration of non-technical uncertainty information, supports decision-making and gives a clearer picture of priority areas (Jha, et al., 2012). Information products for the different end-users of the system are also developed and generated at this stage.

Dissemination. Involves rapid distribution of information to the exposed population with sufficient lead time and in an understandable format (Jha et al., 2012). This may be through web-based viewers, SMS messages, and emails, as in the 'Hidromet' system described by Rodriguez, et al. (2014), or more sophisticated systems like automatic emergency messaging systems (for instance, the standard EDXL (Emergency Data Exchange Language) (OASIS, 2015) used in Task 4.4 of the PEARL Project).

A good data communications system that enables timely transmission of data between components of the system such as 'Forecasting' and 'Decision-Support' is crucial. The same infrastructure could also be used for eventual dissemination of warnings. Thus, the communication links that interconnect the different components of the system could also be categorised as a separate major component of warning systems.

2.1 Real-Time Modelling for Coastal Flood Forecasting

Computational models are valuable tools for flood risk assessment and forecasting (Price & Vojinovic, 2008). Hydrodynamic models, for example, provide high resolution depth and discharge information for flood predictions. These tools offer solid and consistent scientific bases in the form of quantitative and reproducible information that may be used for developing specific risk management strategies, such as the implementation of new coastal protections, or warning systems (Villatoro et al., 2014).

In flood warning systems, models are used for real-time forecasting or offline scenario analysis. Offline analysis involves prior modelling with various system condition scenarios to obtain a catalogue of flooding that may be used as a reference for obtaining future flood estimates. "Real-time", on the other hand, indicates continued information during an event, and real-time flood modelling involves the use of current and short-term future predicted driver and system conditions to determine if, when and where flooding will occur. This report focuses on real-time modelling for coastal flooding applications, i.e. storm surges e.g. in combination with pluvial/fluvial urban flooding.

Coastal flooding is characterized by unusual inundation of inland areas due to the intrusion of sea water over the surface or surcharge of rivers and drainage systems due to high sea levels and/or heavy rainfall. Various parameters involved in coastal flooding for which forecast models are used are shown in Figure 3. These are usually the main driving factors to the flooding, including the flooding itself, and are important to have early knowledge of for early warning as these significantly extend lead times. Rainfall is a major hydrologic driver to urban pluvial and fluvial flooding, and extreme sea levels and storm surges are important factors causing flooding from the sea. The different tools and techniques that are used to model and forecast these phenomena as part of coastal flood warning systems are discussed in succeeding sections.

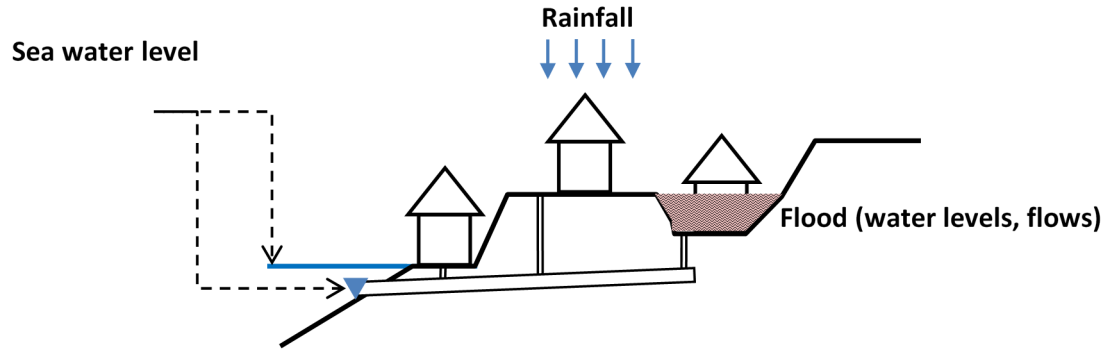

Figure 3 Coastal flooding parameters for which forecasts can be made.

2.1.1 Rainfall

An estimate of precipitation to occur over an area over a time period, or Quantitative Precipitation Forecast (QPF), is obtained using various methods, including Numerical Weather Prediction (NWP), radar-based forecasting, artificial neural network modelling, and knowledge-based nowcasting (Einfalt et al., 2004). Descriptions and application examples of these various QPF methods are also presented in the COST (European Cooperation in Science and Technology) publication on "Quantitative precipitation forecast (QPF) based on radar data for hydrological models" (COST, 2005).

Numerical weather prediction (NWP)

In this method, numerical models of the atmosphere and oceans are used to simulate global atmospheric circulation and predict the weather. The temporal evolution of atmospheric circulation is calculated by integrating the governing equations (i.e. the Navier-Stokes equations in the rotating frame) using initial conditions from current meteorological observations (Kimura, 2002; Lynch, 2008)). Global models, covering the entire earth, and limited-area models (LAMs) or regional models, covering only parts of the earth, are used in NWP.

The ECMWF (European Centre for Medium-range Weather Forecasts) uses a global atmospheric model. ECMWF is an independent intergovernmental organisation that produces and disseminates numerical weather predictions to its member states and users worldwide. Its atmospheric model has a spatial resolution of 25 km with 91 vertical levels, and coupled to an ocean wave model and using initial conditions obtained from conventional and satellite observations, it produces a wide range of global atmospheric and marine forecasts (ECMWF, 2013; Lynch, 2008).

Global models are comprehensive but their coarse resolutions make them inappropriate for localized and short-range forecasts. Regional and meso-scale (MSM) models nested in global models are used instead, which have finer resolutions and use boundary conditions obtained from global models. They provide greater spatial and temporal detail on a range of outputs (e.g. precipitation) appropriate for short-range forecasting.

An example of a LAM is the Weather Research and Forecasting (WRF) Model developed by American national agencies and universities in the late 1990's (Lynch, 2008; "The Weather Research & Forecasting Model", n.d.). It provides various meteorological information in a range of spatial resolutions from tens of meters to thousands of kilometres. Examples of rainfall forecast output using the WRF model by the National Centers for Environmental Prediction (NCEP) is shown in Figure 4.

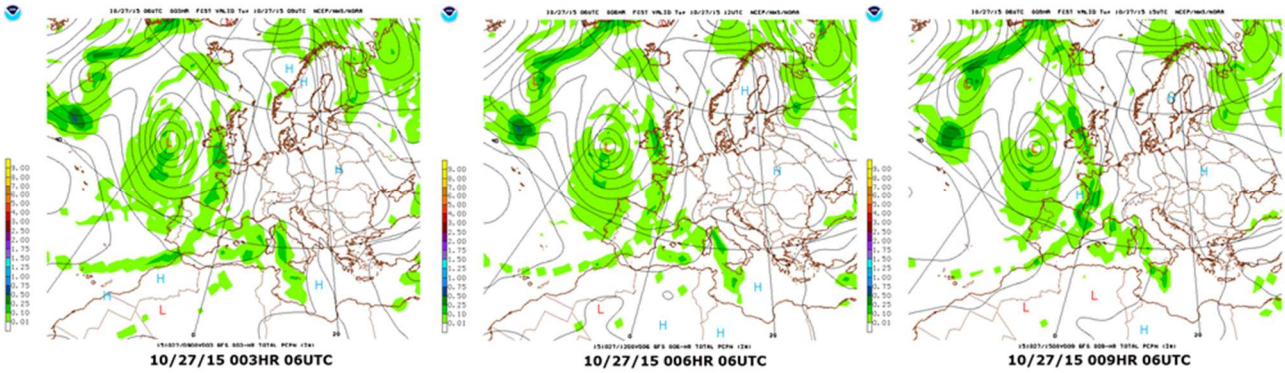

Figure 4 Example series of precipitation forecasts by NOAA National Centers for Environmental Prediction (NCEP) on 27 October 2015 using the WRF Model. The maps show coloured areas for 3-hour accumulated precipitation in inches and contour lines for Mean Sea Level Pressure in millibars in 4 mb intervals. (Source: http://mag.ncep.noaa.gov)

Another example of forecasted rainfall using NWP is shown in Figure 5. These forecasts are in the form of time series of hourly accumulated rainfall for a 0.1 x 0.1 degree area in Denmark, and are made using a WRF model nested in the ECWMF model and run by StormGeo for DHI (StormGeo, n.d.; DHI, 2011) (Figure 6). Hourly rainfall prognoses for a period of 6 days (0 to 144 hour) are obtained twice a day. These StormGeo rainfall forecasts are used in the real-time coastal flood model in the Greve Case Study, which is described in Chapter 3.2. These localized NWP forecasts are accessible from DHI's 'Water Forecast' system (http://www.waterforecast.com/) and are the most readily-available for the area of Greve.

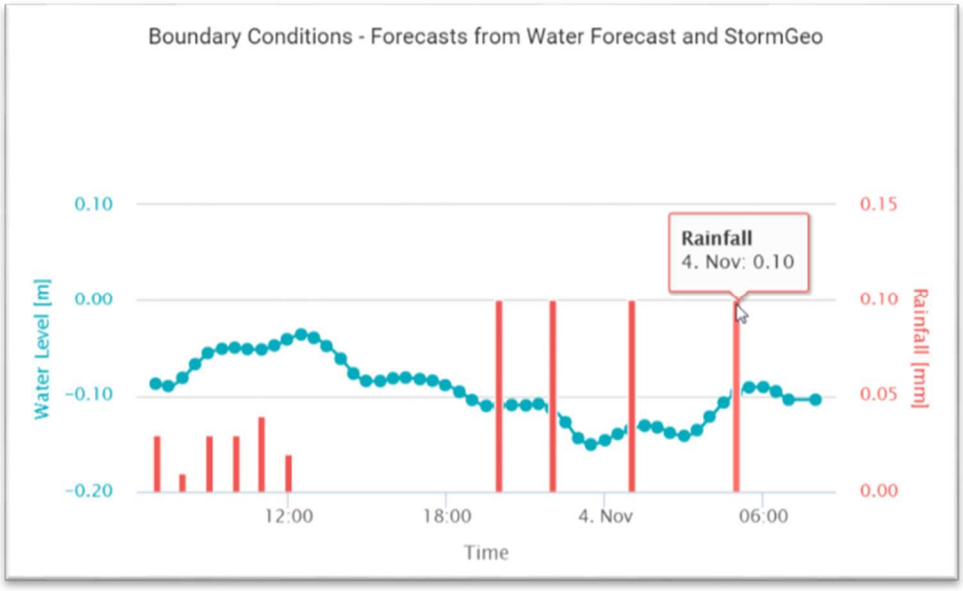

Figure 5 Red bars show time series for forecasted hourly accumulated rainfall (mm) for an area in Denmark. Blue lines show forecasted sea levels, which are described in Chapters 2.1.2 and 3.2. (Source: http://greve.dhigroup.com/)

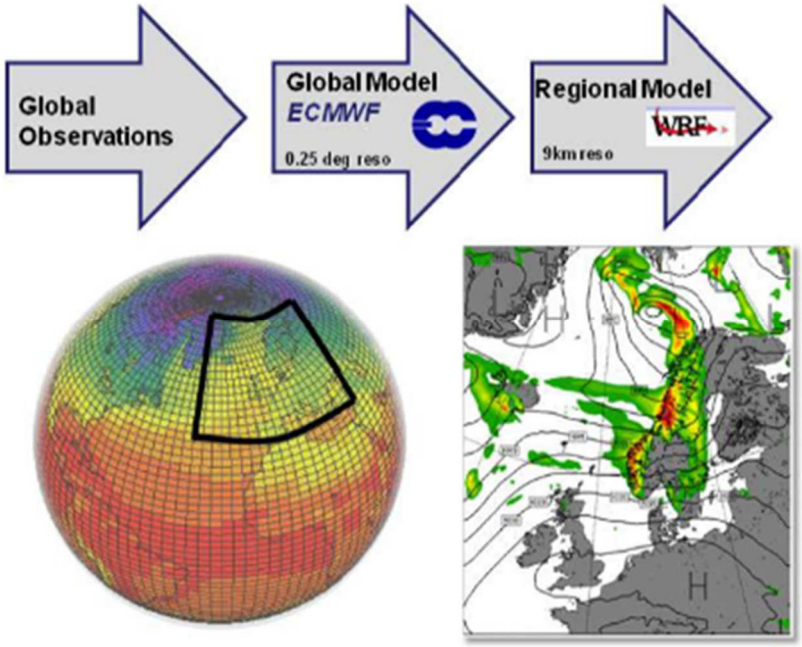

Figure 6 Schematic diagram showing the different NWP models (i.e. the global (ECMWF) model and regional WRF model) used by StormGeo (http://www.stormgeo.com) to obtain rainfall forecasts in parts of Denmark. (Source: DHI, 2011)

Radar-based nowcasting

Obtaining advanced accurate and localized precipitation information over an area is highly advantageous for warning systems, enabling them to better provide accurate information on destructive flood hazards to the public and reduce associated risks to life and property. In urban areas, analysis of hydrological processes requires short-term rainfall forecasts with lead times less than 3 hours (Schilling, 1991). The use of rain gauges is the traditional way of rainfall data collection, and networks of several rain gauges provide information on its spatial variation. Rain gauges are unable to forecast rainfall, and there is a limit to the density of rain gauge networks for practical operation and maintenance. In urban areas, convective rain events can only be identified by a dense network of rain gauges located, on average, every kilometre or by weather radar (Niemczynowicz, 1991). The advantage of using weather radar for precipitation measurement has been recognized as it provides data with high spatial and temporal resolutions. Weather radars detect spatially distributed information that reveal size, shape, intensity, speed, and movement information on rain events. In addition, unlike rain gauge data, weather radar data may be used for short-term forecasting of precipitation using various radar-based QPF methods that have been developed. The radar data can be used to analyse small-scale weather features such as storms in a localised area and make accurate forecasts for a few hours ahead. It is possible to extrapolate the likely location of moving storms from radar data as it provides detailed, virtually continuous, and spatially distributed information on these weather features.

Forecasting rainfall using weather radar essentially involves radar data extrapolation. Various extrapolation techniques are used on a series of radar images to estimate future intensity and position of storms (Einfalt et al., 2004; Berenguer et al., 2013; Liguori & Rico-Ramirez, 2014). Radar echoes are 'tracked' through determination of their velocity and direction of displacement in order to forecast their movement (COST, 2005). The term 'nowcasting' involves detailed description of the current weather and short-period forecasting of less than a few hours ahead (i.e. 0-6 hrs) (Wilson et al., 1998; WMO, n.d.). Nowcasting is very useful for flood warning systems as it provides location-specific forecasts of storm growth and movement, which enables improved flood

forecasting especially in urban catchments with short response times, and allows people at specific locations to prepare for oncoming hazards.

According to the review of radar-based forecasting by Liguori & Rico-Ramirez (2014), the two main types of extrapolation techniques for nowcasting are: (1) cross-correlation methods, and (2) individual radar echo-tracking methods, as summarized by Collier (1981). Cross-correlation involves correlating portions of two subsequent radar images to detect similar patterns of radar echoes, wherein the tracking areas are matched by optimizing the correlation coefficient. The distance between the tracking area and time lag between radar scans determine the displacement vector, which is assumed to characterize the motion of the radar echoes and used to make forecasts (Collier, 1981; COST, 2005). Individual radar echo tracking methods, on the other hand, involve identification of individual radar echoes in a radar image, and matching them in successive images with respect to echo centroids or other characteristics to derive motion vectors, which are then used for forecasting (Collier, 1981).

The 'Hidromet' early warning system, which is being improved under the PEARL Project and described in Rodriguez et al. (2014), makes use of radar nowcasting to obtain rainfall estimates for real-time urban flood modelling and warning. Rainfall forecasts may already be used as a form of first-alert for flood warning (Moore et al., 2005), and a simplified version of 'Hidromet', called 'FloodAlert', does not employ a flood model but primarily uses radar observations and forecasts to issue local flood warnings (Llort et al., 2014). In both systems, cross-correlation techniques are used to derive precipitation motion fields from latest radar images, which are used to extrapolate future (forecasted) precipitation fields (See Figure 7).

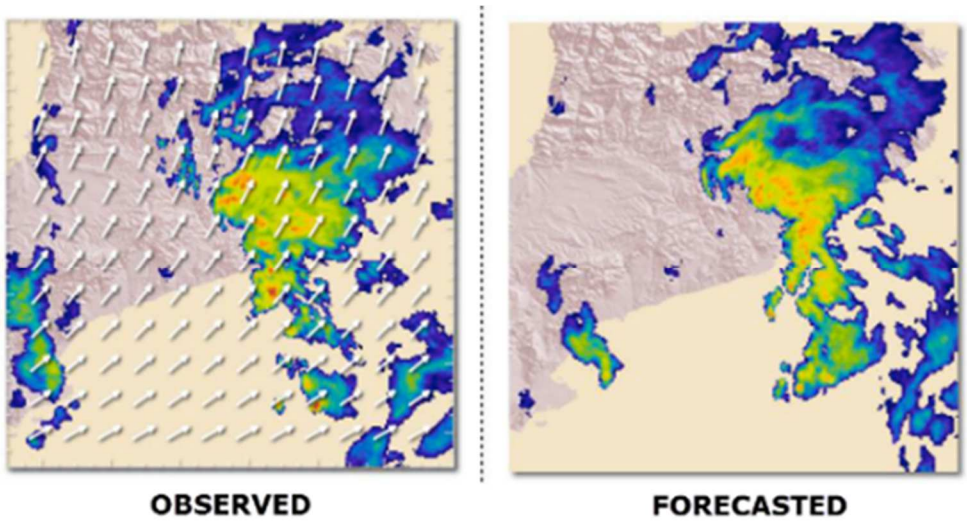

Figure 7 The 'Hidromet' and 'FloodAlert' systems developed under the PEARL Project use the most recent radar observations (Left) to calculate precipitation motion fields (shown as white arrows), which are then used to extrapolate from the last radar image to forecasts (Right). (Source: Rodriguez et al., 2014)

In the 'FloodAlert' system, the derived rainfall motion field is used not only for nowcasting but also for defining critical regions around defined points of interest that dynamically change with the movement of the rain field. Accumulated rainfall values are calculated in these 'critical regions' and compared against user-defined thresholds for possible issuance of warnings (Llort et al., 2014). The cross-correlation technique used in the 'Hidromet' and 'FloodAlert' systems is described in more detail in Berenguer et al. (2005 & 2011).

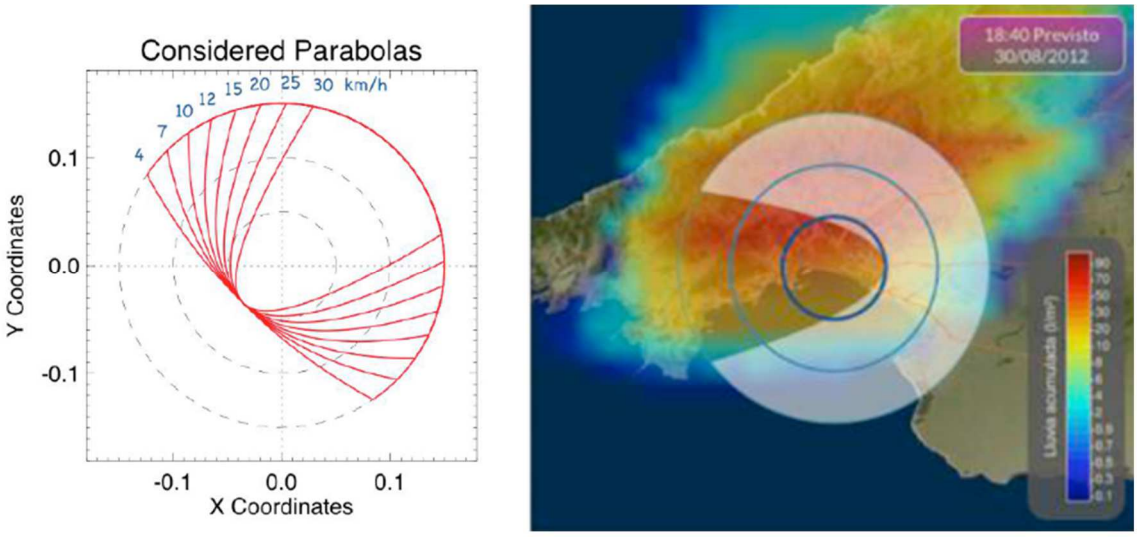

Figure 8 Critical regions at a point-of-interest are assumed to have parabolic shapes that vary in shape and orientation according to the precipitation's derived motion field direction and velocity (Left). The figure on the right shows an example of the critical region around Palma de Mallorca for a forecasted storm 50 minutes before it arrived (30 August 2012 18:40:00) in the FloodAlert system. (Source: Llort et al., 2014)

A cross-correlation technique, detailed in Jensen & Pedersen (2005), is also used in radar-based nowcasting activities at DHI in Denmark. Based on the two most recent radar images, a tool, called 'AutoForecaster', is used to derive the movement vector field of detected precipitation echoes. The derivation of the velocity fields involves sub-division of the earlier of the two radar images into parts for which maximization of pseudo "correlation coefficients" is done between generated displacement scenarios and the latest image. This identifies the 'best' displacement for a sub-image and the velocity is calculated based on the time between radar images. The v_x and v_y values for every radar pixel of the whole image are then determined through interpolation between all sub-images, and used to forecast "forward" movement in the entire area. The movement of each pixel in the last radar image is calculated using the following equations (Jensen & Pedersen, 2005):

$$DeltaX = \frac{X_{vel_{x,y}} DT}{DX}$$

$$DeltaY = \frac{Y_{vel_{x,y}} DT}{DY}$$

Where,
$DeltaX$, $DeltaY$ = Displacement in x- and y-direction, respectively
$X_{vel_{x,y}}$, $Y_{vel_{x,y}}$ = Velocity in x- and y-direction at position (x, y), respectively
DT = Time between images
DX, DY = Grid resolution in x- and y-direction, respectively

DHI's radar-based forecast systems in the areas of Hørsholm, Aarhus, and Odense in Denmark (See Figure 9) use Local Area Weather Radars (LAWRs), which are standard Furuno X-band radars (see Furuno, 2015) that have been modified for signal extraction and remote control. Signal processing, clutter removal, filtering and communication are handled at the radar sites, and then the radar images are transferred to a central computer, which processes and distributes the observations to a website (www.regn.dk). One-hour forecasts are made every 5 minutes. Tests

and evaluations made by Jensen & Pedersen (2005) indicate that the reliability of these completely automatic short term forecasts is about 67% on a 500 by 500 m scale.

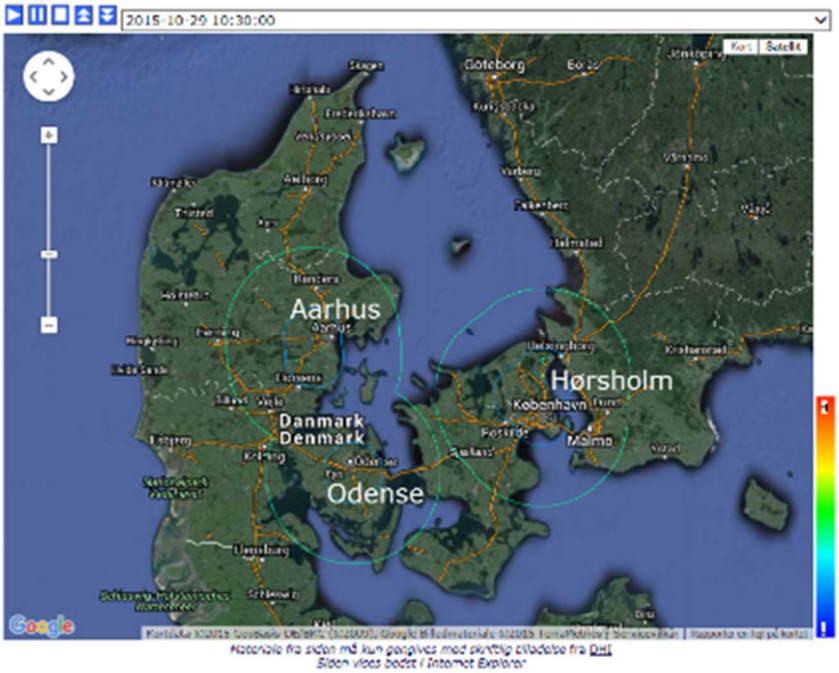

Figure 9 Map showing the coverage (green lines) of DHI's Local Area Weather Radar (LAWR) system installations in Aarhus, Odense and Hørsholm in Denmark. (Source: http://regn.dk/)

Radar nowcasting forecast skills decay quickly with time. The decrease in accuracy with time in terms of hit percentage (rain/no rain) and average deviation (in mm/h) are attributed to the extrapolation technique and disregard of time-dependent developments in rain cells (Jensen & Pedersen, 2005). Nevertheless, radar nowcasting is one of the best short-period precipitation forecasting methods available (Golding, 2000), and with the rapid development of the technique (a new forecast can be calculated every time that new data is available, typically every 5-10 minutes), it is a good tool to use for urban flood forecasting and warning.

Hybrid rainfall forecasting

In order to extend the nowcasting forecasts beyond 6 hours, some use the combination of radar extrapolation techniques with satellite and NWP model (WMO, n.d.). An example of this is the 'Nimrod' system developed by the UK Met. Office and presented in Golding (2000). Tests showed significant improvement of forecasts with the hybrid system compared to pure NWP or nowcasting methods (Golding, 2000). It is apparent that numerical weather prediction and nowcasting methods operate at different space and time scales. Numerical models, although physically based, have limited capacities in describing dynamical processes of sudden localized changes, which are important considerations in averting disasters for early warning systems. Thus, it has been recognized that combining NWP products with conventional observations, radar imagery, satellite imagery and other data offers advantages for rainfall forecasting by capitalizing on the strengths of the different techniques in one method (Lynch, 2008; Yu et al., 2015).

Ensemble and probabilistic rainfall forecasting

It has been recognized that atmospheric processes are chaotic in nature and difficult to predict. For numerical models, unavoidable errors in the initial state grow rapidly and degrade the forecasts after some days (Lynch, 2008). In order to handle this uncertainty, an ensemble of forecasts, each

starting from a slightly different initial state, is run and used to obtain probabilistic forecasts of rainfall or atmospheric conditions.

A probabilistic approach to rainfall forecasting is applied to consider uncertainty in the flood forecasting and warning process. The ECMWF and National Centers for Environmental Prediction (NCEP) have been using ensemble forecasts since the early 1990s (Lynch, 2008). In tests done by Liguori et al. (2012) regarding the use of stochastic probabilistic precipitation forecasting to predict flows in urban catchments, it was found that probabilistic rainfall forecasts have a higher skill than deterministic forecasts for predicting rainfall with lower intensities. In Rene et al. (2013), an approach for probabilistic rainfall forecasting for urban pluvial flooding applications was developed building on methods by Schaake et al. (2007) and Wu et al. (2011), which involved derivation of probability distributions for single-valued forecasts based on comparison of NWP forecasts and rain gauge observations.

In the field of radar nowcasting, probabilistic forecasts have also been created to account for the radar precipitation uncertainties and the uncertainties related to the nowcasting technique itself. The usual way of dealing with the uncertainty has been the use of ensembles (set of equiprobable rainfall fields) to represent the uncertainty in the data. An example is Germann et al (2009)—one of the first to propose a methodology for creating radar precipitation ensembles, or Berenguer et al (2011), illustrating the use of radar-ensemble generation techniques for short term forecasting.

Finally, there are hybrid probabilistic QPF methods that integrate the different techniques involving radar-based and NWP-based rainfall forecasts (Golding, 1998; Liguori et al., 2012). An example is STEPS (Short Term Ensemble Prediction System): a stochastic probabilistic precipitation forecasting scheme developed by the UK Met. Office in collaboration with the Australian Bureau of Meteorology (Bowler et al., 2006; Liguori et al., 2012).

2.1.2 Water levels and storm surges

Coastal flooding occurs from a mix of hydraulic and sediment-related processes, such increased sea levels and wave exposure during storm surges, and dune erosion and dike breach (Christensen et al., 2013). Sea level is actually comprised of several components such as storm surge, astronomical tide, and wind wave effects (i.e. setup, run-up, overtopping, and wave crest elevation) (Bode & Hardy, 1997), and numerical hydrodynamic modelling is used to predict this ocean response to the combined influence of meteorological conditions (i.e. wind and atmospheric pressure), waves, and tides. In this section, numerical modelling techniques for quantifying the predominant hydraulic factors to coastal flooding, such as sea levels, and wave effects (excluding tides) are discussed.

Hydrodynamic modelling

Specific and accurate information for coastal flood warning requires localized, high-resolution data for flood analysis. Thus, hydrodynamic models of local sea areas are used, nested in global circulation and ocean models, to obtain site-specific conditions data, which may then be used for subsequent high-resolution, local flood modelling.

2D Modelling. A 2D hydrodynamic model of a sea region may be used for deterministic storm surge modelling. An example is the 2D model used in the storm surge forecasting and flood management system in Venice, Italy, which is described in Kerper et al. (2002). The model, named Deterministic Venice *Acqua Alta* Forecast System (DVAAFS), was built with MIKE 21 (DHI, 2013), a software tool for simulating two-dimensional free surface flows. The model used nested Cartesian computational grids covering the Mediterranean Sea, Adriatic Sea, and Venice Lagoon, and was driven by wind and pressure fields obtained from global and regional numerical weather prediction (NWP) models, and water level and tide conditions applied at sea boundaries. With the

2D hydrodynamic model, water levels and current velocities could be obtained throughout the model domain.

In Tablazon et al. (2014), the 2D Japan Meteorological Agency (JMA) storm surge model was used to model storm surge heights during historical tropical cyclones in the Philippines to develop a compendium of public storm warning signal (PSWS) and maximum storm surge combinations, and derive recurrence intervals for storm surge heights and resulting inundation. The JMA storm surge model is a numerical model based on the calculation of the shallow water equations in two-dimensions, and is used to model storm surges from tropical cyclones (Higaki et al., 2009). The model is driven by surface wind and atmospheric pressure data from meso-scale atmospheric models, and also uses information on cyclone track, and tides. Model grid sizes down to 1.5-2 km have been used. Details about the JMA storm surge model, including performance evaluation and application in several case studies, are presented in 'Outline of the Storm Surge Prediction Model at the Japan Meteorological Agency' by Higaki et al. (2009).

The Hamburg Case Study conducted under the PEARL Project uses a 2D model for the Hamburg-Elbe estuary (see Chapter 3.1). The model, which covers the Elbe and its hinterland areas from the weir in Geesthacht to Cuxhaven at the mouth of the river (Figure 10), is implemented through the open source modelling system Kalypso. The Kalypso system, jointly developed by Hamburg University of Technology and Björnsen Consulting Engineers, consists of several modules: i) Kalypso-Hydrology for rainfall run-off simulations, ii) Kalypso WSPM for one-dimensional water surface profiles, and iii) Kalypso Hydrodynamic for unsteady coupled 1D2D flows for surface waters (Kalypso 1D2D) and complete 3D modelling of flow conditions. The model of the Hamburg-Elbe estuary uses the Kalypso Hydrodynamic module, which uses Telemac-2D as the calculation core. Telemac-2D, developed by the LNHE (*Laboratoire National d'Hydraulique et Environment*), models unsteady flow and transport processes in free surface waters. The model solves the depth-averaged shallow water equations (Saint-Venant Equation) on unstructured triangular calculation mesh, which allows for different levels of spatial discretization (Telemac, 2014). In Telemac, the partial differential equations are solved using a Finite-Element-Scheme and, therefore, the requirements of the Solver on the calculation mesh are comparatively low.

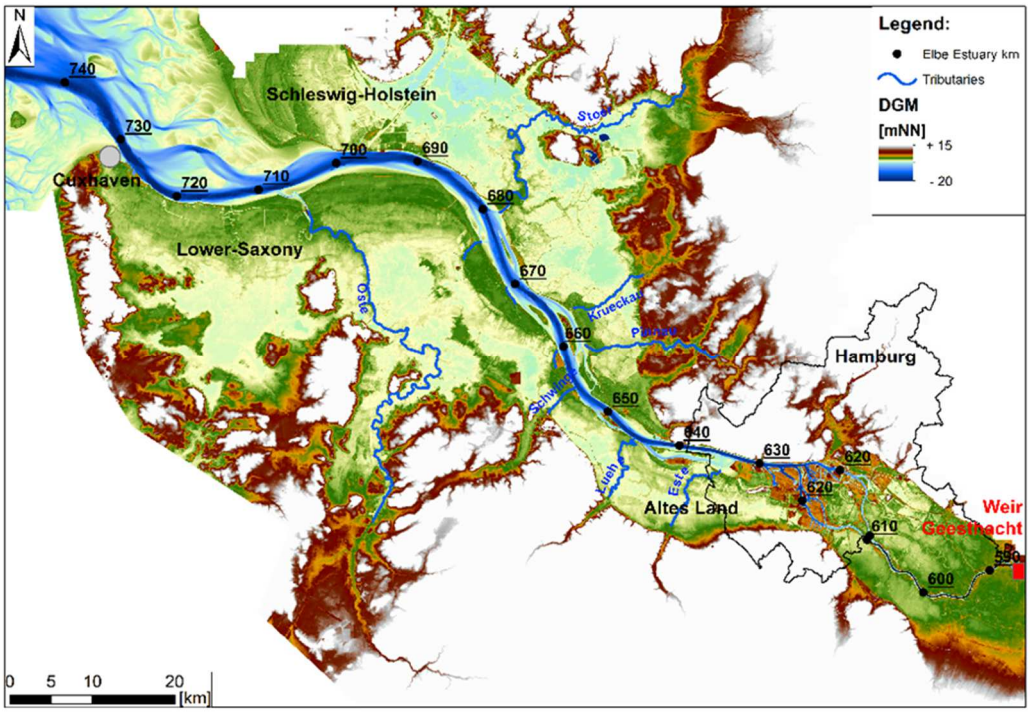

Figure 10 Overview of the Hamburg-Elbe estuary model domain.

The calculation mesh for the Hamburg-Elbe estuary model has approximately 100 000 elements ranging in size from 1 m² to 50 000 m². Different-sized elements are used, which allows for detailed integration of river structures, such as groins, in the mesh (Figure 11).

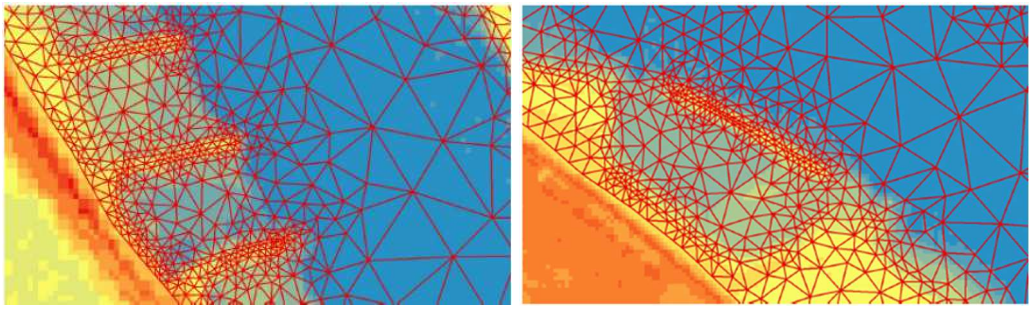

Figure 11 Integration of river structure into the calculation mesh.

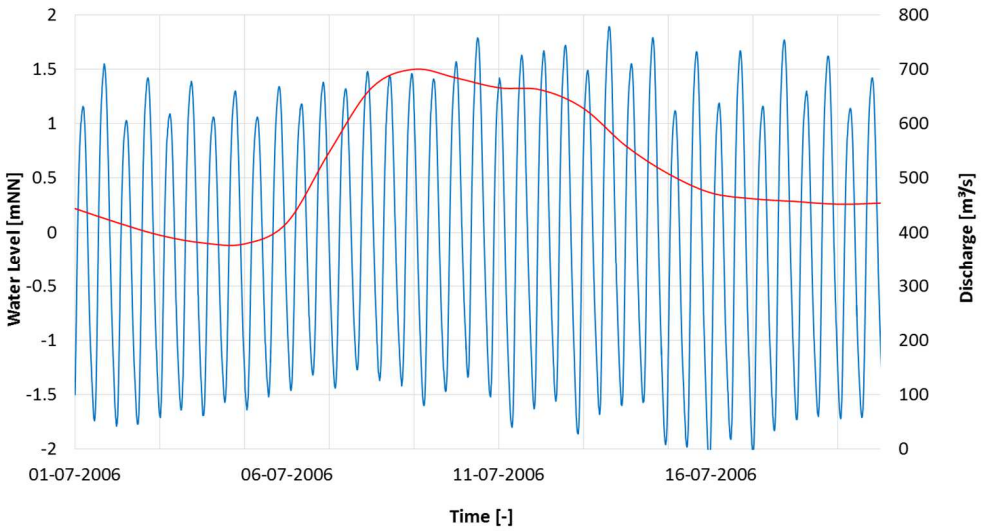

Figure 12 Boundary conditions for the Elbe estuary model. Water level boundary (blue line) applied downstream at Cuxhaven, and discharge boundary (red line) applied upstream at Geesthacht (see Figure 10).

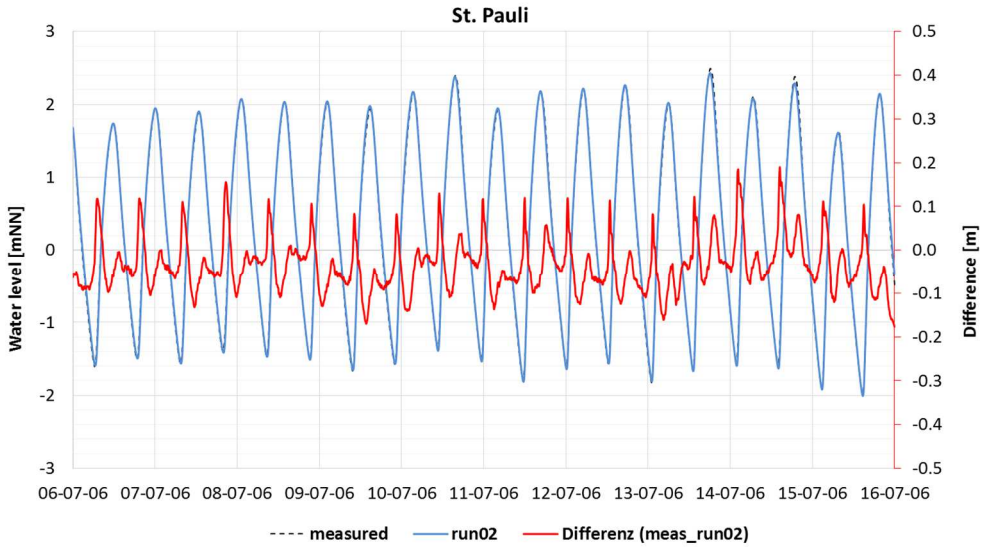

Figure 13 Comparison of measured and simulated water levels for the gauge St. Pauli.

Two different boundary conditions are applied to the model: a discharge boundary upstream at Geesthacht, and a water level boundary downstream at Cuxhaven (see Figure 10 and Figure 12). The model was calibrated against water level and current data from 16 water level gauges in the domain, and verification was performed based on a storm surge event from December 2013. Comparison between measured and simulated water levels show good agreement between observations and model results (Figure 13 and also Chapter 3.1.2).

3D Modelling. The 2D solution, however, neglects stratification and uses a one-layer, depth-averaged approach for the vertical zone. To avoid this assumption and simplification, a 3D hydrodynamic model may instead be used. An example of a 3D hydrodynamic model for a local sea area is the inner Danish waters and the Baltic Sea model described in DHI (2011) and shown in Figure 14. The model, referred to as the 'DKBS' model, is being used for DHI's 'Water Forecast' service (http://www.waterforecast.com/), which is a forecasting service providing hydrodynamic data such, as water level, flux, velocity, salinity and temperature, among other things, for marine, coastal and inland water applications (DHI, n.d.; DHI, 2011). The Water Forecast service is the source of sea water level forecast data driving the flood model for the Greve Flood Warning System, which is described in Chapter 3.2.

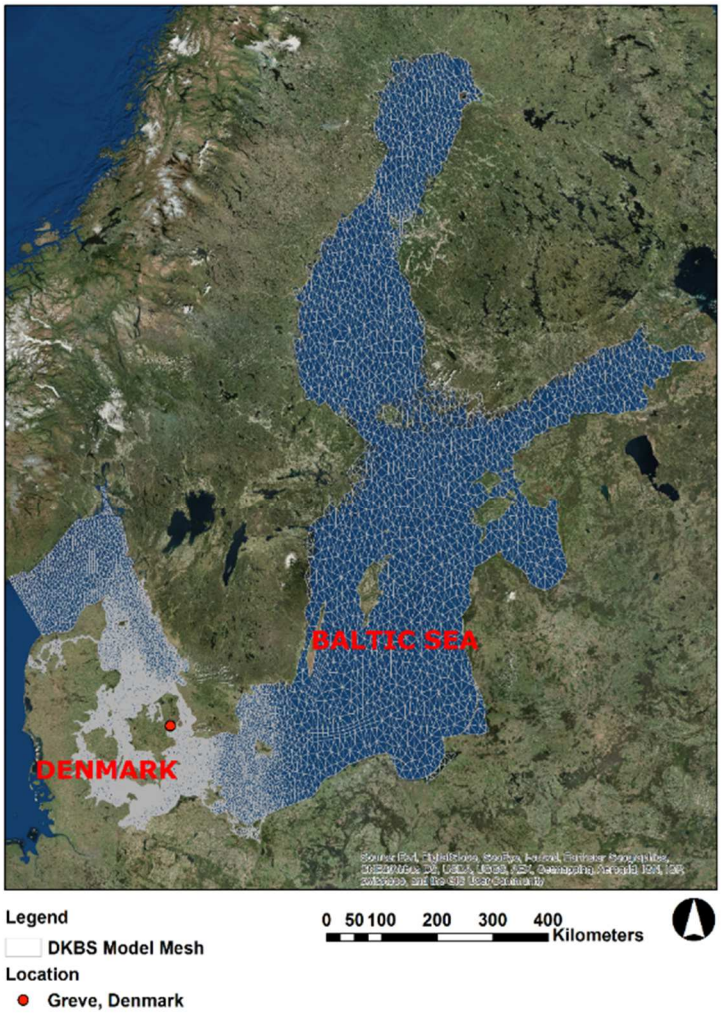

Figure 14 The extents of DHI's 3D hydrodynamic model for the inner Danish waters and the Baltic Sea (a.k.a. 'DKBS' model) showing the computational mesh elements (grey outlines). (Source: DHI, 2011)

Three-dimensional (3D) hydrodynamic models are based on solving the incompressible Reynolds-averaged Navier-Stokes equations in 3 dimensions. Physical conditions data, such as bathymetry and bed resistance, are used to model the physical system, and calculations are driven by inputs, such meteorological data of pressure and wind (i.e. from an atmospheric meteorological model), boundary water levels and fluxes, and tidal variation, among others. The computational grid for describing and discretizing the 3D model domain may be a Cartesian grid or a layered flexible mesh (see Figure 15). In a mesh-based 3D model, the horizontal space is discretized with an unstructured mesh, while for the vertical domain, the mesh may be structured or unstructured. The output from these models includes water levels, flux densities, velocities, densities, temperatures, salinities, current speed and direction, wind velocities, and air pressure. The use of forecasted meteorological boundary data, such as those from NWPs, would subsequently result in forecasts of local parameters that may be used for high-resolution coastal flood analyses for flood warning.

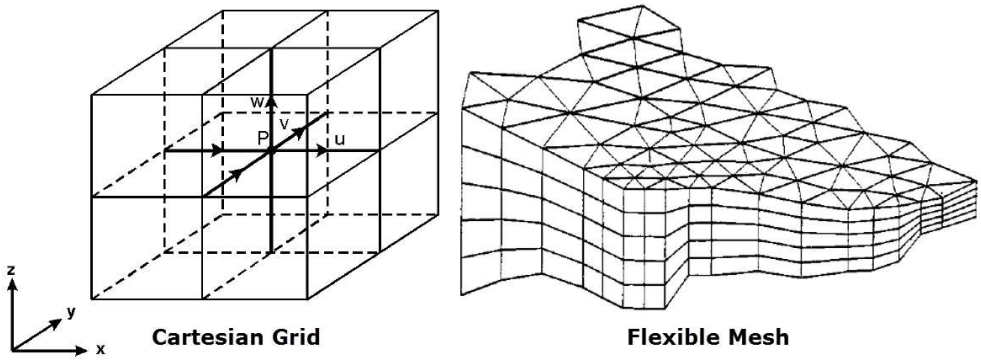

Figure 15 Comparison of Cartesian and flexible mesh computational grids that may be used in 3D modelling. The left figure shows the computation grid in the x, y and z-space (known as the Arakawa C-grid) used in a Cartesian grid-based 3D model. The right figure shows a layered mesh used in flexible mesh-based 3D modelling. (Source: DHI, 2013)

DHI's DKBS model (Figure 14) was built using MIKE 3 FM, a software tool for modelling unsteady three-dimensional flows, which uses a flexible mesh calculation grid (hence, 'FM') taking into account density variations, bathymetry and external forcing, such as meteorology, tidal elevations, currents and other hydrographic conditions (DHI, 2013). Meteorological forcing for the model is obtained from a WRF (Weather Research and Forecasting) limited-area numerical weather prediction model (see Chapter 2.1.1) covering Northern Europe with a resolution of 0.1 degrees (see Figure 6), which is run by StormGeo in Norway (StormGeo, n.d). The DKBS model provides 6-day forecast results twice a day (every 12 hours), which are stored in the Water Forecast system (see Figure 16).

The computational mesh of the DKBS model has a resolution ranging from 0.5-1 km in the Femern Belt area between southern Denmark and Germany, to 5-20 km in the eastern Baltic Sea. The vertical domain is a combined sigma-z domain, with the upper 10 m of the water column represented by 10 sigma layers and the remainder represented by a number of z-layers depending on local water depth. A vertical resolution of 1 m is used for the main part of the western Baltic Sea and the Belt Sea including Femern Belt (DHI, 2011). The hydrodynamic model was calibrated and validated against water level, current, temperature and salinity observations from 14 stations across the inner Danish Waters and the Baltic Sea, and good agreement between model results and measurements was achieved. More information about the calibration, and the model in general, are given in DHI (2011).

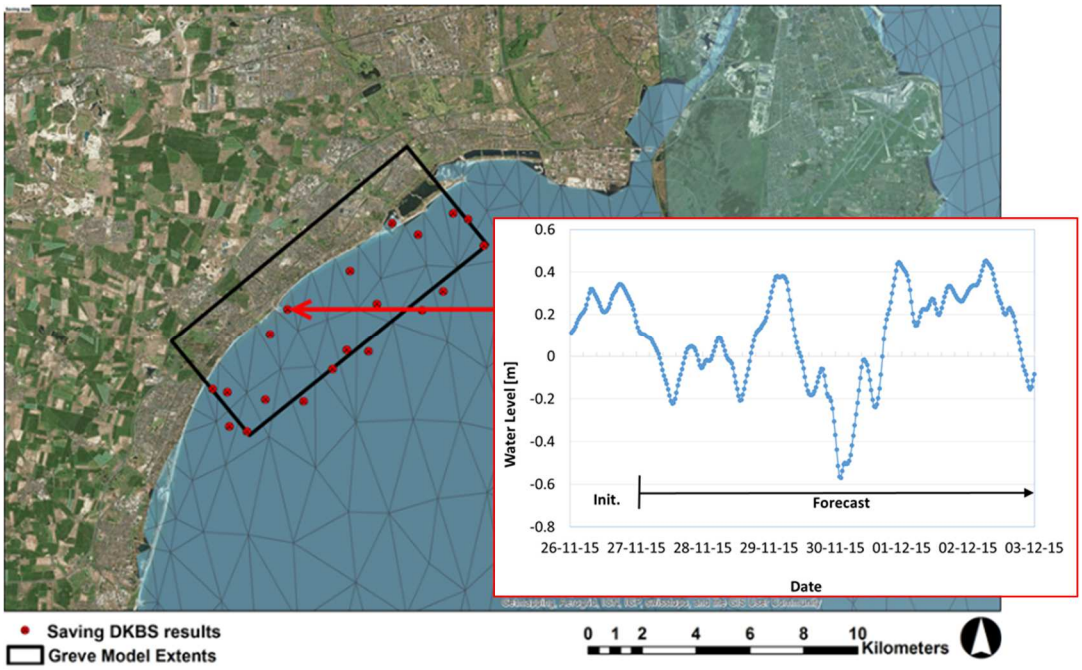

Figure 16 Example 6-day water level forecasts (obtained 27-11-2015) from the DHI DKBS model at a point along the coast of Greve, Denmark. The domain of the Greve Flood Warning System (see Chapter 3.2) is outlined in black, and the red points indicate locations where DKBS model results are being saved for subsequent coastal flood forecasting in Greve.

Wave modelling

Numerical wave modelling involves the computation of wave characteristics, primarily under wind action, using energy balance equations (Cavaleri et al., 2007). With respect to the analysis of flooding from the sea, wave modelling would be relevant for coastal and port areas where flooding due dynamic wave action and overtopping of dikes and structures are of main concern.

Different types of wave modelling tools are currently available, as reviewed in Cavaleri et al. (2007). Most can accurately predict surface waves in deep ocean areas (Komen et al., 1996; Booij et al., 1999), but for coastal flood warning applications, localized, high-resolution wave data are needed for subsequent overtopping analysis at the coast. Wave computation tools used in coastal flood analysis must then be adaptable to small-scale and high-resolution computations, and applicable in shallow water regions, such as coastal areas (Booij et al., 1999).

An example of high-resolution wave modelling is that for the inner Danish waters and the Baltic Sea setup for DHI's Water Forecast service, which was built together with the hydrodynamic model (DKBS model) described in the previous section (also see Figure 14). The wave model was built using MIKE 21 SW, a spectral wind-wave modelling tool simulating the growth, decay, and transformation of wind-generated waves and swells in offshore and coastal areas (DHI, 2013). The tool is applicable for regional- as well as local-scale analysis. It uses a flexible mesh computational grid, and thus, coarse spatial and temporal resolutions may be used to model offshore regions, and high-resolution boundary and depth-adaptive meshes may be used for shallow coastal environments. Traditionally, the tool is used to assess wave conditions in offshore and coastal areas, and to simulate sediment transport. The DHI spectral wave DKBS model is forced by spatially and temporally varying wind and ice coverage data, and water level and depth-integrated current inputs are obtained from the hydrodynamic DKBS model. Computation results include full wave spectra, and wave parameters, such as Significant Wave Height, Peak Wave Period, etc. As

with the hydrodynamic model, more details about the spectral wave DKBS model are found in DHI (2011).

Wave modelling is used in the HIDRALERTA Project (Raposeiro et al., 2013; Fortes et al., 2013), which focuses on flood occurrence from wave action, and is about developing a warning and risk assessment system for wave overtopping and flooding in coastal and port areas in Portugal. The system has a 'Wave Characterization' module, wherein wave characteristics at a location is forecasted using a series of nested numerical models for sea wave propagation (Fortes et al., 2013). The system uses SWAN (Simulating Waves Nearshore) (Booij et al., 1999), a third-generation numerical wave model for the coastal areas, and DREAMS, a linear mild-slope wave propagation model for port areas. Flooding is then estimated using wave overtopping analysis, which uses wave level results from preceding wave modelling, and GIS mapping. In HIDRALERTA, wave overtopping analysis is done using neural network modelling for port areas, and empirical modelling for coasts.

The SWAN wave model was also used by Gallien, et al. (2014) for urban coastal flood prediction in Newport Beach, California. Spatially-distributed significant wave height values were obtained from the wave model, which were then used in static and hydrodynamic wave overtopping flood modelling. They used a grid resolution of 28 m x 22 m for the wave model, and applied measured deep water spectral data as boundary condition 10 km offshore.

2.1.3 Flood Modelling

Coastal flooding is characterized by the inundation of inland areas not usually inundated due to raised sea levels. Flood waters are conveyed inland over the coastal terrain or via channels and drainage networks connected to the sea. Many different types of flood modelling methods are available, including conceptual routing models, empirical black-box models, and physically-based hydrodynamic models. In DANVA's 'Cookbook for Analysis of Climate Change Effects on Floods in Cities', a range of techniques for modelling flooding from the sea is presented (Figure 17). The different techniques range from simple terrain analysis using digital terrain models (DTMs) to advanced coupled 1D-2D hydrodynamic flood models, which are recommended for use depending on the application type (DANVA, 2007). In this study, as the focus is on coastal flood forecasting and warning, hydrodynamic modelling tools, which calculate spatially-distributed values of water depths and discharges, are mainly of interest.

The aim in flood modelling is to obtain accurate predictions of water levels from hydrologic (e.g. rainfall) and hydraulic (e.g. sea water levels) conditions. When the flood model is used for warning systems and run in real-time, another important consideration, besides accuracy, is calculation speed. Short computation times are one of the most important criteria for selecting models for real-time flood warning applications, wherein reliable information on flooding before as well as during events are to be continuously calculated.

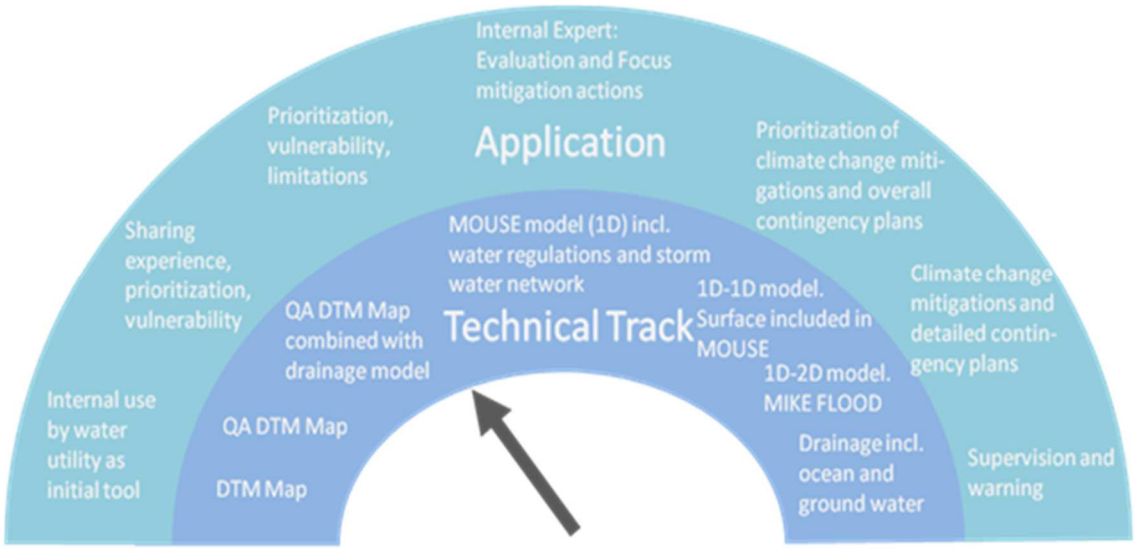

Figure 17 Modelling tools for coastal flood analysis. (Source: DANVA, 2007)

Empirical Flood Forecasting

Flood forecasting may be empirically-based, using past observations and experiences to estimate the occurrence of flooding (Henonin et al., 2013). Observations from past flood events are used to set threshold values for parameters, such as accumulated rainfall, sea levels, or upstream river stage, as indicative of flooding. In relation to the forecasting techniques discussed in the previous sections, 'empirical' flood forecasting, as described here, may be considered an implicit part of forecasting the 'drivers' (i.e. rainfall and water levels), and thus, there are simplified flood warning systems issuing warnings based only on rainfall forecasts. However, additional qualification and interpretation of these rainfall or water level forecasts are needed to determine their implications in terms of flooding in the area of interest, as in 'empirical' flood analysis.

Rainfall-runoff modelling has traditionally been much associated with flood forecasting, especially when flooding mechanisms are dominantly driven by runoff, as in fluvial flooding. It involves the calculation of catchment hydrologic response to precipitation (i.e. flow hydrographs) through the use of conceptual models approximating runoff mechanisms of catchments. Examples of conceptual runoff models are the unit hydrograph method, linear reservoir method, and time-area diagram method (Butler & Davies, 2011). Information on runoff volume (and timing) from rainfall-runoff models may be directly used in flood warning systems as flood indicators when values are compared against set thresholds (levels) that in the past have resulted in flooding (i.e. empirical flood forecast).

An example of a system employing an empirical flood forecasting method is the real-time online pluvial flood warning system in the Municipality of Hvidovre in Denmark. As described in Jensen & Pedersen (2009), this system, which uses radar rainfall data, employs radar nowcasting and a simple hydrological book-keeping model that calculates accumulated catchment rainfall depths that are compared to critical levels. Warnings by SMS and email are issued if critical levels are exceeded within the forecast period.

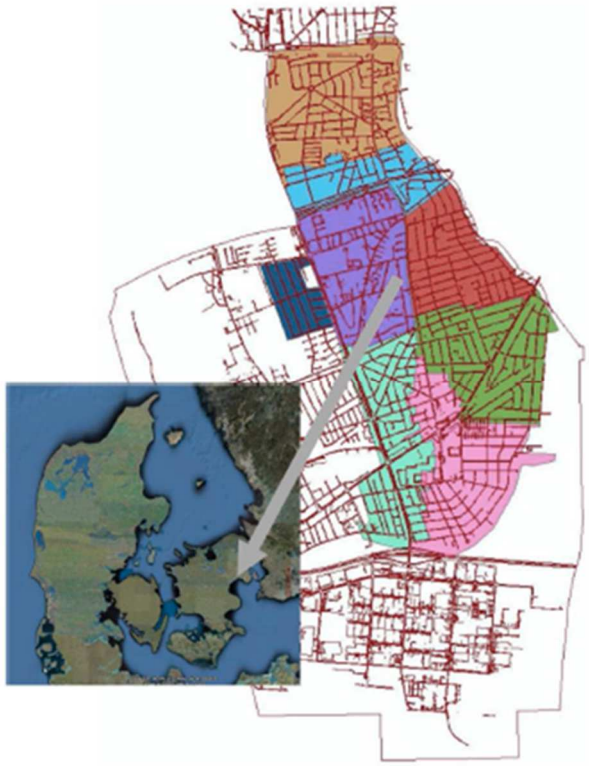

Figure 18 Map showing the location of Hvidovre Municipality in Denmark (55°39′26.45 N, 12°28′23.18 E) and a close up of the 22 urban catchments used in the pluvial flood warning system. (Source: Jensen & Pedersen, 2009)

Results from the rainfall-runoff modelling may also be used as further input to hydrodynamic models, such as network models or surface flow models, for more accurate simulation of flood depths, discharge and propagation. These types of flood models are discussed in succeeding sections.

Flood Modelling Based on Terrain Analysis

In this method, flood inundation is calculated by comparing boundary condition/'driver' water levels (e.g. sea level, river stage) against terrain levels; and areas where the terrain is below the water level are considered inundated. Using digital terrain models (DTMs) with spatially distributed ground surface elevation information allows not only estimation of whether flooding will occur or not but also derivation of 'flood' maps that show areal extents and depths for estimated flooding, which may be used for dissemination of warnings in the forecast system (see Figure 20).

For coastal flooding applications, maximum sea level estimates may be used as 'boundary conditions' to estimate inland flooding (see Figure 19). The method assumes that all surfaces are completely impermeable, and all areas below the sea level boundary will be flooded, even local inland depressions surrounded by high terrain (see left figure in Figure 20). The technique may also be modified by re-classifying these inland depressions as non-flooded areas (see right figure in Figure 20).

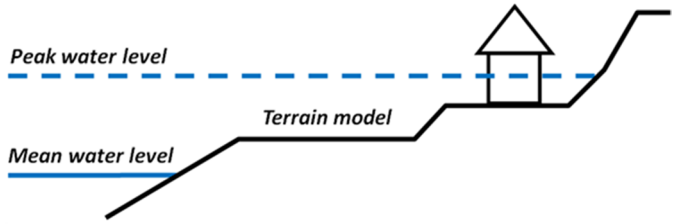

Figure 19 Illustration of terrain analysis method for coastal flood modelling. Terrain model elevations are subtracted from (peak) sea water levels (dashed lines) to calculate overland flood depths.

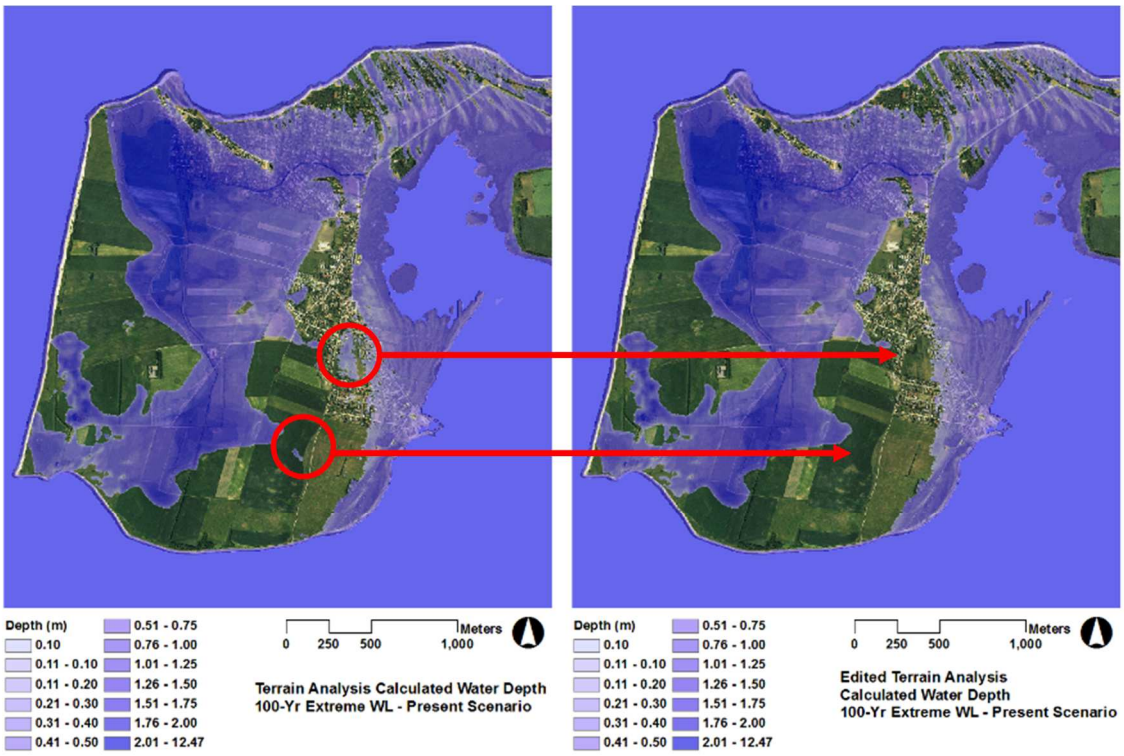

Figure 20 Example maps showing calculated coastal flooding through terrain analysis. Inland depressions surrounded by elevated terrain (in red outlines) may be re-processed as non-flooded areas in a modified version of the terrain analysis method (right).

1D Flood Modelling

This method uses the basic one-dimensional free surface flow equations (Saint Venant equations) to simulate flows in drainage networks, such as sewers and rivers. The use of 1D models for flood forecasting is discussed in this report despite its limited direct use in coastal flooding applications because it is relevant for pluvial and fluvial flooding analyses, which are also of interest in the study. In addition, when used in combination with other techniques, such as terrain analysis or GIS mapping, 1D modelling may be used to obtain spatially distributed results that are applicable for e.g. coastal flooding analyses, and provides a computationally fast and more physically-based method for flood simulation.

Various 1D modelling software tools are available for modelling urban drainage and river networks. It is not applicable for modelling storm surges, but a 1D flood model might be used in conjunction with a 2D flood model of the storm surge. However, 1D models are unable to accurately simulate

network surcharge conditions, wherein overflows from the network to the terrain/floodplain occur at, for example, sewer manholes or over river banks. 1D models, therefore, indicate if and where along the network surcharge conditions (and potential flooding) occur, but cannot accurately simulate flooding. Use of these models for inland flood estimation requires the use of GIS mapping to project calculated head levels along the network onto adjacent floodplains or inland areas. Flood level estimates using this technique are therefore not based on realistic physics-based simulation of the surcharge, and normally leads to overestimation of flood depths (Vojinovic & Tutulic, 2009; Mark et al., 2004; Maksimovic & Prodanovic, 2001). Vojinovic & Tutulic (2009) evaluated the use of 1D models against coupled 1D2D models for urban flood prediction. It was found that using 1D models in steep areas with irregular terrain, flow prediction along channels are realistic, but projection of 1D model results onto a 2D map for flood estimation uses assumptions that introduce large inaccuracies and produce misleading results, which, to avoid, require careful consideration of the topography and corresponding modification of the mapping technique.

Figure 21 The 'Hidromet' system application in La Laguna, Canary Islands. The left panels show time series for sensor parameters. Horizontal colour lines show user-defined threshold levels for the given sensor. The right panel shows the sewer network with critical points shown as dots. (Source: Rodriguez et al., 2014)

In the 'Hidromet' flood early warning system by Rodriguez et al. (2014), a 1D hydrodynamic model, which could be an EPA-SWMM, MOUSE, or HEC-HMS model, is placed in the cloud, and is used to simulate sewer and river network flows using observed and forecasted rainfall data (from radar and rain gauge observations and radar nowcasting). The model is run with updated data whenever available, and simulates flows and water levels throughout the sewer network. 'Hidromet' issues flood warnings based on simulated parameters and user-defined thresholds, and does not use GIS mapping and projection techniques to derive spatially distributed flood maps (Figure 21). Thus, the 'Hidromet' system currently uses the 1D network model in a more 'empirical' way of flood forecasting and avoids the inaccuracies introduced by the projection of 1D results onto 2D flood maps. Tests with a 1D-2D flood model using Infoworks ICM are also being conducted under the PEARL Project.

2D Flood Modelling

Two-dimensional (2D) models are based on computations with the 2D incompressible depth-averaged Navier-Stokes equations. Complex terrain, such as in highly built-up urban areas, may

be accurately described with 2D models. The spatial discretization, which also describes the surface topography, is an important component of 2D models. It must describe surface features in sufficient detail as well as allow proper computation and description of depths and flow variations within the model domain. Spatial and computational discretization may be in regular grids or meshes of non-overlapping elements/cells (Figure 22). They compute spatially-distributed and time varying flow and water level values over the whole model domain, and flood maps are showing maximum flood extents, as well as time-varying surface flow, velocity and level variations, may be easily derived from 2D model results.

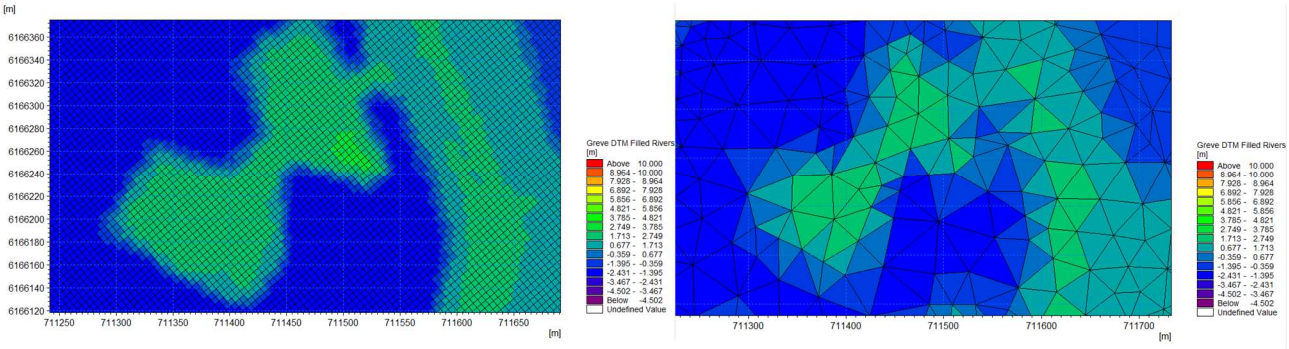

Figure 22 Topography and computational grids for 2D surface flow models may be a regular grid of cells (left) or a mesh of (triangular or quadrangular) elements (right). The figures show the terrain for the same area with grid cells (left) and with an element mesh (right).

Cell Grid Model. 2D models using Cartesian cell grids can simulate flooding with high resolution and reliability (Schmitt et al., 2004; Sto. Domingo et al., 2010; Henonin et al., 2013; Leitão et al., 2013). However, these models are computationally expensive and are often too slow to run real-time simulations (Vojinovic & Tutulic, 2009; Chen et al., 2012, Yu & Lane, 2006). Increasing grid resolutions (i.e. smaller cells) for detailed description of the terrain causes corresponding significant increase in total number of computational points and computation time for the model since a uniform cell size is used in the whole domain. Grid sizes of around 1 to 5 meters are usually recommended for urban areas for the topography to reflect major surface features such as roadways and buildings (Prodanovic et al., 1998; Mark et al., 2004).

Element Mesh Model. The use of element meshes can reduce computation times for 2D hydrodynamic models in comparison with conventional Cartesian models without compromising numerical accuracy (Sleigh et al., 1998, Namin et al., 2004). The mesh is usually comprised of triangular and quadrangular elements that may be of different sizes, which helps optimize model accuracy and computation times. This is a major advantage in using flexible meshes, as the mesh may be locally refined in specified regions according to users' needs allowing description of highly complex terrain surfaces (Walters et al., 2009; Danilov, 2013; Liu et al., 2013). Areas that require finer computational grid resolutions, such as built-up areas with various structures characterizing the terrain, may be represented by smaller elements, while other areas with more uniform terrain, may be represented by bigger elements (see Figure 23). Thus, meshes are also very suitable for modelling coastal areas as they can easily represent irregular coastlines (Shen et al. 2006). In addition to the computation time improvements afforded by element meshes, parallel computing techniques, such as Graphical Processing Unit (GPU), further improve the computational efficiency of 2D flood models (Hankin et al., 2008; Neal et al., 2010; Kalyanapu et al., 2011; Ghimire et al., 2013; Smith et al., 2014), allowing their use in flood warning applications.

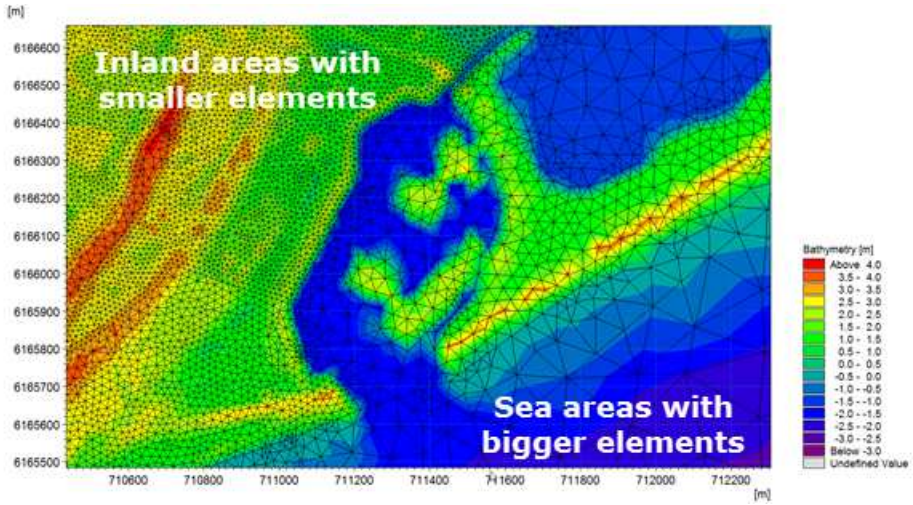

Figure 23 An element mesh is used for a 2D model of a coastal area. Smaller-sized elements are used for the built-up inland areas, and bigger elements are used for the sea areas (in blue).

In the Hamburg Case Study (see Chapter 3.1), 2D flood modelling was performed using Telemac-2D. Telemac-2D, developed by the LNHE *(Laboratoire National d'Hydraulique et Environment of the Electrité de France)*, is applied to model unsteady flow processes and transport processes in free surface waters (Telemac, 2014). Modelling the failure of protection works is important to assess risks in coastal and estuarial areas. Telemac-2D can integrate dike breaches and dike breach development, as well as the failure of similar protection works, in the calculation of potential and real inundation areas behind protection structures. It is possible to specify the timing of the breaching process or the process of dike breach development (supercritical flow). Figure 24 and Figure 25 show results of such a dike breach scenario as a consequence of a storm surge event. Figure 24 shows the location of the dike breach, while Figure 25 shows results of a dike breach simulation, wherein inundation areas and flow vectors are shown at different times during the breaching process.

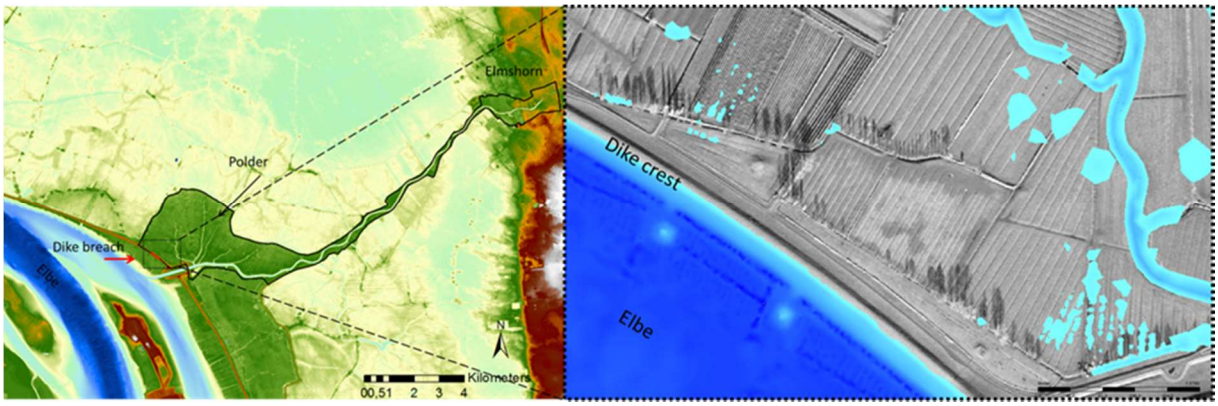

Figure 24 Location of the dike breach.

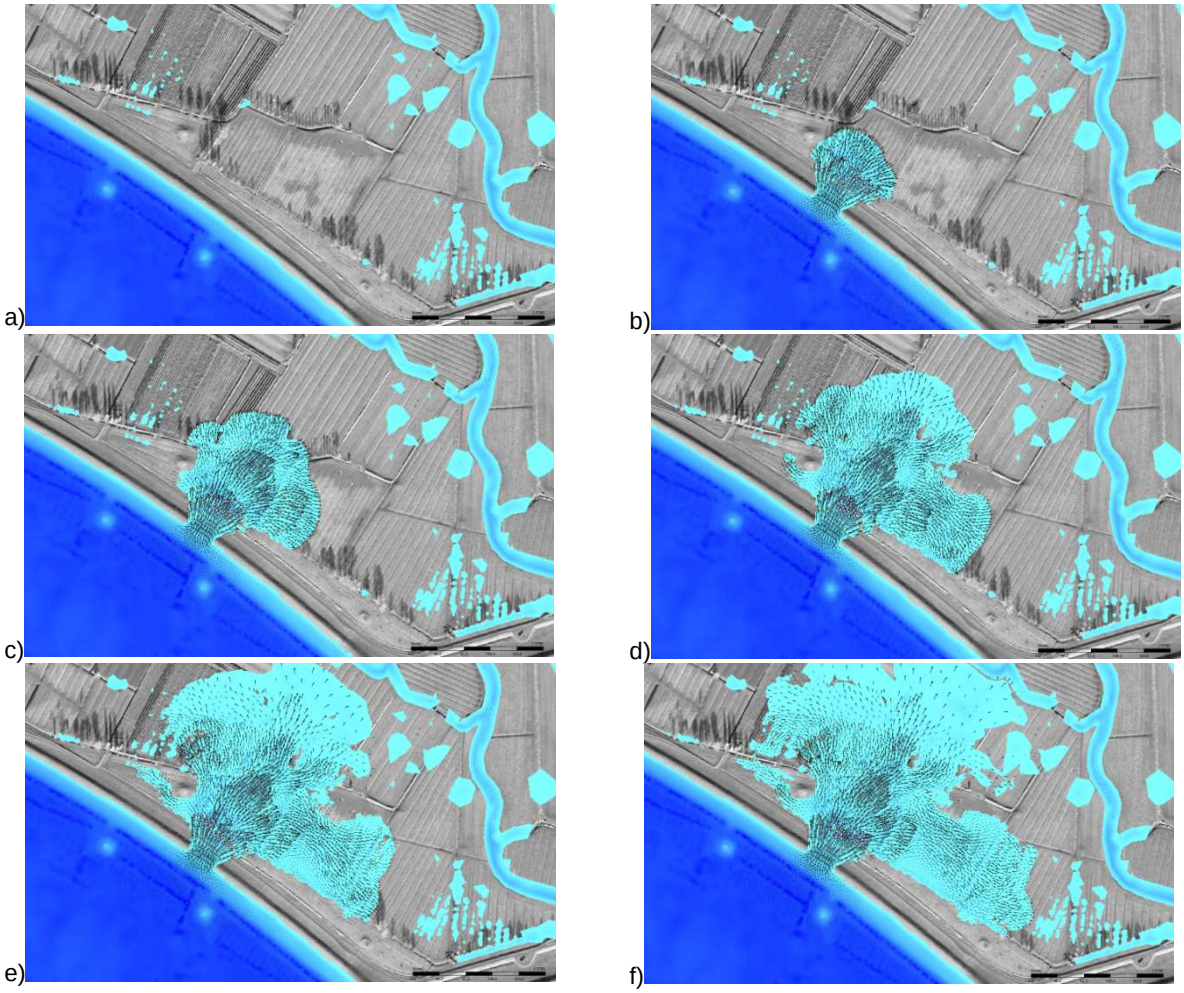

Figure 25 Results of the dike breach scenario in the form of inundated area and flow vectors.

For coastal flooding applications (i.e. flooding from the sea), flows between the sea and inland areas are normally simulated by applying sea level and flux conditions at sea boundaries of the 2D model. Runoff processes may also be approximated with 2D hydrodynamic models, as inputs (e.g. rainfall) as well as losses (e.g. evaporation) may be applied to each grid element. Underground sewers and pipes are not represented in 2D models. But if required, the presence of sewers may be approximated through the application of sewer system losses to the rainfall input. Thus, 2D flood models are most relevant for urban coastal flood applications where the sewer network is not a significant factor in the flood process, or when sewer network data are missing preventing the use of coupled 1D-2D flood models discussed in the succeeding section.

1D-2D Flood Modelling

This technique dynamically links a 2D surface model to a 1D model of the drainage network for flood simulation. It is widely used in urban flood analysis (Schmitt et al. 2004; Carr & Smith, 2006; Mark & Djordjevic, 2006; Henonin et al., 2013) and is also highly suited for urban coastal flooding applications (Sto. Domingo et al., 2010). Flows and water levels along drainage networks and over the land surface, and the flow interactions between the two systems are simulated with 1D-2D models. In this approach, the areal topography is represented in the 2D model, which simulates water levels and flows over the surface with the 2D shallow water equations. The drainage system is represented by the 1D model, which simulates flows through the network using equations of flow in one dimension. The two systems are linked at network structures, such as manholes (nodes),

and coinciding grid cells, and flow exchanges are determined according to computed head differences (i.e. using the weir or orifice equations) between the two.

Coupled 1D-2D models consider the role of underground sewers or channels in conveying water from the sea to inland areas. This is an improvement over 2D models for coastal flood modelling, especially when the urban coast is flat and low-lying and have drainage networks connected to the sea (e.g. at sewer or river outlets). These connections may convey water through channels or underground pipes, causing surcharge in low-lying areas further inland (Figure 26).

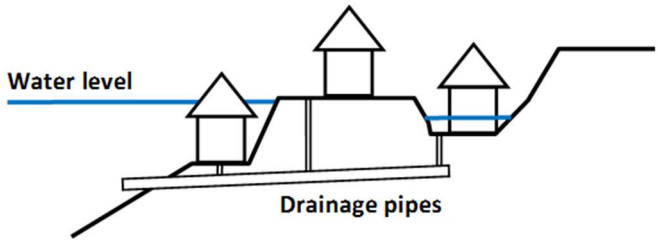

Figure 26 Illustration of how drainage networks may convey flooding from the sea further inland.

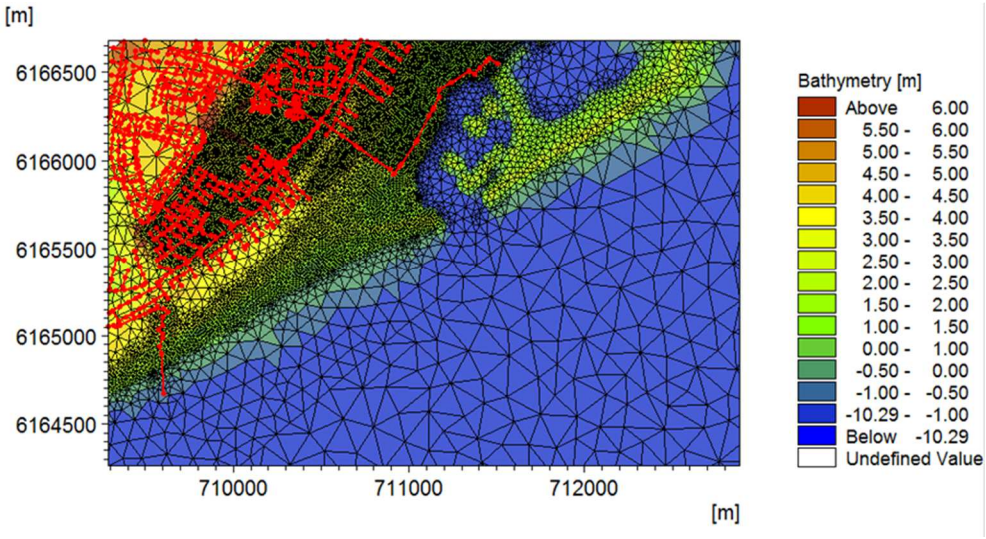

Figure 27 An example of a 1D-2D urban coastal flood model linking a 1D drainage network model (red lines and points) and a 2D flow model using mesh elements (element outlines in black). Finer elements are used to describe inland areas to the north-west, while sea areas to the south-east are described by larger elements.

Similar to 2D models, 1D-2D models are computationally expensive, mainly due to the large number of computation points in the 2D component. This limits their practicality for real-time applications (Leandro et al., 2009), but various techniques are now available for improving their computational efficiency—usually focusing on the 2D model efficiency. These approaches include the use of multiple-resolution grids, such as the 'Multi-cell Overland Solver' technique described in Hartnack et al. (2009), which combines coarse and fine grids for computations and result presentation. Also, as described in the previous section, the use of mesh elements instead of Cartesian grids for the 2D model (Figure 27) significantly improves the computational efficiency of the flood model (Berbel Roman, 2014). Moreover, there are strategies involving parallel processing and hardware modifications, such as the use of Graphics Processing Units (GPUs) instead of

Central Processing Units (CPUs) for model computations, affording further shortening in computation times.

A summary of the different techniques for coastal flood modelling that have been discussed is shown in Table 1. Each is evaluated with respect to real-time modelling considerations.

Table 1 Summary of coastal fluvial and pluvial flood modelling methods and their potential for real-time forecasting applications. (Source: Based on Henonin et al. (2013) and Berbel Roman (2014))

Real-time Model Criteria	Empirical, Conceptual	GIS	1D	2D	1D-2D
Data requirements	Low to moderate	Low	Moderate to high	Moderate	High
	Historical hydrologic and flood conditions	Topography	Drainage network	Topography	Drainage network, Topography
Computation time (actual/computation)	N/A	N/A	57	1.18 (Cartesian)* 4.43 (Flexible Mesh)*	3.48 (Flexible Mesh 2D)*
Flood computation	Calculated indicative flood parameters	Estimated maximum depths and extents	Calculated surcharge points and flood depth estimates	Calculated flood depths, extents, velocities	Calculated flood depths, extents, velocities
Flood map accuracy	Low	Low	Low to moderate	Moderate to high	High

*****Source: Berbel Roman, 2014)

2.2 Flood Hazard Mapping

Hazards are physical events, phenomena or human activities that may cause loss of life or injury, or economic, social or environmental damages (UNISDR, 2007). Flood hazard maps provide information on likelihood and magnitude of flood events (de Moel et al, 2009), which could be of fluvial, flash flood, urban pluvial, or coastal flooding types. The maps normally show spatial data on flood parameters, such as extent, depth, and velocity. But also, as the maps should be easy to understand, both for technical as well as non-technical users, the contents may be customized according to user-specific requirements. A 'Handbook on good practices for flood mapping in Europe' has been published by EXCIMAP (2007). It suggests ways of presenting flood-related information on maps (Van Alphen et al., 2009), and could be consulted for ideas regarding standard map scales, content layer presentation, and other cartographic details.

Flood maps are useful tools for understanding flood occurrence in an area. They are important components of early warning systems providing spatial hazard visualization crucial for decision-support, reduction of damages and risk, civil protection, and information dissemination (Alfieri et al., 2012). In Europe, flood mapping has been required of EU Member States through the EU Floods Directive (Directive 2007/60/EC) (EU, 2007). Enforced in October 2007, it provides a framework for the assessment and management of flood risks, and requires, among other things, that flood mapping is performed for water course and coastal areas at risk.

Flood hazard mapping involves flood assessment and subsequent geospatial mapping of results. There are different approaches to flood mapping, combining statistics, meteorology, hydrology, hydraulics and geography (Jha et al., 2012). Hazard mapping involves flood estimation, which could employ simple terrain analysis methods, or data-driven/empirical, conceptual, or hydrodynamic modelling. Flood estimates are then combined with topographic, infrastructure, and other geospatial data using Geographic Information Systems (GIS) tools for map creation.

For coastal flooding applications, state-of-the-art mapping techniques involve assessment methods similar to those presented in Chapter 2.1.3 for flood forecasting. These techniques are discussed further with respect to mapping (i.e. geospatial presentation of flood data) in succeeding sections.

2.2.1 *Terrain analysis*

The Terrain Analysis method, also called 'raster-based' method (Gallien et al., 2014), assumes that all inland areas below a certain level, such as an estimated maximum sea level, are going to be inundated, and are shown on the coastal flood map as such. It uses a digital terrain model (DTM), which contains spatially-distributed terrain elevation data throughout the model domain (also see Chapter 2.1.3). Thus, flood maps obtained with this technique show spatially-distributed but static flooding information—showing flood extents, and providing flood depth values at all points within the domain, but not giving information on flow velocities or directions. An example of a coastal flood map generated using the Terrain Analysis method is shown in Figure 28.

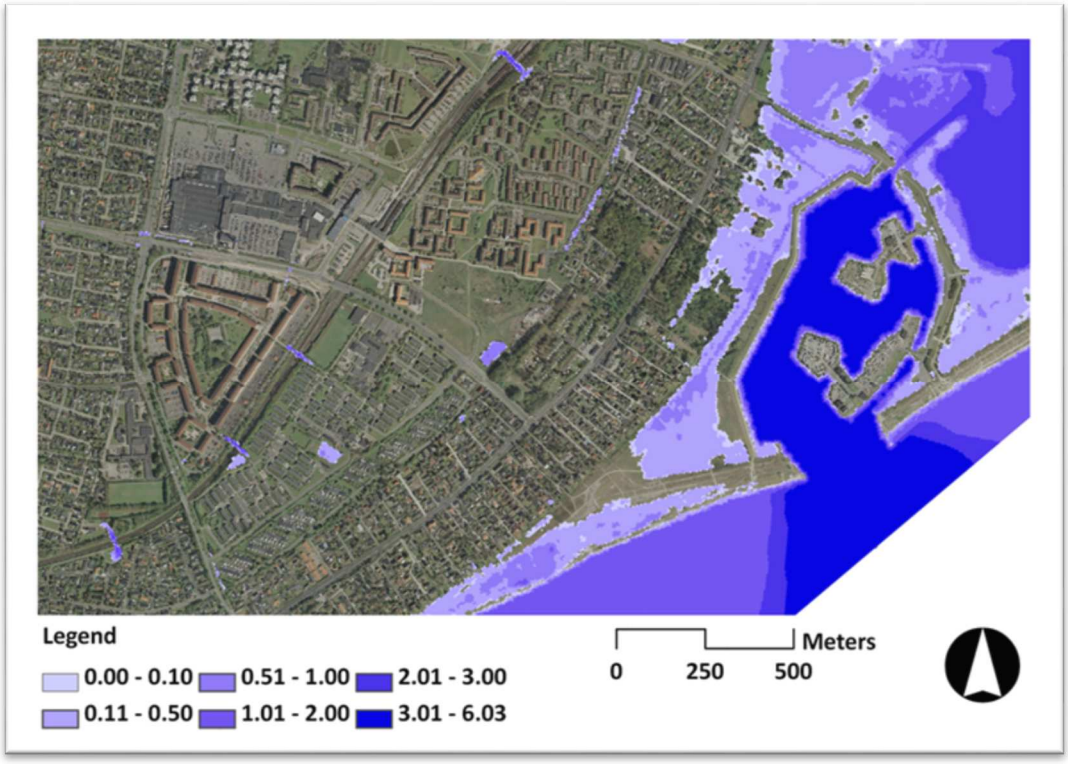

Figure 28 Example flood map for a coastal area obtained using Terrain Analysis Method. Inland areas behind elevated terrain are inundated as flow paths to all low-elevation areas from the sea are assumed to exist.

Modified Terrain Analysis Mapping

The Terrain Analysis method assumes that flow paths exist between low-elevation areas (see Figure 28 and Figure 29), but this may not always be the case. A modified Terrain Analysis technique may then be applied, wherein inundation only occurs when overland flow paths exist according to the DTM, and flooding could be hindered by embankments or high-elevation areas.

Flooding is overestimated with Terrain Analysis (Berbel Roman, 2014; Gallien et al., 2014; Sto. Domingo, et al., 2010) as it assumes the event has a long enough duration to cause uniform flood levels, and that maximum depths are reached instantaneously in all inundated areas. Nevertheless, the method is quick and straightforward to implement with low data requirements. It

provides a fast overview of potential flood risk areas, and is thus useful for initial flood risk assessment.

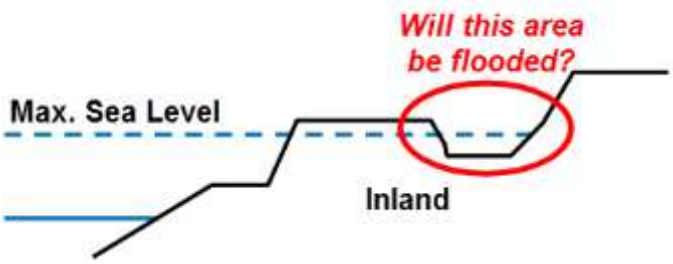

Figure 29 Flow paths are assumed to exist for the Terrain Analysis method.

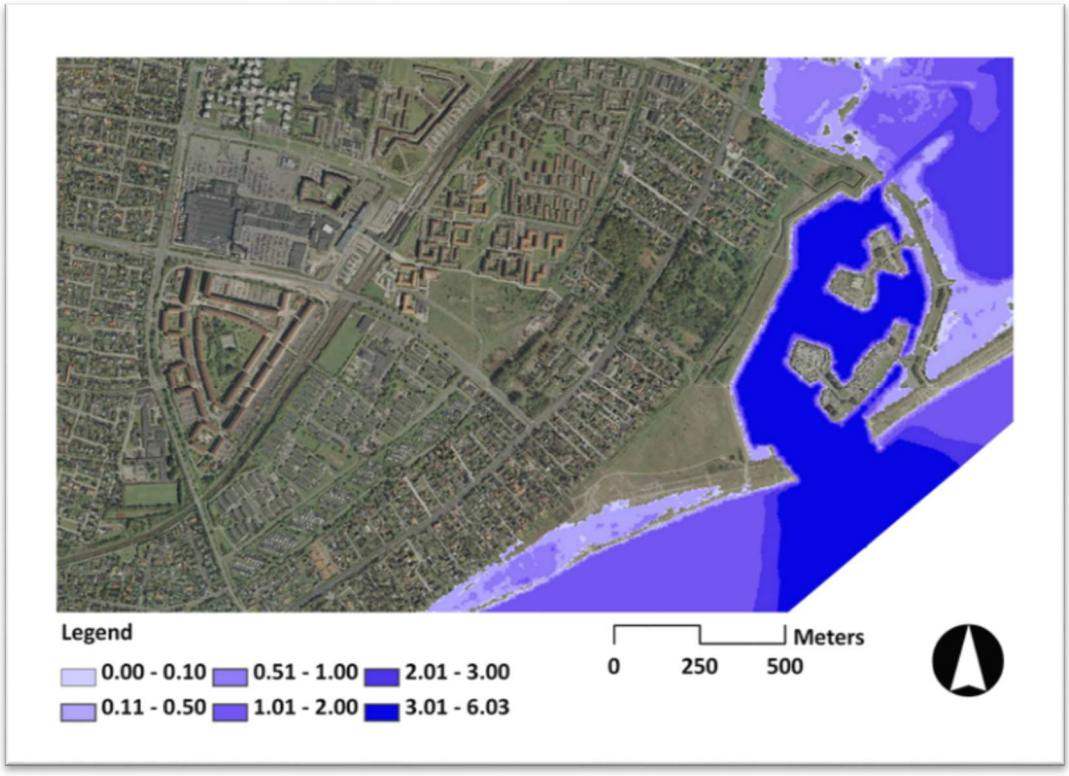

Figure 30 Flood map for the same coastal area shown in Figure 28 using Modified Terrain Analysis method. Inland areas behind elevated terrain are not inundated.

2.2.2 Hydrodynamic modelling

Flood maps obtained from hydrodynamic modelling have stronger scientific basis compared to terrain analysis methods. They simulate flooding using physics-based equations. Gallien et al. (2014), in their comparison of flood forecasts using hydrodynamic and raster-based models in Newport Beach, California, found that hydrodynamic model predictions had good agreement with measurements, while the raster-based model substantially overestimated flooding.

For mapping purposes, hydrodynamic modelling that can simulate (at least) 2D surface flows (e.g. 2D, 1D-2D or 3D models) are most relevant, since spatially-distributed information is ideal for flood

mapping. Results from 1D network models may be post-processed with GIS tools to project flood level results onto the DTM and obtain spatially-distributed values for mapping. But this flood projection method is a mere approximation of overtopping, and similar to the Terrain Analysis method, may overestimate flooding.

2D Model Mapping

Two-dimensional (2D) hydrodynamic models are widely used for overland flow modelling, and the Environment Agency (2010) has made a study of the method and reviewed and evaluated various available 2D modelling packages in terms of performance and predictive capability. These models are based on computations with the incompressible depth-averaged Navier-Stokes equations in 2 directions. They compute spatially-distributed and time varying flow and water levels over the entire model domain. Flood maps showing maximum flood extents, as well as time-varying surface flow, velocity and levels, may be easily derived from 2D model results (Figure 31).

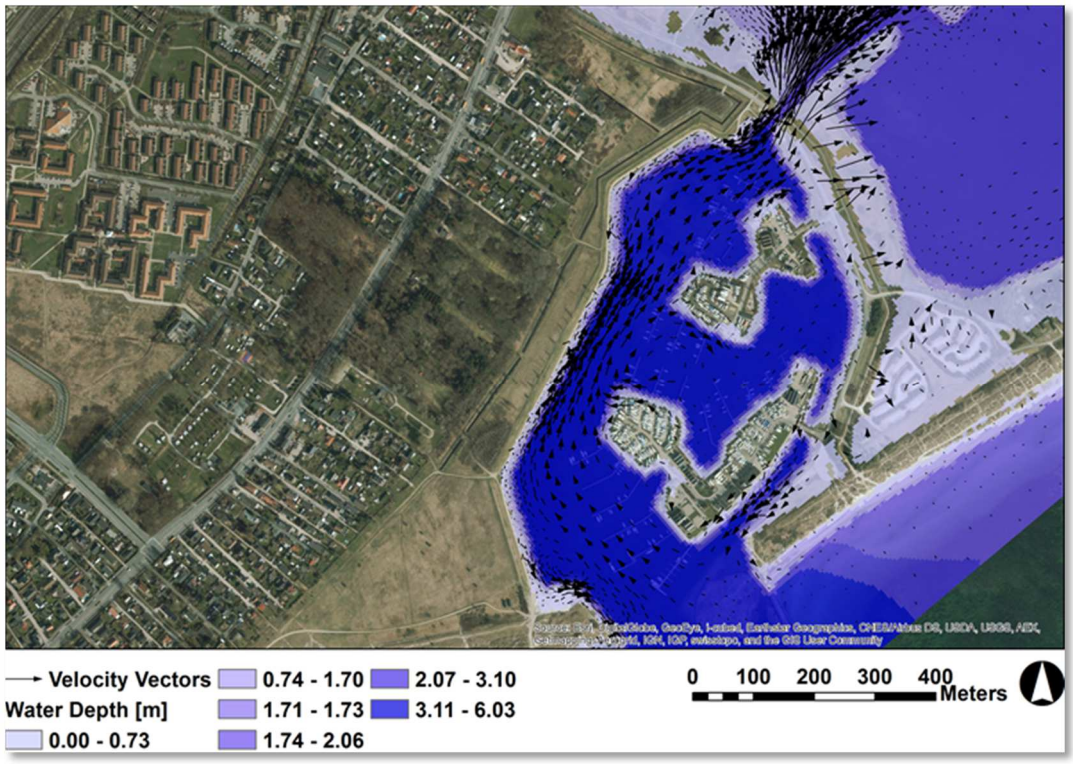

Figure 31 Example flood map for a coastal area obtained using 2D surface flow modelling. Besides water depth information (blue fill), velocities and flow directions (at a particular point in time) may also be obtained from 2D model results and plotted on a map (black arrows).

Two-dimensional models, however, do not simulate underground drainage networks in coastal flooding. In highly built-up coastal areas with dense sewer networks well-connected to the sea, the role of the drainage network in conveying potential flooding from the sea further inland may be significant. The use of 2D models to map flooding in these areas may overestimate flooding if potential storage in the underground network is neglected, or it may underestimate flooding inland where flooding from the sea may be conveyed through underground pipes.

1D-2D Model Mapping

This assessment method uses a 2D surface model dynamically linked to a 1D network model to simulate flooding. Flows over the terrain surface are simulated with the 2D model, which calculates

water levels and flows overland, while the 1D model represents the drainage network, and simulates flows and water levels in the network. The two systems are linked at structures where flow exchange between the two systems may occur. Coupled 1D-2D models consider the role of drainage networks in conveying flooding from the sea further inland. This is an improvement over 2D models for coastal flood modelling, especially in low-lying urban coasts with drainage networks that are well-connected to the sea.

Flood information obtained from 1D-2D model results include spatially-distributed and time-varying flows and levels over the 2D model domain, as well as throughout the 1D drainage network. Maximum flood extent information, as well as time-varying values for surface flows, velocities and water depths, may be easily obtained from 2D model results. In addition, flows and water levels in the drainage network may also be obtained from 1D model results and plotted as time series graphs.

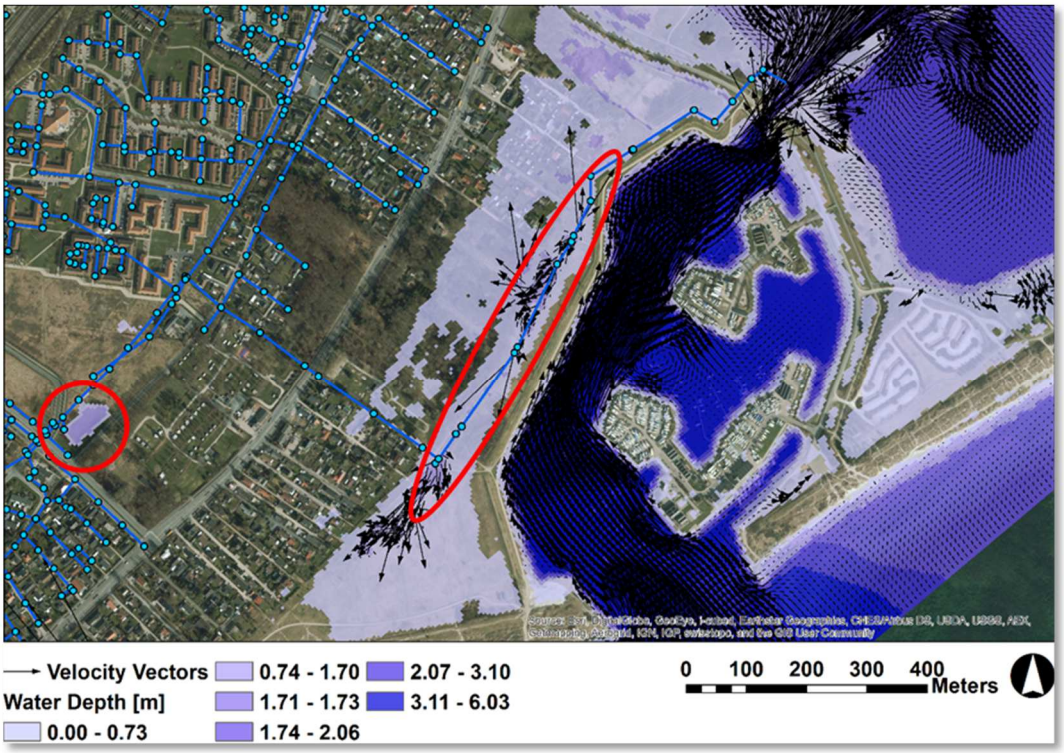

Figure 32 Example flood map for a coastal area obtained using a 1D-2D model showing flood depths and velocity vectors. The urban drainage network (blue lines) may bring water from the sea further inland, even in areas behind dikes (e.g. encircled areas).

Table 2 below summarizes the various types of information obtained from the different flood mapping methods that have been discussed. The advantages of methods employing 2D hydrodynamic modelling, such as 2D or 1D-2D modelling, are apparent, especially with respect to the accuracy and number of spatially-distributed flood information that can be obtained and easily used for mapping.

Table 2 Summary of result types obtained from various flood hazard mapping techniques previously discussed.

	Terrain Analysis	2D Model	1D-2D Model
Flood map accuracy	Low	Moderate to high	High

	Terrain Analysis	2D Model	1D-2D Model
Spatially-distributed results	Yes	Yes	Yes
Time-varying results	-	Yes	Yes
Model results:			
Flood extents	Yes	Yes	Yes
Surface water levels	Yes	Yes	Yes
Surface velocities	-	Yes	Yes
Drainage network water levels	-	-	Yes
Drainage network velocities	-	-	Yes

2D Computational Grids. The type and resolution of the 2D model computational grid influence the accuracy, as well as graphical quality, of the resulting flood map. The grid is used for discretizing the governing equations for numerical model computations, and it represents the topographical characteristics of the model domain. Thus, as highlighted in Chapter 2.1.3, it is crucial that the computational grid describes surface features in sufficient detail and allow for proper computation and description of depths and flow variations within the model domain. Computational grids may be Cartesian grids or meshes of non-overlapping elements/cells (Figure 22).

In Henonin et al. (2013), the impact of Cartesian grid size on the representation of surface features in 2D models was discussed and highlighted (see Figure 33). Using larger grid sizes dampens surficial relief features, but on the other hand, very fine resolutions cause longer computation times with the 2D model. A balance between model accuracy and computation time must be targeted in selecting computational grid sizes. For flood assessment and mapping in urban areas, the selected grid size should be able to represent important features that affect flow paths, such as roads, streets and buildings, and thus, grid sizes from 2-4 m are recommended (DANVA, 2007).

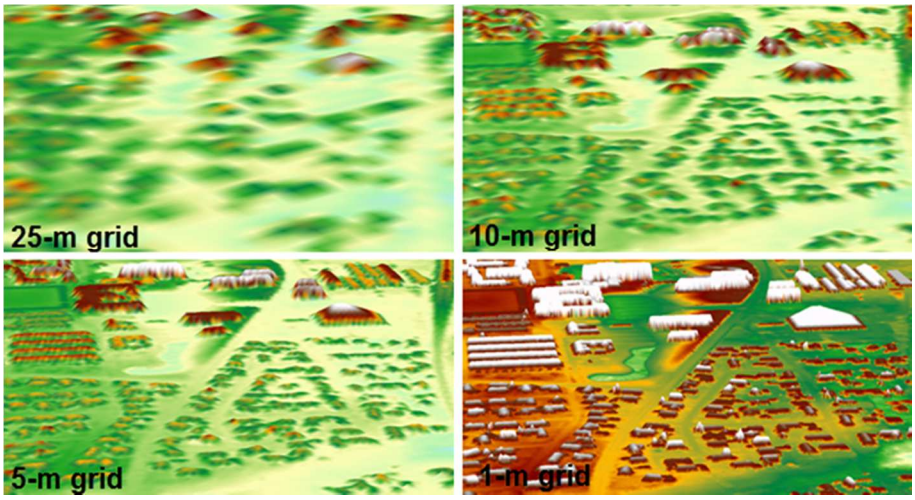

Figure 33 Illustration of how Cartesian grid resolution impacts the representation of terrain surface and structures in urban 2D models. (Source: Henonin et al., 2013)

Probabilistic Flood Mapping. The various flood mapping methods that have been presented were discussed with respect to a deterministic approach to flood mapping, wherein, e.g. well-delineated flood extents could be plotted for various flood events. However, various uncertainties exist in flood assessment, such as with the model structure, model parameters, and inputs. Thus, flood mapping may be improved by reflecting the certainty of flood estimates, especially as decision-makers referring to these maps have to consider the effect of uncertainties in making

decisions. In Di Baldassarre et al. (2010), a probabilistic flood map was developed for a river flood plain in the UK. An ‘uncertain flood extent map’, taking into account the uncertainty of model parameters, was generated, wherein a grid map with graded values between 0 and 1 was used to plot flood extents reflecting the likelihood of inundation at a point for the simulated flood event.

This type of mapping, which includes information on probability, may be a more correct representation of flood hazards. Thus, probabilistic flood mapping will be additionally explored in the course of the PEARL project. Mapping ‘best-practices’ for these ‘uncertain flood maps’ should be developed, as ultimately, these hazard maps should be easy to understand, both for technical as well as non-technical users, and they should present ‘uncertainty’ information in the most understandable manner.

3 Case Study Applications

Online coastal flood warning systems have been developed and implemented for several PEARL case study areas, such as Hamburg (Germany), Greve (Denmark) and Castries (Saint Lucia) (Figure 34). These systems are presented in this Chapter, and the use of each system of some of the modelling tools and techniques in Chapter 2 is discussed.

Figure 34 Map showing locations of PEARL case study areas with online coastal flood early warning systems that are presented in this Chapter.

3.1 Hamburg, Germany

The city of Hamburg and the Elbe River are located in the north of Germany (Figure 35). The Elbe has its source in the Czech Republic, flows through Germany and drains into the North Sea. On its way to the North Sea, the river flows through Hamburg, the second biggest City in Germany and one of the 16 German federal states. Hamburg is a comparatively densely populated metropolitan area with approx. 1.7 million inhabitants on an area of approx. 755 km². Within the Hamburg metropolitan area the port of Hamburg is located. The Port of Hamburg is the second biggest seaports in Europe.

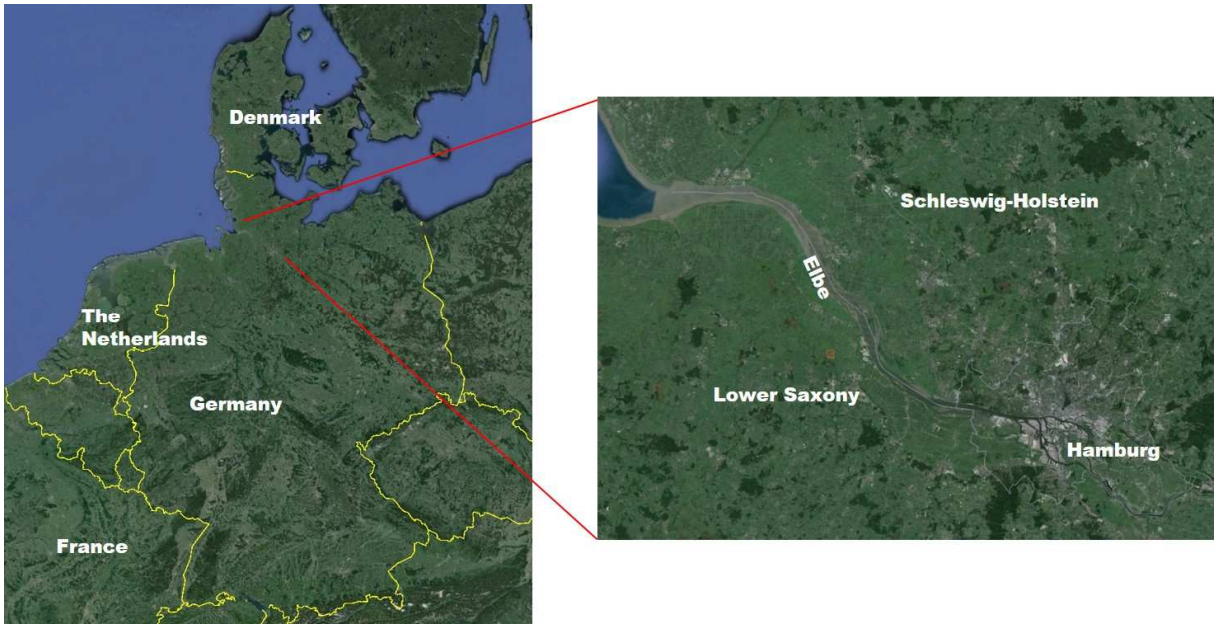

Figure 35 Overview of the location of the Elbe River and Hamburg.

The case study area (Figure 36) includes the tidal influenced section of the Elbe (tidal Elbe) between the weir in Geesthacht (Elbe km 586) and the navigational mark Kugelbake at Cuxhaven (Elbe km 728). This section is called Lower Elbe and has a length of 142 km. The Lower Elbe is generally divided into three sub-sections. The first and most upstream sub-section of the tidal Elbe includes the area in the so called Vier- und Marschlande between Geesthacht and Hamburg. Within the metropolitan area of Hamburg, the Elbe furcates into the Norderelbe and the Süderelbe forming the island of Wilhelmsburg as well as parts of the port of Hamburg – second section. At Elbe km 625, Norder- and Süderelbe re-unify and conflate. This is the start of the third sub-section of the Elbe so called Niederelbe, draining into the North Sea. In this third sub-section, the river morphology is characterized by several small river islands (e.g. Neßsand, Lühesand, Pagensand and Rhinplatte). Additionally, several tributaries (e.g. Krueckau, Pinnau, Este and Schwinge) drain into the Elbe in this third sub-section.

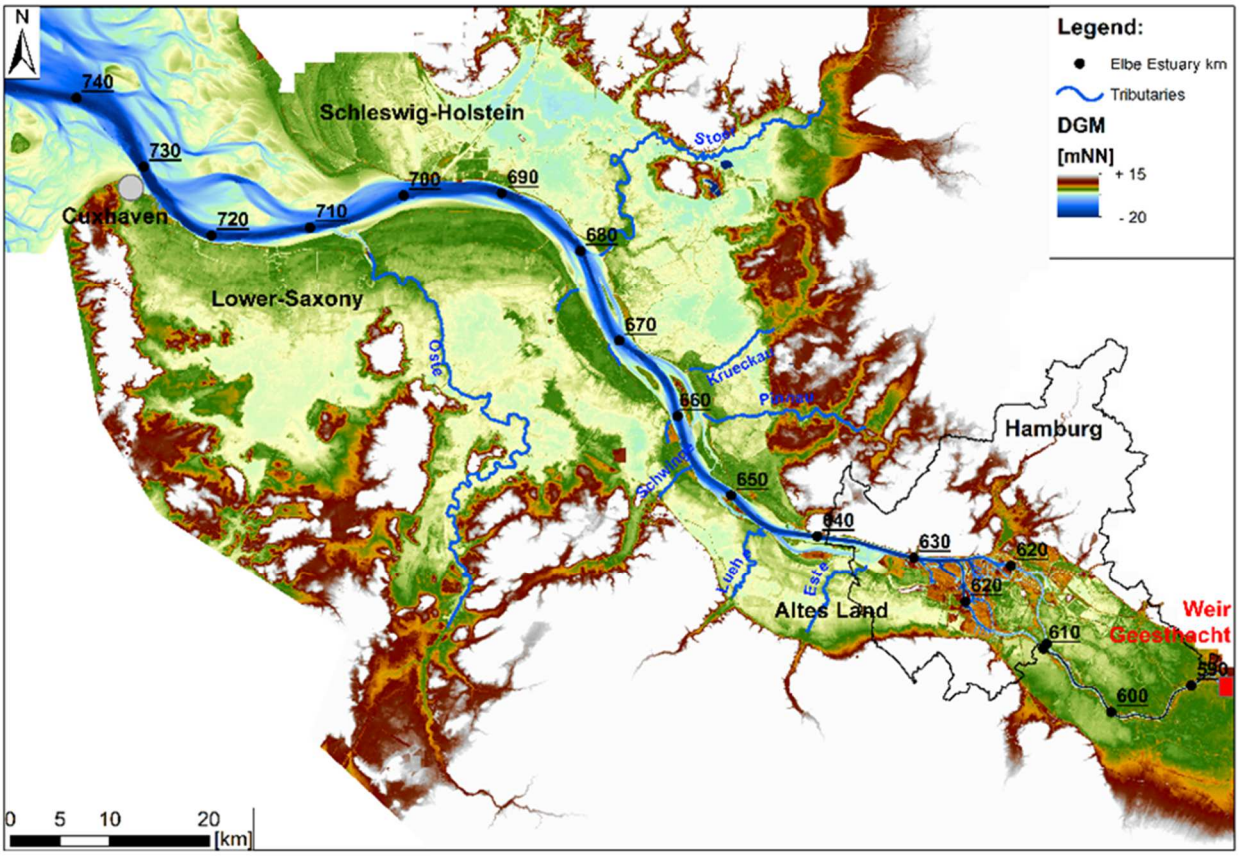

Figure 36 Overview of the Hamburg-Elbe estuary case study.

The actual protection level along the Elbe seems to allow more or less safe utilization of the flood prone protected areas. But, a residual risk of flooding is still existing, especially, if climate change induced effects are taken into consideration. It is expected that extreme storm surge events will occur more frequently and with a longer duration (IPCC, 2014) leading to higher hydrodynamic loads on the flood protection infrastructure. In addition, higher storm water levels have to be expected in the future.

As the flood prone Elbe estuary region and the flood prone metropolitan region of Hamburg are densely populated with a high utilization pressure, it is of crucial importance for the responsible authorities to have reliable forecasts of the water level along the Elbe, especially in the case of storm surges. Hence, an early warning systems based on real-time simulations has been developed within PEARL on the basis of the multi-regression gauge based forecast system developed and implemented by BSH, the German Federal Maritime and Hydrographic Agency. The so-called MOS-forecast system provides point-wise water level forecasts for up to 6 days for several locations (gauge stations) along the Elbe River. Since it is a point-wise forecasting system, no information about the spatial distribution and the spatial development of the water level along the river exists. This information together with flow velocities and wave information is necessary to assess the safety of the constructions and is consequently generated by the PEARL forecast approach as basis for the holistic risk assessment.

3.1.1 *Framework and methodology*

The early warning system for the Elbe estuary is based on the hydrodynamic model of the Elbe Estuary. The general aim is to calculate the actual status and a forecast over up to 3 days of the temporal and spatial development of the water level and respective currents along the Elbe estuary

and to detect potentially endangered sections of the flood protection infrastructure. Figure 37 shows the operational sequence of the early warning system.

The forecast of the water levels and currents in the Elbe estuary are based on a Model Output Statistics (MOS) approach applied to water levels, which has been developed for the Elbe estuary by BSH (German Federal Hydrographical Service) and is in daily operational use. MOS is a multiple regression approach. In this approach, predictands are related to one, two or more predictors. The most important predictors are: i) Surge observations at several points, ii) Model forecast results with meteorological input, iii) The output of the MOS System of BSH, iv) last observation of the predictand, v) wind components and others. Predictands are in general the surge levels for different time steps at 9 water level gauges (Müller-Navarra & Knüpfer, 2010).

In addition, results of a 2D barotropic model of the North Atlantic and a 3D baroclinic model of the North Sea and the Baltic Sea as well as results of a high resolution 3D model of the German bight and the Western Baltic Sea with an extension into the Lower (Tidal influenced) Elbe estuary are used. All models, except the barotropic model of the North Atlantic, are double-sided and simultaneous coupled models (Müller-Navarra & Bork, 2012).

Basically, the operational sequence of the early warning system consists of three threads. First of all, the water level data (MOS data) is downloaded from the external server of the BSH to the local database at TUHH (see Figure 37, blue thread). The downloaded water level data is obtained in a format that cannot directly be used and, hence, the data sets have to be converted and are then stored in a local database as continuous time series. The second thread covers the data pre-processing and the simulations (see Figure 37, green thread). The processed data from the local database are copied as boundary conditions to the numerical models. After the data transfer is finished, the simulations are started. The model results are stored into a database. For each successfully finished simulation (see Figure 37, yellow thread) the resulting water level is evaluated with respect to a critical predefined water levels in order to detect endangered sections of the flood protection infrastructure in the forecast area. The results of the evaluation are stored in an alert database. A scheduler manages the processes described above.

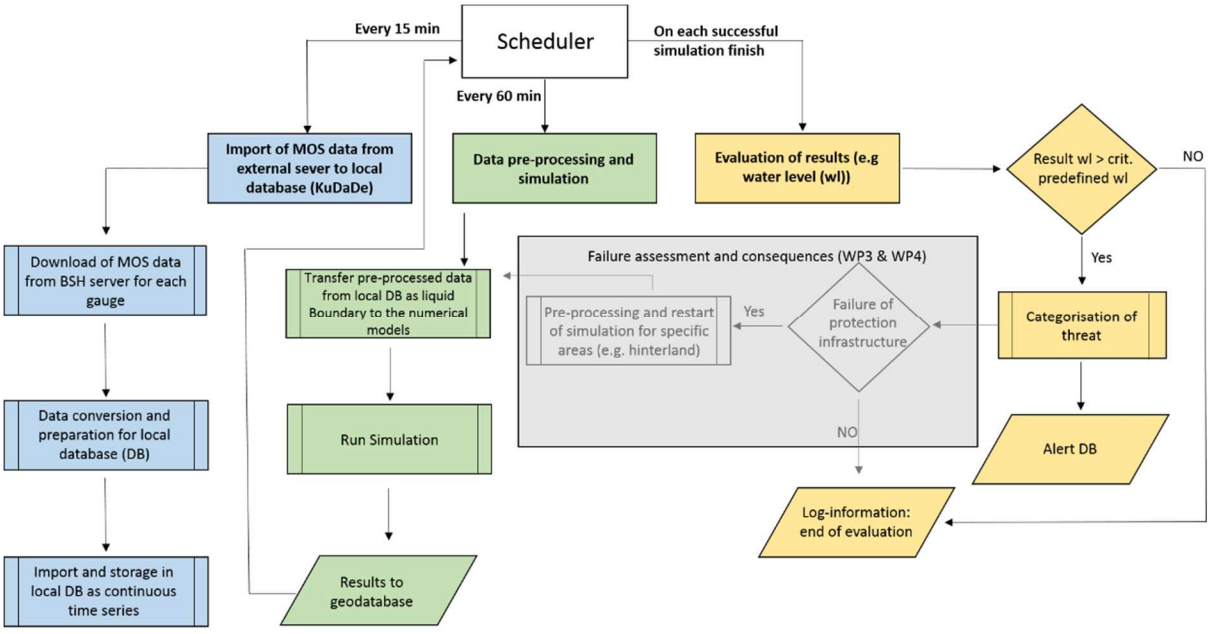

Figure 37 Flow chart of the early warning system for the Elbe estuary.

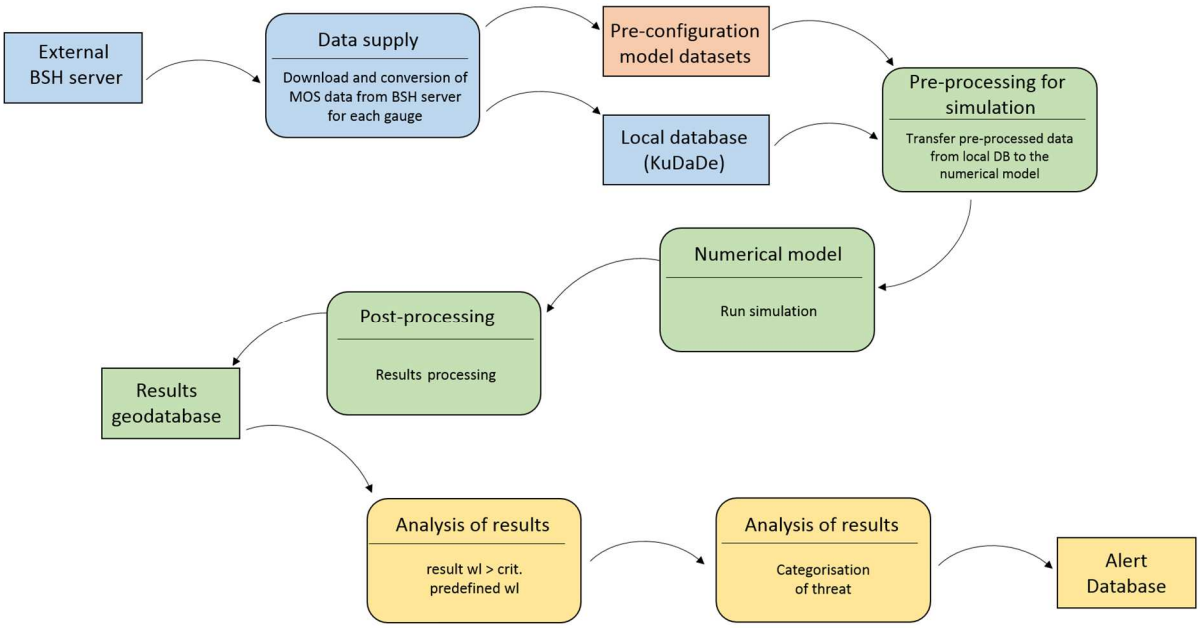

Figure 38 Data flow chart of the early warning system.

Data Acquisition and Data Conversion

As previously described the numerical model of the Elbe estuary uses water level data and discharges as boundary conditions for the open boundaries. The real-time forecasting and warning model for the Elbe Estuary is operated based on the MOS water level forecast data provided by the German Maritime and Hydrographic Agency (BSH). The basis for the derivation of the water level forecast is the operational forecast model of the BSH (MOS-model see above). Within the MOS-forecast, water levels are forecasted for 9 specific gauge locations:

- Cuxhaven
- Brunsbüttel
- Glückstadt
- Stadersand
- Brokdorf
- Schulau
- Hamburg St. Pauli
- Zollenspieker
- Geestacht

along the Elbe (see Figure 40) covering forecast periods of up to 6 days. An example forecast is shown in Figure 39. The MOS-forecasts are updated every 15 min.

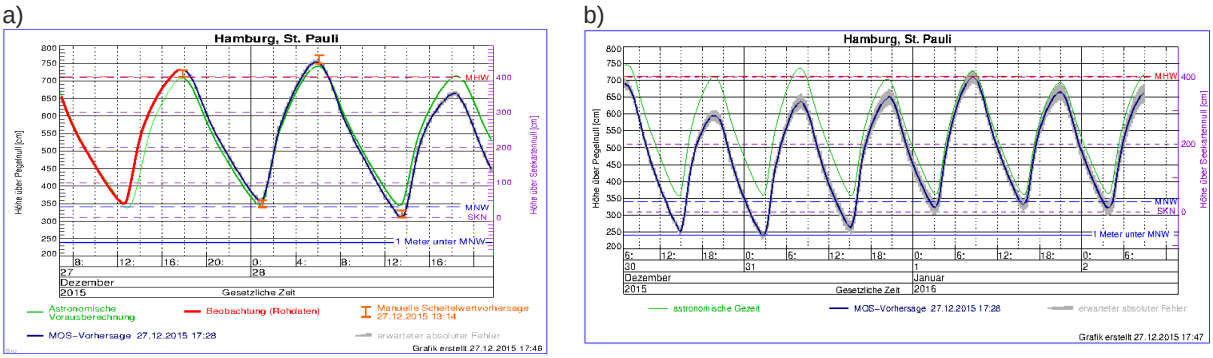

Figure 39 *Example of the water level forecasts of the BSH, a) 24 hours forecast, b) 6 days forecast.*

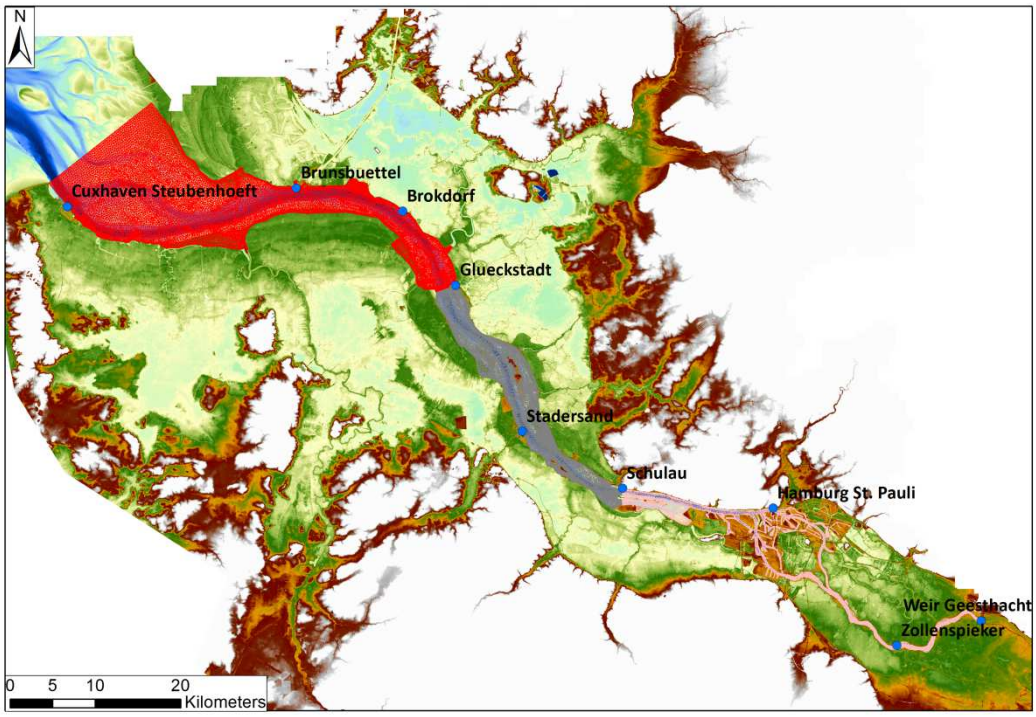

Figure 40 *Location of the water level forecast gauges along the Lower Elbe.*

For each gauge a zip-file containing a water level forecast for the next 3 days is downloaded automatically every 15 min from the external BSH server to the local server of TUHH (see Figure 37, blue thread. Figure 38, blue elements).

Each water level forecast file has a tabular structure (Figure 41) where all forecast relevant information are stored. For the purpose of an early warning system for the Lower Elbe the following information are used: (i) gauge (specified by numbers), (ii) valid forecast time, (iii) calculated astronomical tide and (iv) wind set-up (see Figure 41).

The data stored in the downloaded tables cannot be used directly for the model system and has therefore to be converted and pre-analysed for the assimilation into the early warning system. The forecasted water level has to be calculated by summation of the calculated astronomical tide and the forecasted wind set-up. The format of the timestamp has to be converted into the format of the

numerical model and the model input file has to be generated. The data is stored in a database and then used as a boundary condition in the numerical model (see Figure 37, blue thread).

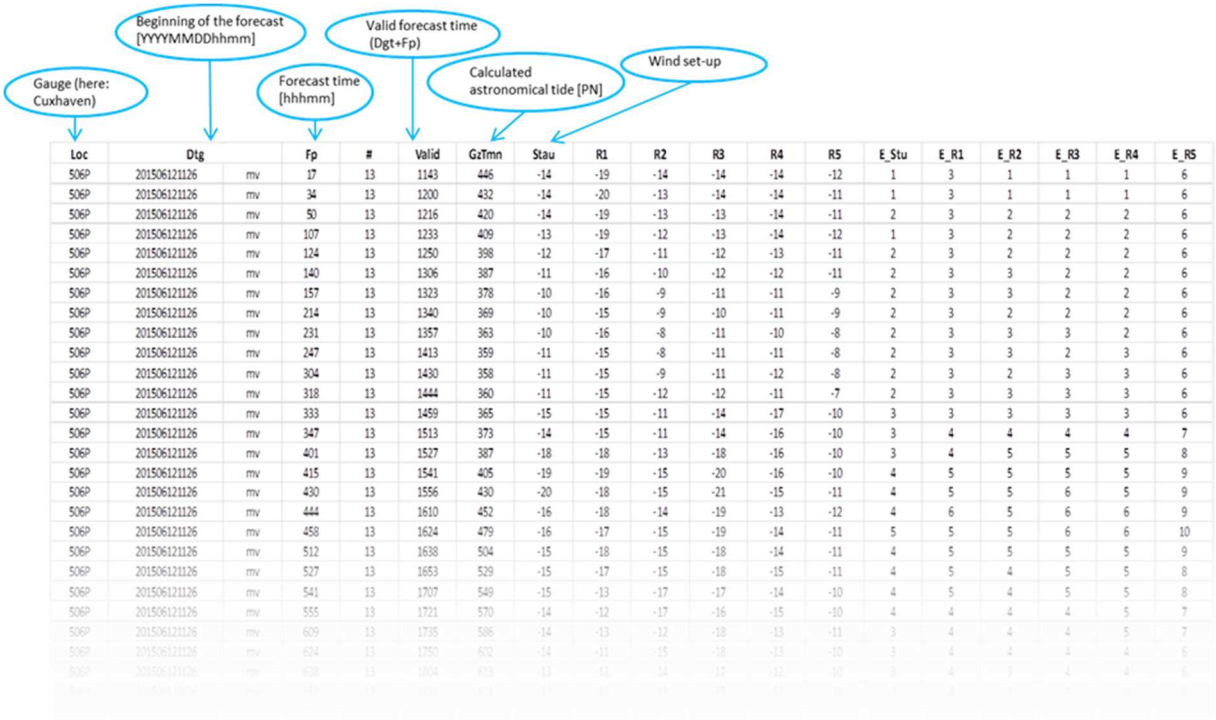

Loc	Dtg		Fp	#	Valid	GzTmn	Stau	R1	R2	R3	R4	R5	E_Stu	E_R1	E_R2	E_R3	E_R4	E_R5
506P	201506121126	mv	17	13	1143	446	-14	-19	-14	-14	-14	-12	1	3	1	1	1	6
506P	201506121126	mv	34	13	1200	432	-14	-20	-13	-14	-14	-11	1	3	1	1	1	6
506P	201506121126	mv	50	13	1216	420	-14	-19	-13	-13	-14	-11	2	3	2	2	2	6
506P	201506121126	mv	107	13	1233	409	-13	-19	-12	-13	-14	-12	1	3	2	2	2	6
506P	201506121126	mv	124	13	1250	398	-12	-17	-11	-12	-13	-11	2	3	2	2	2	6
506P	201506121126	mv	140	13	1306	387	-11	-16	-10	-12	-12	-11	2	3	3	2	2	6
506P	201506121126	mv	157	13	1323	378	-10	-16	-9	-11	-11	-9	2	3	3	2	2	6
506P	201506121126	mv	214	13	1340	369	-10	-15	-9	-10	-11	-9	2	3	2	2	2	6
506P	201506121126	mv	231	13	1357	363	-10	-16	-8	-11	-10	-8	2	3	3	3	2	6
506P	201506121126	mv	247	13	1413	359	-11	-15	-8	-11	-11	-8	2	3	3	2	3	6
506P	201506121126	mv	304	13	1430	358	-11	-15	-9	-11	-12	-8	2	3	2	3	3	6
506P	201506121126	mv	318	13	1444	360	-11	-15	-12	-12	-11	-7	2	3	3	3	3	6
506P	201506121126	mv	333	13	1459	365	-15	-15	-11	-14	-17	-10	3	3	3	3	3	6
506P	201506121126	mv	347	13	1513	373	-14	-15	-11	-14	-16	-10	3	4	4	4	4	7
506P	201506121126	mv	401	13	1527	387	-18	-18	-13	-18	-16	-10	3	4	5	5	5	8
506P	201506121126	mv	415	13	1541	405	-19	-19	-15	-20	-16	-10	4	5	5	5	5	9
506P	201506121126	mv	430	13	1556	430	-20	-18	-15	-21	-15	-11	4	5	5	6	5	9
506P	201506121126	mv	444	13	1610	452	-16	-18	-14	-19	-13	-12	4	6	5	6	6	9
506P	201506121126	mv	458	13	1624	479	-16	-17	-15	-19	-14	-11	5	5	5	6	6	10
506P	201506121126	mv	512	13	1638	504	-15	-18	-15	-18	-14	-11	4	5	5	5	5	9
506P	201506121126	mv	527	13	1653	529	-15	-17	-15	-18	-15	-11	4	5	4	5	5	8
506P	201506121126	mv	541	13	1707	549	-15	-13	-17	-17	-14	-10	4	5	4	5	5	8
506P	201506121126	mv	555	13	1721	570	-14	-12	-17	-16	-15	-10	4	4	4	4	5	7
506P	201506121126	mv	609	13	1735	586	-14	-13	-12	-18	-13	-11	3	4	4	4	5	7
506P	201506121126	mv	624	13	1750	602	-14	-11	-15	-18	-13	-10	3	4	4	4	4	6
506P	201506121126	mv	638	13	1804	633	-13	-12	-14	-17	-12	-10	3	4	3	4	4	6

Figure 41 Example of the structure and content of a file with forecasted water level data.

Numerical Scheme for Real-Time Flood Forecast

The numerical model, which is used as the basis for the early warning system is described in the previous section.

For the application as real-time early warning system, the base model is adjusted in order to implement the BSH MOS – forecast data. The complete model is divided into three sub-models along the Lower Elbe (see Figure 40), i.e.:

- Model I: section between the weir Geesthacht and the gauge Schulau
- Model II: section between the gauge Schulau and gauge Glückstadt
- Model III: section between gauge Glückstadt and gauge Cuxhaven.

The extension of the three sub-models are chosen with respect to the location of the available BSH - MOS forecast points (gauges) for the Elbe. Furthermore, the sub-models are chosen in a way that the MOS forecast data can be used unambiguously as model boundary data. Hence, use of the location Hamburg St. Pauli (see Figure 40) as sub-model boundary is inappropriate, since the Elbe is in this area subdivided into the Norderelbe and the Süderelbe where no water level is available in the Süderelbe.

Each sub-model area covers at least one additional MOS forecast point for calibration, validation of the numerical scheme and for the direct assessment of the model output compared to the forecast. Comparison calculations show that with the use of the MOS forecast data (Cuxhaven-Steubenhöft, Glückstadt, Schulau and Geesthacht, see Figure 40) as a boundary for the early warning model (three sub-models) the accuracy of the model output is significantly improved compared to an early warning system with one complete Elbe model, only.

At the model boundaries of each sub-model, the downloaded and processed MOS – forecast water level data sets are used as boundary conditions and the model run is automatically started to calculate the spatial distribution of the water level. This process is repeated every 60 min based on the update interval of the MOS - water level forecasts (see Figure 37, blue and green thread). The forecast period is three days (Figure 44).

At the model boundaries, the water level forecasts are used directly as boundary conditions. In addition, discharge data at the downstream boundary of the respective sub-models is used as a boundary. The discharges are calculated from the results of the forecast runs at the downstream boundary of the upstream sub-models, respectively. This means that at each upstream sub-model boundary i) water level data (MOS-results) and ii) discharge data is applied as a boundary condition and that at each downstream boundary water level data (MOS-results) is used as a boundary condition.

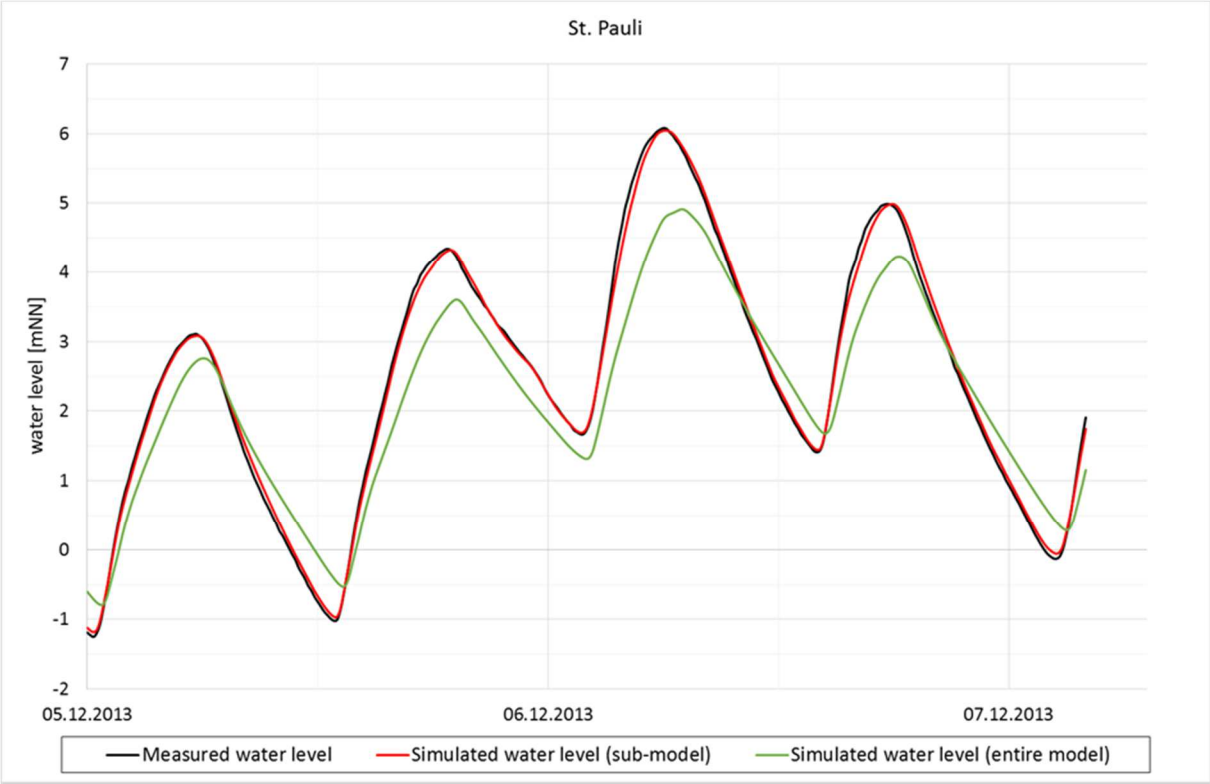

Figure 42 Comparison of water levels resulting from the entire Elbe estuary (green solid line), the sub-model (solid red line) and measured water level (solid black line) for the gauge St. Pauli.

For the Model I (the most upstream model) measured discharge data at gauge Neu Darchau (see Figure 36) is used as an upstream boundary condition (see Figure 40).

This procedure implies a sequential run of the simulations of the sub-models.

At present, each sequential run of simulations is restarted every 60 min with the updated boundary conditions. The model results are stored in a database (see Figure 37, green thread, Figure 38, green thread).

3.1.2 *Results and evaluation*

The numerical model approach is validated based on measured data from the storm surge event "Xaver" which occurred in December 2013. Figure 43 exemplarily shows the comparison between measured and simulated water levels based on the modelling scheme described in 3.1.2. The good agreement between modelled and measured water levels can be clearly seen from Figure 43.

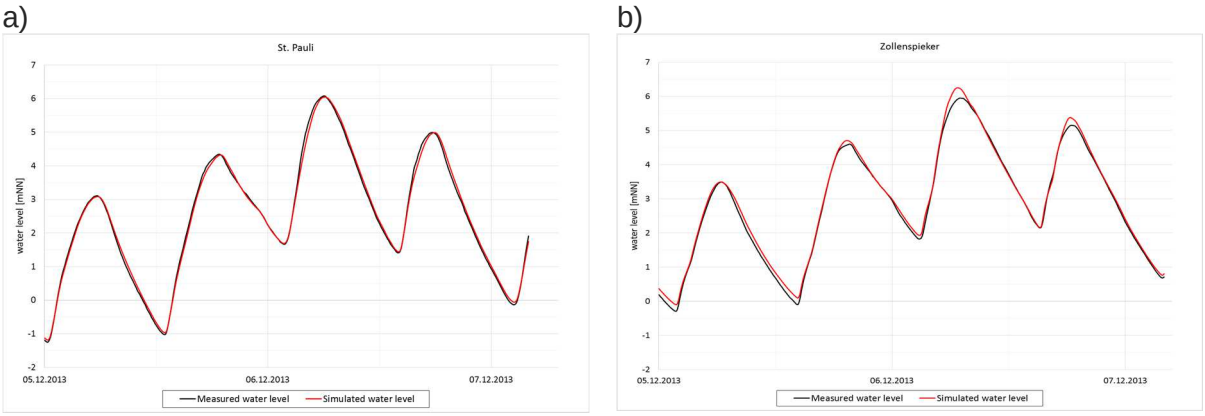

Figure 43 Comparison of measured and simulated water levels for the gauges a) St. Pauli and b) Zollenspieker.

All model results are stored in a database (Figure 37, green thread). Within the implemented Elbe river early warning system, model results are analysed with respect to the water level distribution along the Elbe (see Figure 37, yellow thread, Figure 38, yellow thread). By comparison of the forecasted water levels with the known heights of the flood protection structures, potentially endangered areas are determined and specified as a basis for early warning.

The results of the forecast are consequently the input for the assessment of the failure of flood protection structures and the analysis of the consequences (Figure 37) in the PEARL work-packages WP3 and WP4.

The simulation results will be made available via a web platform. The content includes:

- GIS data layer including model extent (see Figure 40)
- Time series of selected gauges
- Spatial presentation of the water levels from the model runs
- Display of potentially endangered sections of the flood protection infrastructure

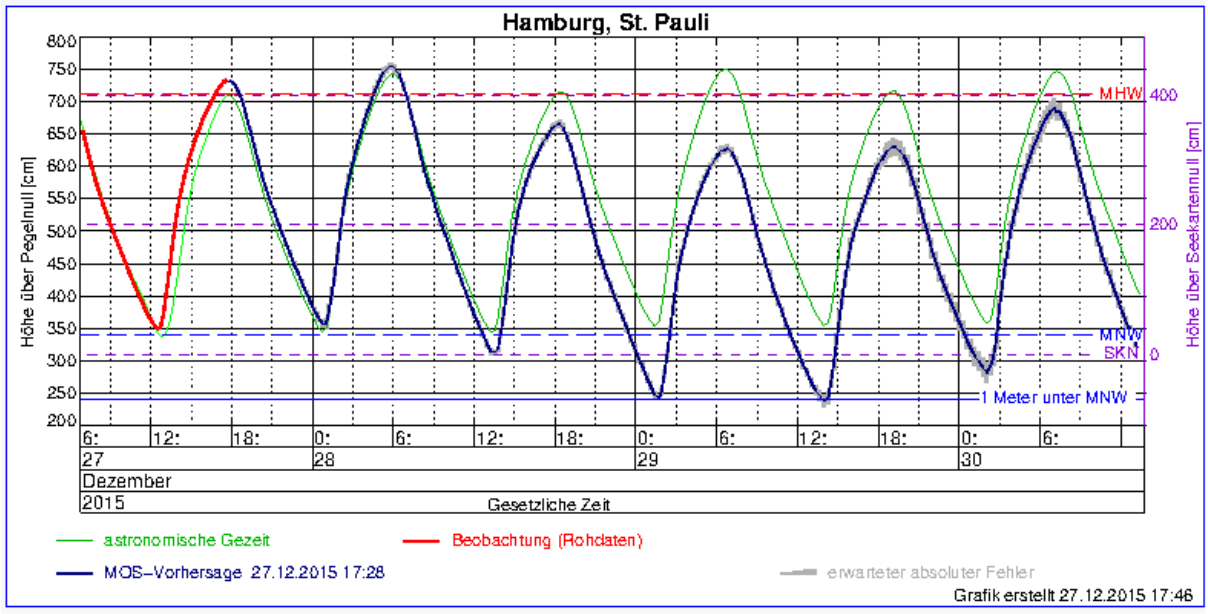

Figure 44 Example of the water level forecast of the BSH, 3 days.

The described early warning system provides real time forecast information about increased water levels along the Elbe estuary. Sections of the protection infrastructure, which are endangered by high and extreme water levels, are detected. For the potentially endangered sections, a subsequent reliability analysis is carried out to determine the probability of failure of the protection infrastructure. In the case of an increased risk of failure, an inundation simulation (see Figure 37, grey thread, Figure 25) is carried out to determine the potentially inundated area. For this purpose, a numerical model of the hinterland area behind the endangered section of the flood protection infrastructure is added to the respective sub-model of the Elbe estuary (The principles of dike breach modelling are described in Chapter 2.1.3). This extended model is then re-started with the forecast data in order to determine the possible inundation area. Results of the inundation analysis (e.g. Figure 25) are additionally the basis for the damage assessment and for possible evacuation measures.

3.2 Greve, Denmark

Greve is a municipality in eastern Denmark. It is a sub-urban area about 20 km southwest of Copenhagen. It has a total area of around 60 km^2 and has 9 km of coast to the southeast bordering Køge Bay, which is part of the Baltic Sea (Figure 45). The coastal area is the most densely built-up part of Greve, and it is characterized by relatively flat terrain with elevations between 2 and 6 m (above MSL).

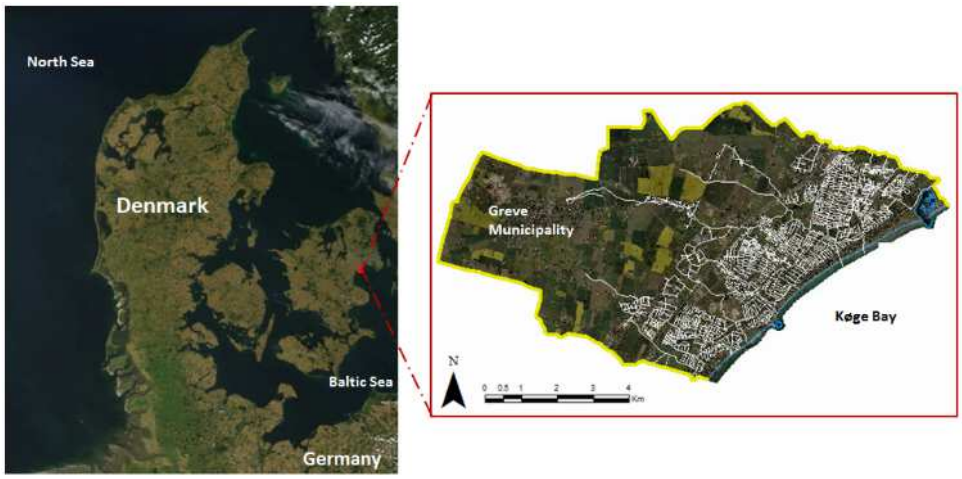

Figure 45 Location of the Greve case study area in eastern Denmark.

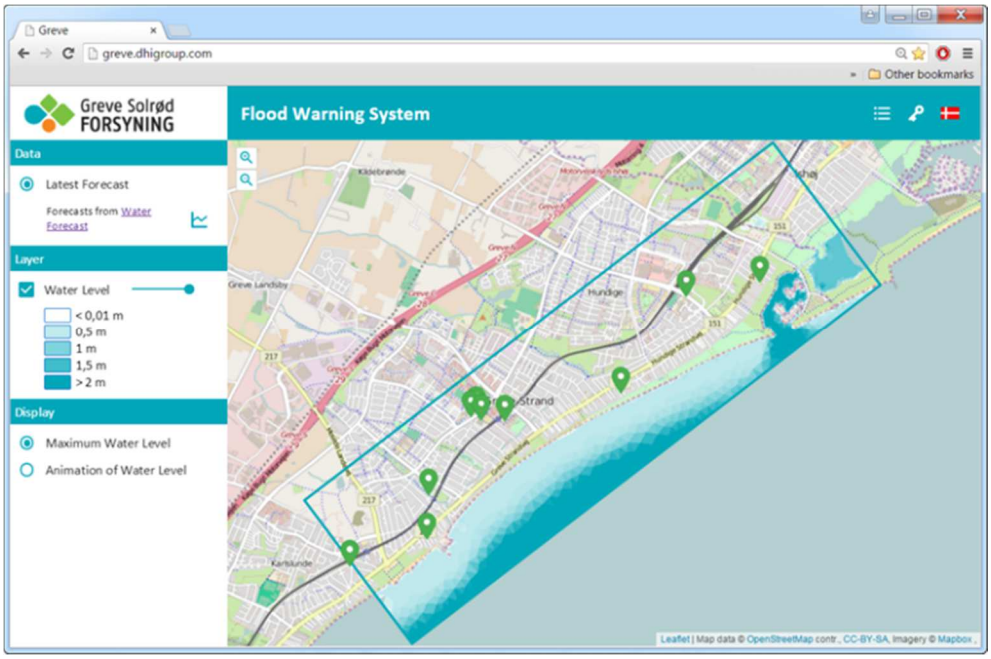

Figure 46 Homepage for the online coastal flood warning system in Greve, Denmark (www.greve.dhigroup.com). A map of the most recently calculated maximum water depths is displayed by default. Pre-determined critical points (see place markers) are colour-coded from green to red depending on the magnitude of forecasted flooding.

In July 2007, a series of rain events with an estimated return period of 500 years caused severe flooding in Greve (Greve Kommune, 2007). In addition to extreme rainfall, Greve is also vulnerable to flooding from extreme sea levels along its coast. Greve is at risk from coastal flooding due to

storm surges and general water level increase because of its location in Køge Bay (Vestergaard, 2011), which has been identified as 1 of 10 most at-risk areas in Denmark from coastal flooding (NIRAS, 2014).

Thus, a coastal flood warning system has been developed for the municipality of Greve (Figure 46). It employs a 1D-2D hydrodynamic flood model for flood forecasting, which makes use of NWP rainfall forecasts and 3D hydrodynamic model water level forecasts as boundary conditions. Details on the different components and functionalities of the warning system are presented in the following sections.

3.2.1 *Framework and methodology*

The Greve coastal flood warning system employs a hydrodynamic flood model that calculates potential flooding using forecasted rainfall and sea water levels. The main components of the system are illustrated in Figure 47. Data collection and processing of flood forecasts are done through a desktop client, and a website is used to show flood forecast information as well as system data (see Figure 46).

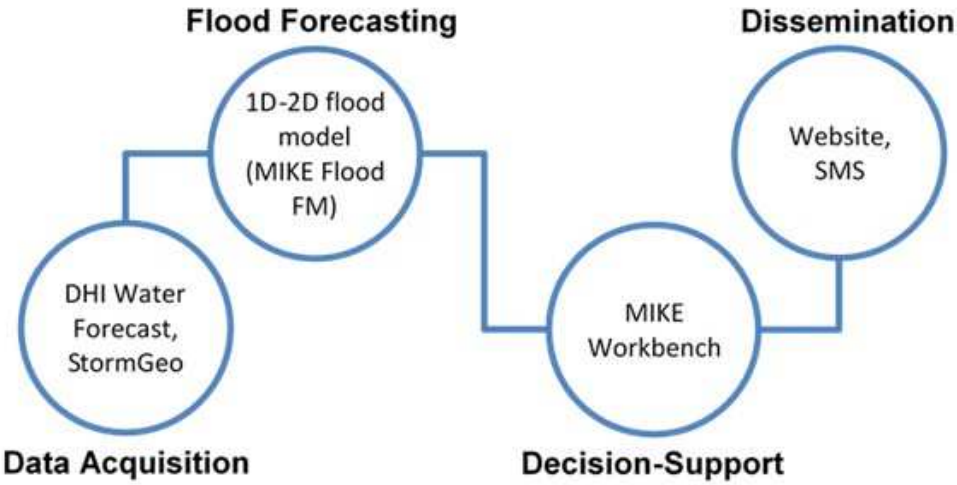

Figure 47 Diagram showing the main components of the Greve Flood Warning System.

Data Acquisition from DHI Water Forecast and StormGeo

Forecasted sea water level and rainfall data are obtained and used as boundary conditions for the coastal flood model. In the acquisition process, data are routinely collected from two sources: Water Forecast by DHI (DHI, n.d.) and StormGeo (StormGeo, n.d.). DHI's Water Forecast provides 6-day sea level forecasts in Køge Bay every 12 hours, using results from a 3D hydrodynamic and wave model covering the Inner Danish Waters and the Baltic Sea (DHI, 2011). The data is accessed from an internal MySQL database located at DHI. The rainfall forecast for the next 24 hours over the area of Greve is also acquired from the Water Forecast database, which retrieves and stores NWP rainfall forecasts from StormGeo. The collected data are stored through MIKE Workbench, a desktop client for interactive data analysis and processing, and are processed to ensure that they cover the flood model simulation period. The processed data are converted to *.dfs0-format files and used as boundary conditions for the flood model. The files are updated for every forecast, and the simulation period for the flood model is adjusted accordingly. Information on the rainfall and water level forecast data are published on the website as time series plots (Figure 48).

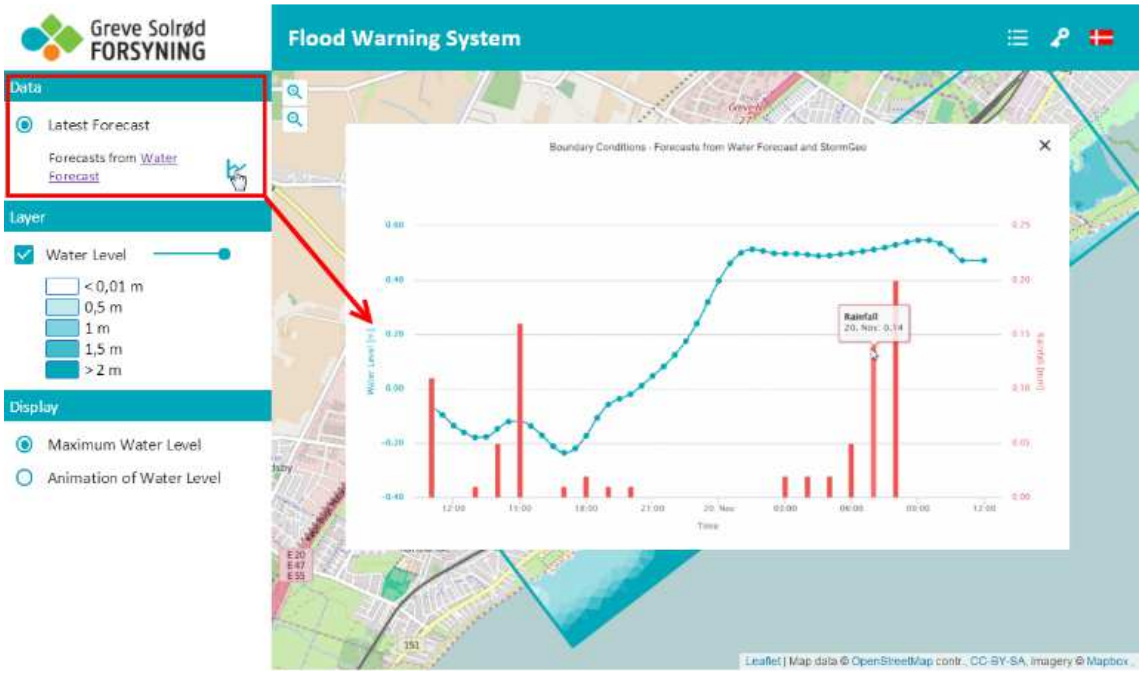

Figure 48 Forecasted sea water level (blue lines) and rainfall (red bars) data used to drive the coastal flood model in the Greve Flood Warning System. Plots of the most recent data may be viewed on the website (http://greve.dhigroup.com/).

Flood Forecasting with MIKE Flood FM

A 1D-2D hydrodynamic model is used for calculating potential flooding in the coastal area of Greve. It was built using MIKE Flood FM, a modelling system integrating one-dimensional and the two-dimensional models into one dynamically coupled model (DHI, 2013d). It comprises of a 1D model of the drainage system comprising of stormwater sewers and streams, coupled to a 2D surface flow mesh model of the inland and sea areas along the coast (see Figure 49). The drainage network is included in the flood model to ensure simulation of pluvial and fluvial flooding, and consider the influence of the drainage network in conveying flooding from the sea further inland.

The 1D network model is relatively comprehensive and detailed, covering most of Greve Municipality and consisting of around 7 000 nodes, 6 500 links and 9 outlets to the sea. The model employs a conceptual (Time-Area) runoff model to calculate rainfall runoff from the 6 000 sub-catchments of the area, and a 1D fully hydrodynamic pipe flow model simulating water levels and flows through the underground pipes and open channels comprising the drainage system. Forecasted rainfall data obtained from StormGeo is used to calculate runoff, which is then applied as an input to the network model.

MIKE 21 FM, a 2D modelling system based on a flexible mesh approach, was used to build the 2D model in Greve. The model covers 53 km^2 of the area made up of sea and inland regions along Greve's coast (see Figure 49). It uses a flexible computational mesh to represent the terrain surface. The mesh elements, which could be triangular or quadrangular in shape, vary in size depending on the required/specified computational resolution at an area. The Greve 2D model computational mesh is comprised of 49 000 elements that vary in size from 9 m^2 to 20 000 m^2. Small mesh elements were used for built-up areas, roadways and flood plains, and bigger elements were used for rural areas and the sea. The element mesh representing the terrain is an important component of the 2D model, and must include and appropriately represent surface features, such as dikes, waterways and overland flow paths, as these are important factors

influencing overland flows and flood propagation. Small-sized elements may be used to achieve appropriate computational resolutions at these critical flow areas. In Greve, Terrain Analysis (see Chapter 2.1.3) using the estimated maximum sea level ever recorded in Køge Bay (i.e. 3.7 m above MSL on 13 October 1760) was employed to identify these critical areas, and small mesh elements were specified in regions with terrain elevations below 3.7 m. In flood modelling, sea water level forecasts are applied as boundary conditions to the 2D model at its open boundaries to the sea (see Figure 49).

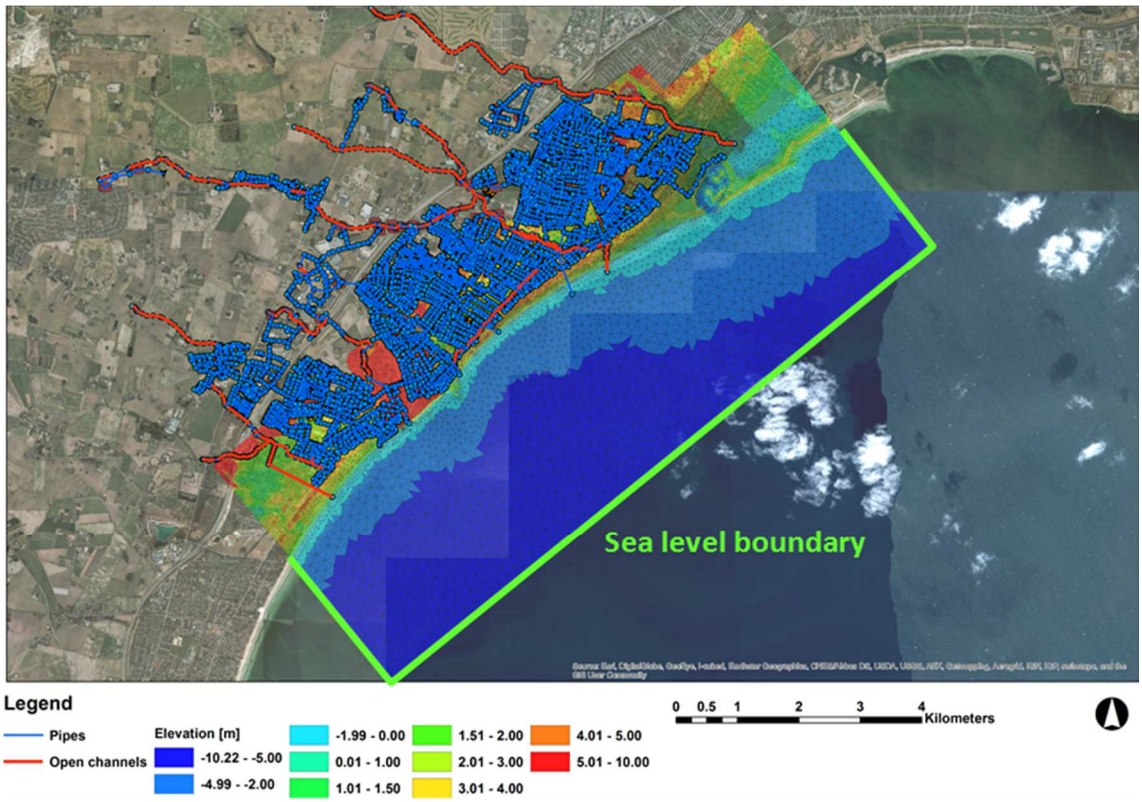

Figure 49 A map showing the 1D-2D coastal flood forecast model for Greve. A 1D model of the drainage system comprising of streams (red lines) and stormwater sewers (blue lines and points) is linked to a 2D mesh model of the coast (coloured areas). The triangular elements of the terrain mesh and open boundaries of the 2D model are also shown.

The 2D surface flow model and1D network model were linked at points where the exchange between the two systems could occur, such as at drainage outlets, stormwater inlets, unsealed manholes, and open channels. The computational links were modelled using the weir equation, which calculates flows based on head differences at linked network nodes and terrain elements (Mark and Djordjevic, 2006). Flows between the two systems can occur in both directions. Drainage network outlets to the sea are explicitly linked to the 2D model at coinciding mesh elements, such that calculated water levels at the linked element are used as water level boundary conditions for the corresponding linked drainage outlet.

Flood forecasts for the next 24 hours are made every 4 hours at 00:00, 04:00, 08:00, 12:00, 16:00, 20:00 CET. The Greve flood forecast model takes around 2 hours computation time to simulate a period of 24 hours. Computation results are shown on the website, wherein static maximum water depths and time-varying water depth animations are plotted on a map.

Decision-Support with MIKE Workbench

Flood model results are stored and processed using the MIKE Workbench desktop client. The results are analysed at pre-identified important points in the model domain, which are plotted as colour-coded place markers on the flood map (Figure 50). Warning information is disseminated according to exceedance of set water depth thresholds (0 cm, 20 cm and 40 cm) by forecasted flood depths at these pre-defined important locations.

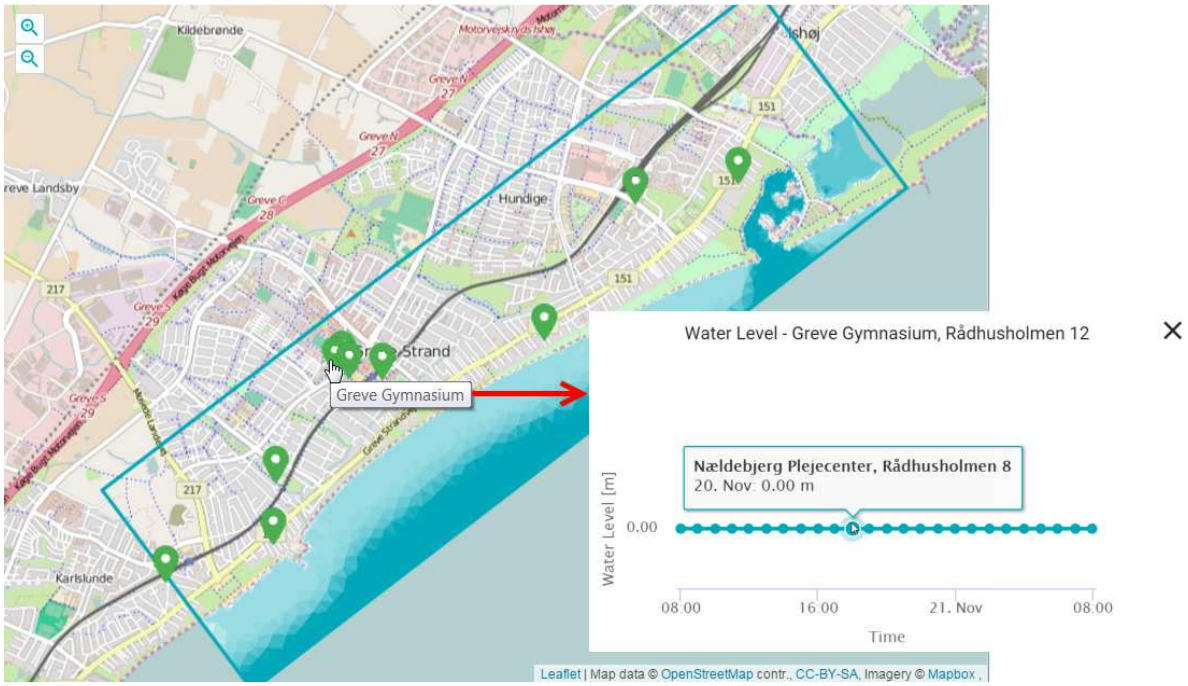

Figure 50 The flood map on the website shows place markers for pre-identified important places in the coastal area of Greve. The markers are colour-coded according to computed flood depths from green (0-20 cm) to yellow (20-40 cm), and to red (above 40 cm).

Information on important locations, such as coordinates, name and location type, as well as the computed flood time series, are stored in a spreadsheet in MIKE Workbench. The time series are extracted for the locations from the flood model result files and stored in MIKE Workbench. The time series are then analysed to identify the maximum value, which is then written back into the spreadsheet for the location. The result files are additionally made available for the website. The data that is available for the website to display are:

- GIS data layer with the model extent
- Spreadsheet with a list of locations and their maximum depth values for the next 24 hours
- Result files for 2D animation of water depth as well as display of maximum water depth
- Time series for water depth at important locations
- Time series for boundary conditions

Dissemination through 'http://greve.dhigroup.com/'

The website was built using Polymer (Polymer, 2015) linking to the DHI Web API (Application Programming Interface), which supports data access in MIKE Workbench. The website allows viewing most recent forecasts, as well as results from extreme event scenarios (see Figure 51). The extreme event scenario results are, however, only available through login for confidentiality reasons. By default, the maximum water depth is displayed on the page, but the user can switch over and display an animation that shows the propagation of flooding.

The important locations are shown on the map colour coded by the flood state. Maximum depth of 0-20 cm is shown as green, 20-40 cm yellow, and above 40 cm red. The user can click on the place markers to see a time series of the water depth as well as click on the left hand side on the time series icon to see the boundary conditions used for the model run.

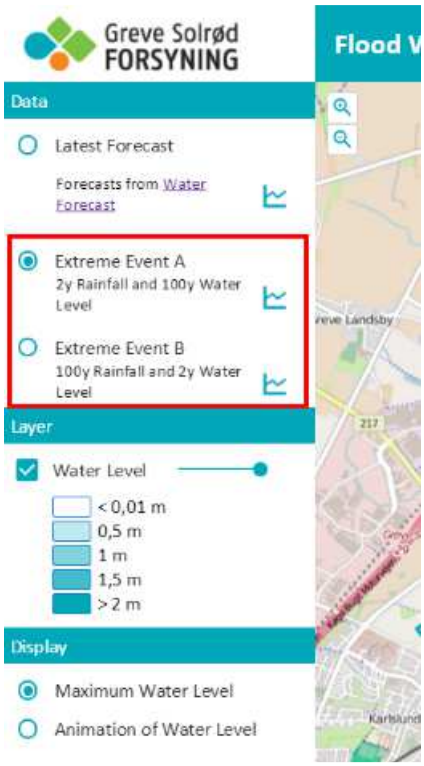

Figure 51 Besides real-time flood forecasts, results from other flood modelling scenarios are also shown on the website, although accessible only with login information.

3.2.2 Results and evaluation

The online Greve Flood Warning System was launched in September 2015, and there have been 2 down periods to date—in early September 2015 for 6 days (29 forecasts), and early November 2015 for 4 hours (1 forecast), which indicates that the system has been 'reliable' 94% (492/522) of the time.

This type of information on system performance may be viewed through a functionality implemented in the system's decision-support component in MIKE Workbench. Job statistics data on 'Duration' are recorded and stored, showing a time series of model computation time for each flood forecast (Figure 52). This data gives information not only on model efficiency but also on whether the system is functioning properly, as 0 h calculation duration is unlikely and most probably indicates a system malfunction.

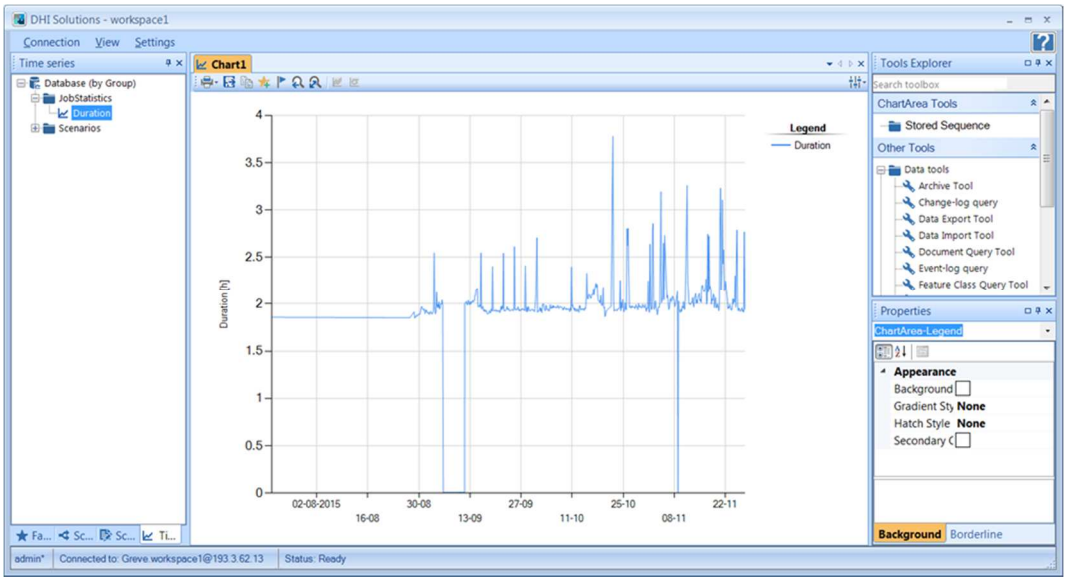

Figure 52 Job statistics recorded in MIKE Workbench indicating system status for the Greve Flood Warning System. The 'Duration' time series show the computation times used for each flood forecast. The data shows that there have been 2 periods when the system was down since its launch in September 2015, indicated by the 0 h duration values. Data before September 2015 are for a preliminary test period.

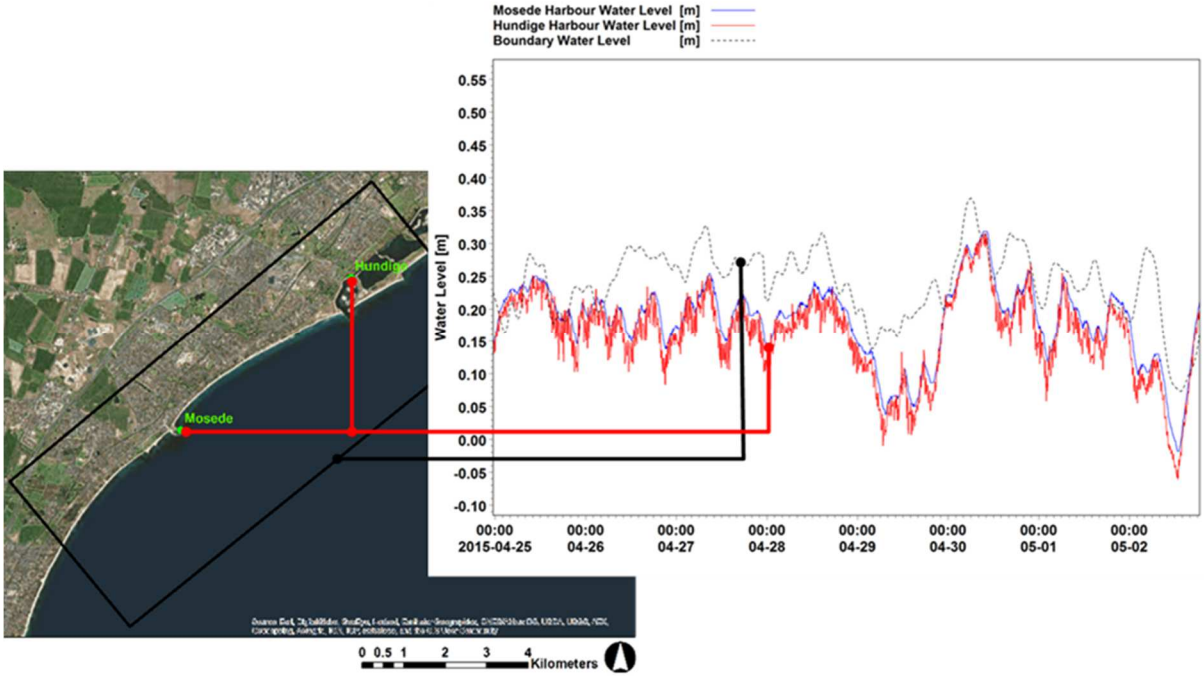

Figure 53 The map shows water level measurement stations at Mosede and Hundige harbour in Greve. The coastal flood model domain is indicated in black outline. Plots of water level measurements at Mosede (blue line) and Hundige (red line) harbour in Greve are shown on the right. The black broken line shows forecasted sea levels at the sea boundary of the flood model.

There have been no coastal flood events in Greve in recent years, and thus, the flood model has, so far, been only verified at periods of 'normal sea level conditions'. Model verification involved the

ex post comparison of calculated/forecasted water levels to actual measurements at Hundige and Mosede harbour for the period 25 April to 5 May 2015 (see example comparison in Figure 54). Rainfall and sea level forecasts retrieved from the DHI Water Forecast system were used as boundary conditions to the Greve flood model, as described in Chapter 0.

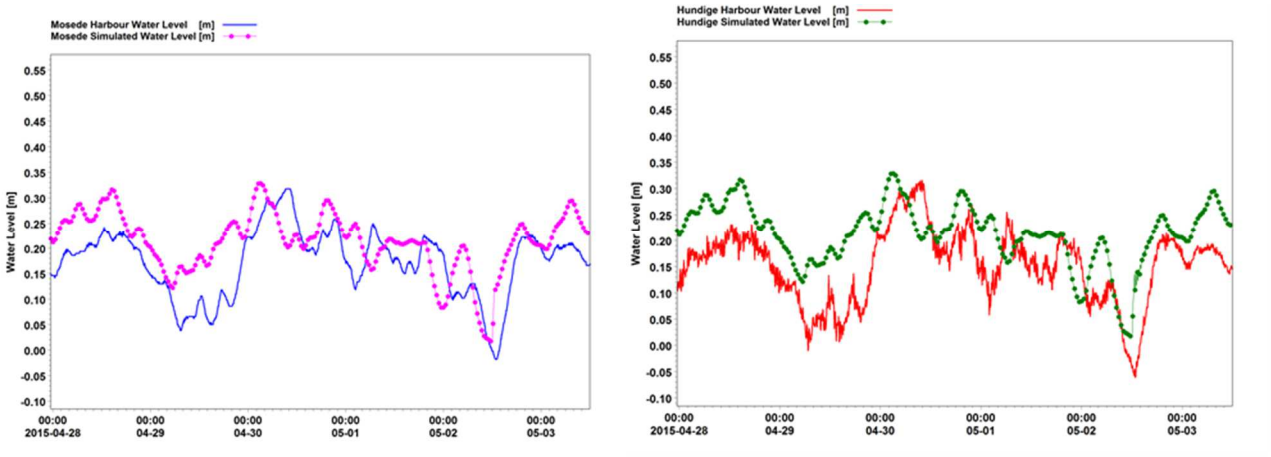

Figure 54 Comparison of observed (thick solid lines) to simulated (dotted lines) water levels in Mosede (left) and Hundige (right) harbour for the forecast period 27/4/2015 23:30 – 3/5/2015 12:00.

Comparison of observed and simulated water levels at the measurement stations over different forecast periods show maximum errors of up to 20 cm in Mosede and 25 cm in Hundige, with the larger discrepancies occurring mostly after 2 days into the 5-day forecast period (see Figure 55 and Figure 56). Root Mean Squared Error (RMSE) values averaged over different forecast periods, as shown in Table 3, indicate how forecasts degrade over time, with average RMSE values increasing with forecast period duration. More information about the accuracy of the Greve coastal flood forecast model can also be found in Jensen (2015), a thesis study on integrated storm surge modelling in Greve that was conducted under the PEARL project.

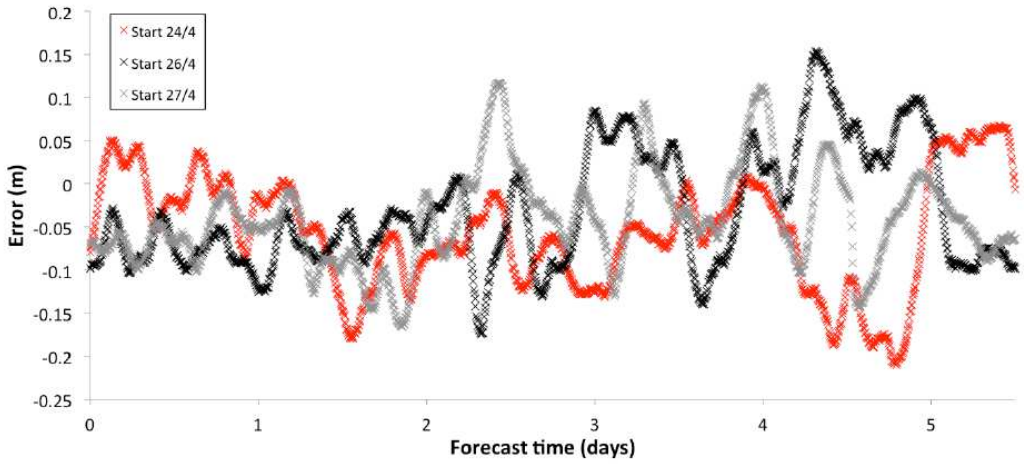

Figure 55 Plot of absolute error from comparison of simulated and observed water levels at Mosede harbour. (Source: Jensen, 2015)

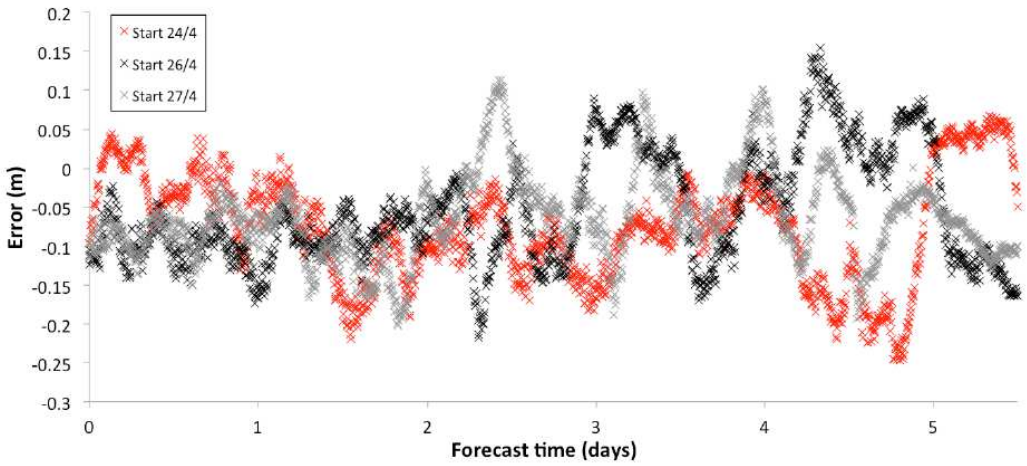

Figure 56 Plot of absolute error from comparison of simulated and observed water levels at Hundige harbour. (Source: Jensen, 2015)

Table 3 Average error statistics over different forecast period durations [h]. (Source: Jensen, 2015)

		Forecast Period Duration [h]										
		12	**24**	**36**	**48**	**60**	**72**	**84**	**96**	**108**	**120**	**132**
Mosede	**ME [m]**	-0.046	-0.048	-0.053	-0.063	-0.057	-0.057	-0.051	-0.048	-0.045	-0.045	-0.043
	RMSE [m]	0.060	0.060	0.064	0.076	0.075	0.075	0.074	0.072	0.075	0.078	0.077
Hundige	**ME [m]**	-0.064	-0.068	-0.073	-0.083	-0.077	-0.078	-0.071	-0.068	-0.065	-0.065	-0.064
	RMSE [m]	0.074	0.077	0.083	0.095	0.093	0.093	0.091	0.089	0.090	0.093	0.093

The water utility company Greve Solrød Forsyning (http://www.gsforsyning.dk/), which is the institution responsible for the drainage system in Greve Municipality, has also been consulted and involved in testing and evaluating the online Greve Flood Warning System. They helped identify areas in the municipality that are critical with respect to coastal flooding (see 'critical points' in Figure 46). The system will continue to be evaluated and improved within the course of the PEARL Project. Recent consultation with the company has identified several points for improvement for the system, which includes:

- **Refinement of the flood model**. Initialize the flood model with previous forecast results.
- **Adding dissemination media**. Finalizing the implementation of SMS and email service for flood warnings.
- **Adding plots of observed water levels.** Plotting sea water level measurements against sea level forecasts at Mosede port in real time.
- **Adding time series plots in results presentation.** Showing measurements against calculated water levels from the 5 critical locations inland.
- **Adding flood risk information.** Showing outlines of houses that are potentially flooded.

3.3 Castries, Saint Lucia

An online coastal flood warning system was developed for Castries, Saint Lucia (see Figure 57). Castries City is the capital of Saint Lucia, which is an island nation in the eastern Caribbean region (Figure 58). The city centre is relatively small with an area of around half a square kilometre (Figure 59). The area is at risk from pluvial flooding, especially during short duration high intensity rainfall, as well as fluvial flooding from the river located south of the city. A real-time pluvial flood warning system for Castries has been earlier developed and tested by Rene et al. (2015). Coastal flooding in the area is apparently rare but may occur during storm events. Therefore, given its coastal location in a hurricane-prone region, the earlier pluvial flood forecast model was extended to also consider flooding from the sea, and used in this new Castries urban coastal flood warning system developed under the PEARL project.

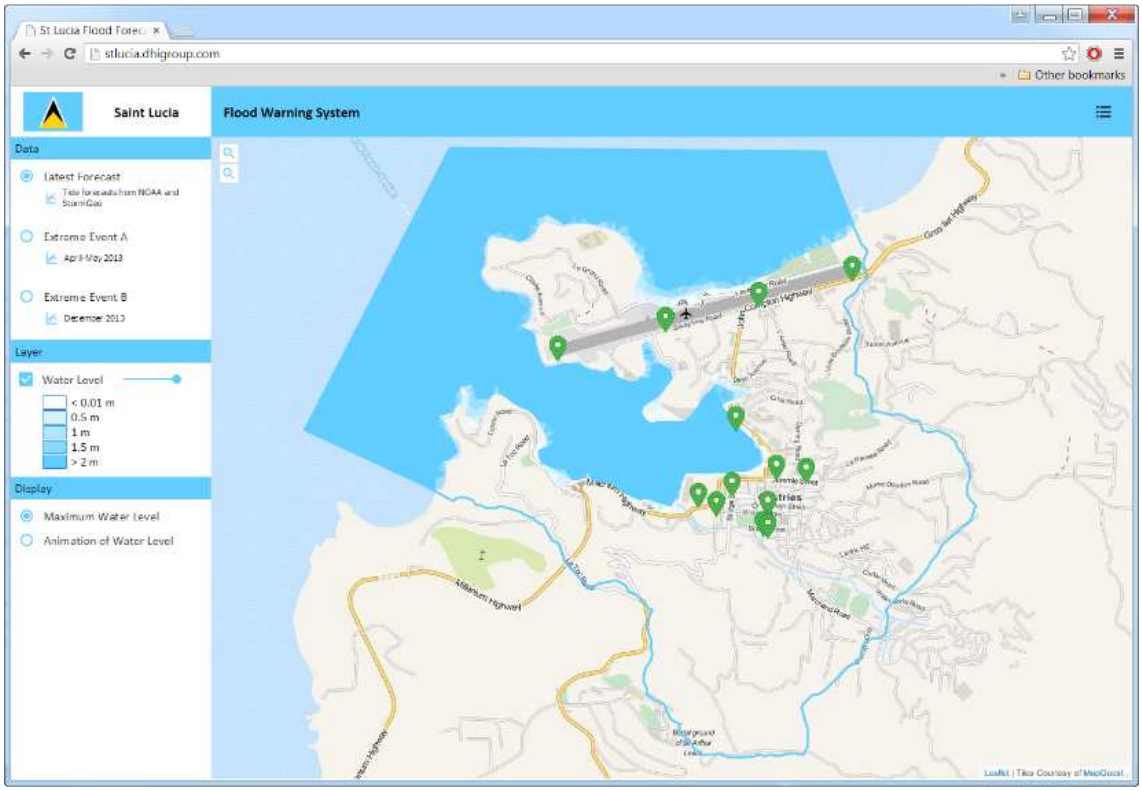

Figure 57 Homepage for the Saint Lucia Flood Warning System – and online coastal flood warning system in Castries, Saint Lucia (www.stlucia.dhigroup.com). A map of the most recently calculated maximum water depth forecast is displayed by default. Pre-identified important locations are plotted using place markers ( ) that are colour-coded from green to red depending on the magnitude of estimated flooding.

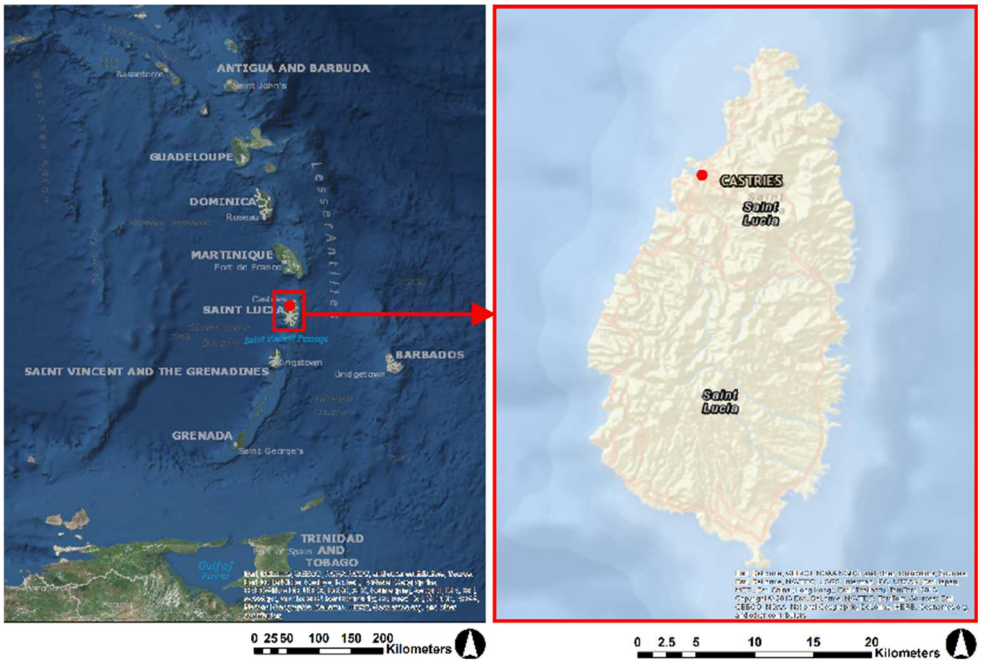

Figure 58 *Location of the Castries case study area in Saint Lucia in the Caribbean.*

Figure 59 *Castries city centre (red outline) in Saint Lucia.*

The new Castries Flood Warning System was built following the earlier pluvial flood warning system developed by Rene et al. (2015). However, in this new system, a more efficient flexible mesh approach is used for the 2D flood model instead of Cartesian grid discretization (see Figure 60). Coastal flooding (i.e. flooding from the sea) has also been included in the simulated processed in addition to pluvial flooding, and the model domain has been extended to include not only the city centre but also upstream sub-catchments and the land and sea areas around the port.

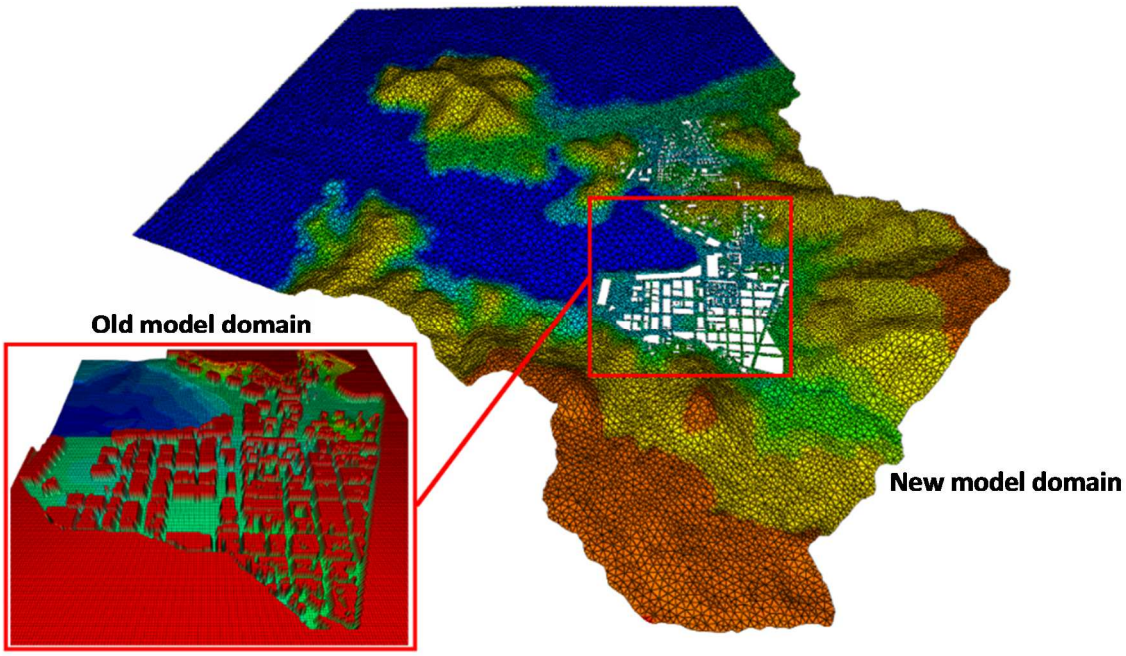

Figure 60 Figures showing the 2D model domains and computation grids for the earlier pluvial flood warning system (lower left) and the new coastal flood warning system (right) for Castries, Saint Lucia. The red outlines indicate the location of the old model domain in the new expanded model area.

3.3.1 Framework and methodology

The Saint Lucia Flood Warning system employs a 2D hydrodynamic model to forecast coastal flooding in Castries. The flood model is driven by rainfall and sea water level forecasts, and the forecasted results as well as various information about the system are published (in real-time) on a website (www.stlucia.dhigroup.com). The various components of the system are illustrated in Figure 61 and further described in succeeding sections.

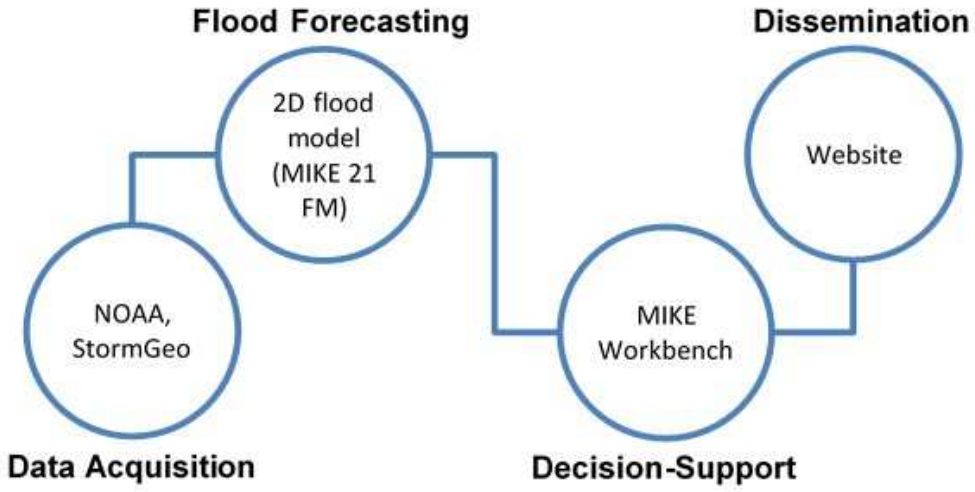

Figure 61 Diagram showing the main components of the Saint Lucia Flood Warning System.

Data Acquisition from NOAA and StormGeo

The flood forecast model is driven by forecasted sea level and NWP rainfall data routinely obtained from NOAA (NOAA National Ocean Service, 2013) and StormGeo (StormGeo, n.d.). During data acquisition, sea level data are retrieved from a NOAA website, and rainfall forecasts from DHI's Water Forecast system (DHI, n.d.) database holding StormGeo data. Data from the NOAA website are read and data mined to derive sea levels from Mean Lower Low Water (MLLW) tide level values (MLLW is 0.173 m below Mean Sea Level (MSL) in Saint Lucia). At the same time, NWP rainfall forecasts from StormGeo for the next 24 hours are obtained from the Water Forecast database located at DHI. Both time series are collected and stored through MIKE Workbench, and are then processed to ensure that the data time series cover the flood model simulation period. Finally, the time series are set as boundary conditions to the flood model, which is routinely run by the system.

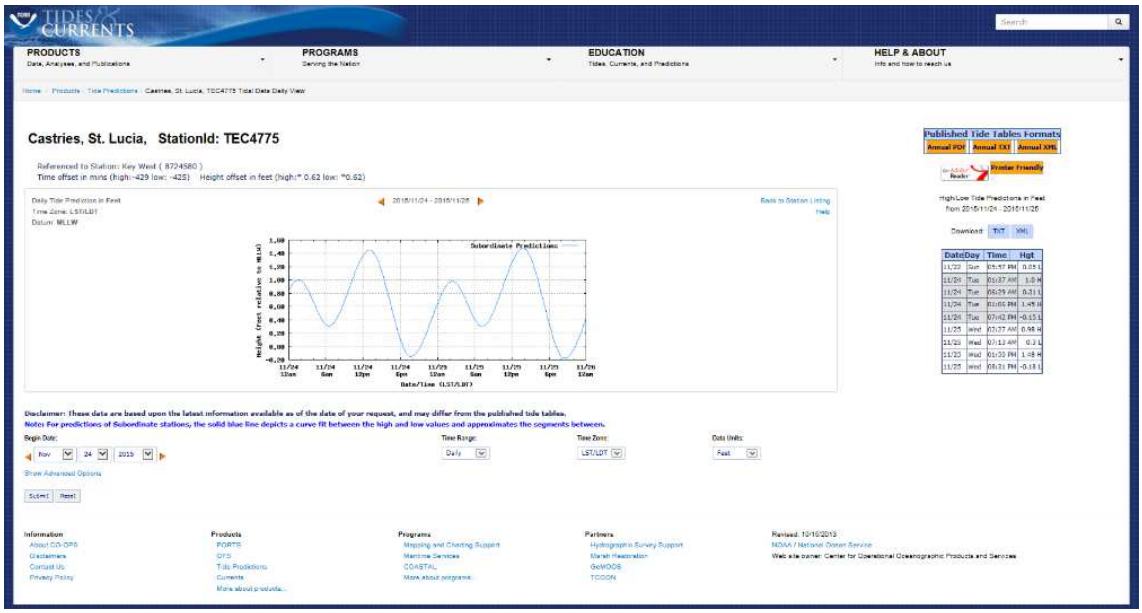

Figure 62 The NOAA website from where sea level data are obtained (https://tidesandcurrents.noaa.gov/noaatidepredictions/NOAATidesFacade.jsp?Stationid=TEC4775). (Source: NOAA National Ocean Service, 2013)

Flood Forecasting with MIKE 21 FM

A 2D flexible mesh model is used for coastal flood forecasting in the Castries Flood Warning System. The model was built using MIKE 21 Flow Model FM, a modelling software that calculates two dimensional flows based on the 2D incompressible Reynolds-averaged Navier-Stokes equations. It employs a flexible mesh approach that uses a cell-centred finite volume method for spatial discretization in the calculations (DHI, 2013).

The 2D model covers around 8.5 km^2 of inland and sea areas around the port in Castries (Figure 63). The element mesh comprises of around 32 000 triangular elements ranging in size from around 0.5 to 1 200 m^2. With the assumption that buildings in the area are largely impervious to surface flows, the presence of these structures is considered by removing them from the calculation mesh (see Figure 64). This means that calculations are not performed over these areas, and flows are simulated to occur around/between these structures reflecting their influence on surface flows. Small mesh elements are used to describe most of the inland areas (Figure 64), since small elements are needed to properly resolve (flow-influencing) structures on the complex urban terrain, such as streets, alleyways between buildings, and building corners. Relatively larger

mesh elements are used to represent sea and rural inland areas, which helps optimize the number of computational elements, and hence computation time, for the model.

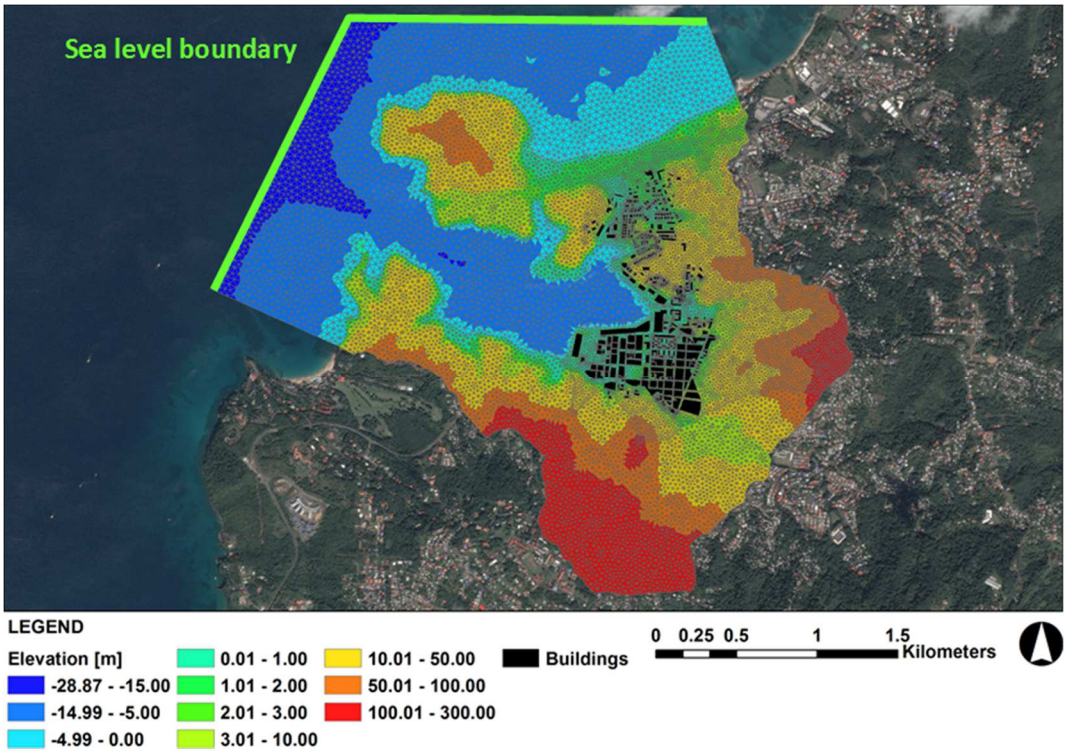

Figure 63 A plot showing the 2D coastal flood forecast model for Castries. The 2D model for the inland and sea areas around the harbour (coloured areas) employs a mesh of different-sized triangular elements. The presence of buildings is considered in the mesh (black shapes), and the sea boundaries of the 2D model are indicated in the figure (green lines).

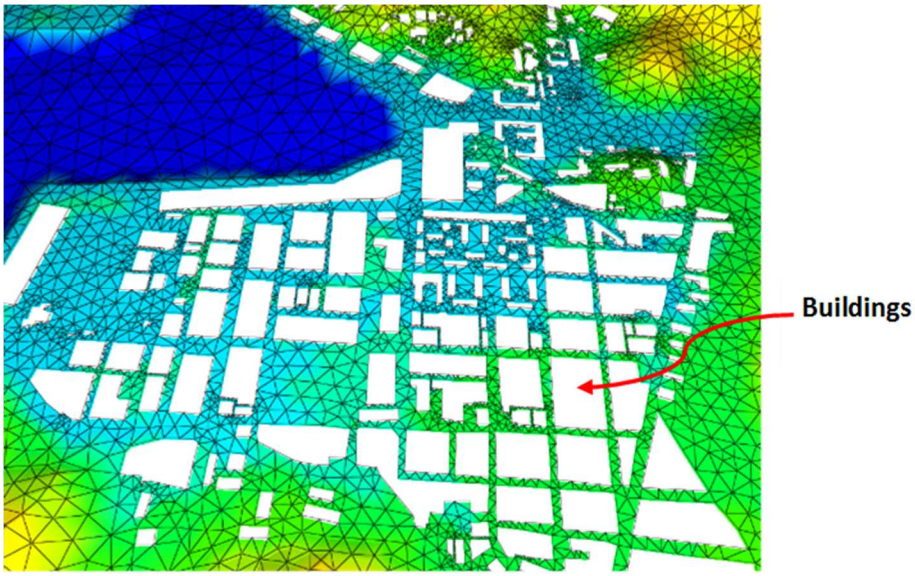

Figure 64 A closer view of the 2D model element mesh representing the terrain at the centre of Castries. Buildings are removed from the mesh (shown as white spaces) as a way to consider the influence of structures on surface flows.

Forecasted rainfall from StormGeo is used as spatially-distributed precipitation input to the 2D flood model. The surface runoff process is approximated using the rain-on-grid approach in the 2D model. Also, for the Castries flood model, rainfall over buildings is assumed collected by the urban sewer system and not applied to the 2D grid. The technique could also be further refined by pre-processing the rainfall time series input considering (i.e. subtracting) the design capacity of the urban drainage system. Forecasted sea levels from NOAA are also applied to the 2D model as water level conditions at the open sea boundaries towards the Caribbean Sea (see Figure 63).

In the system, 24-hour flood forecasts are made every 4 hours at 22:00, 02:00, 06:00, 10:00, 14:00, 18:00 CET. The Saint Lucia flood forecast model takes around 20 min computation time to simulate a period of 24 hours. Results are shown on the website as static maximum water depths and time-varying water depth animations.

Decision-Support using MIKE Workbench

Important locations in the study area were identified, and noted in a spreadsheet in MIKE Workbench (see Figure 65). After each flood simulation, results at these important points are extracted, stored, and analysed to derive maximum values upon which flood warning information is issued. Coloured place markers are used to represent these points in flood map on the website, and the colours are changed according to whether flooding is forecasted to occur at a point or not. Calculated water depth time series at the pre-identified critical points could also be viewed on the website.

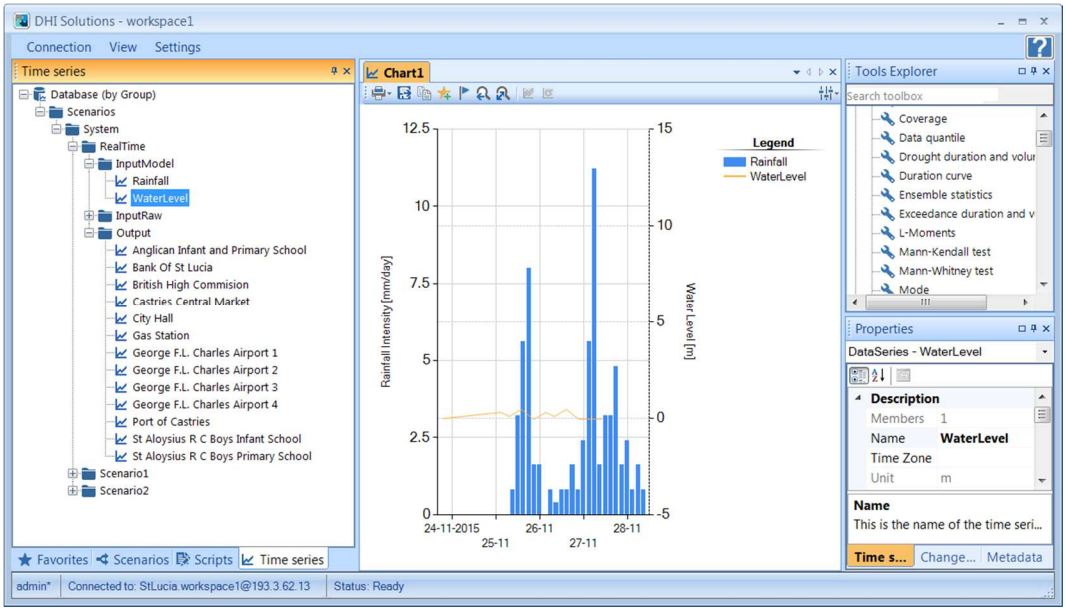

Figure 65 The MIKE Workbench interface showing the various input and output data being handled by the Saint Lucia Flood Warning System.

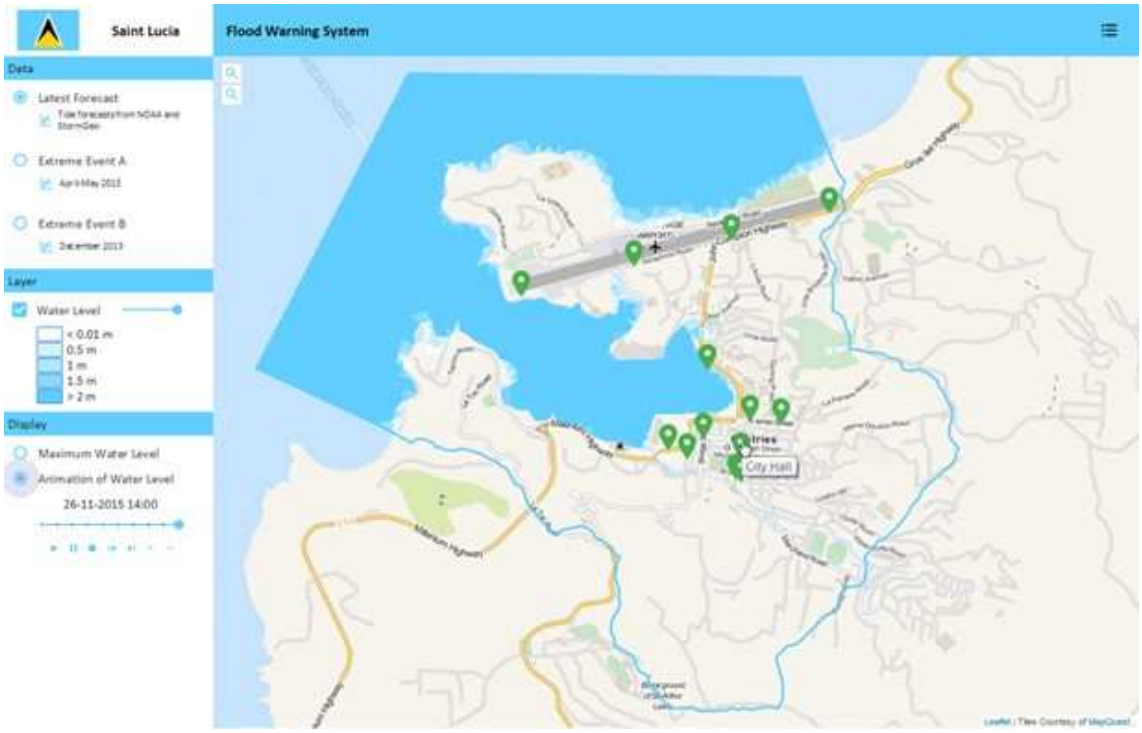

Figure 66 The flood map on the website shows place markers for pre-identified important places (e.g. the City Hall) in Castries. The markers are colour-coded according to computed maximum flood depths for the next 24 hours from green (0-20 cm), to yellow (20-40 cm), and to red (above 40 cm).

A summary of the various data that may be viewed on the website include:

- GIS data layer showing model extents
- Spreadsheet with a list of critical locations and maximum calculated flood values for the next 24 hours
- 2D water depth animation and static maximum water depth map
- Time series for water depth at critical locations
- Time series for boundary conditions used in the flood modelling

Dissemination through 'http://stlucia.dhigroup.com/'

Information on the Saint Lucia Flood Warning System and real-time flood forecast results are published on the website 'http://stlucia.dhigroup.com/'. The site was built using Polymer (Polymer, 2015) linking to the DHI Web API (Application Programming Interface), which supports data access in MIKE Workbench. The website shows information on real-time forecasts as well as results from historical event simulations (Figure 67). By default, the maximum simulated water depth is displayed on the map, but the user can also display an animation showing the propagation of flooding. Pre-identified important locations are shown on the map with markers coloured according to calculated maximum flooding as green (0-20 cm), yellow (20-40 cm), or red (above 40 cm). The user can click on the place markers to view calculated water depth time series at each location, and boundary conditions used for the flood simulation may be viewed through the time series icon under the 'Data' menu (see Figure 67).

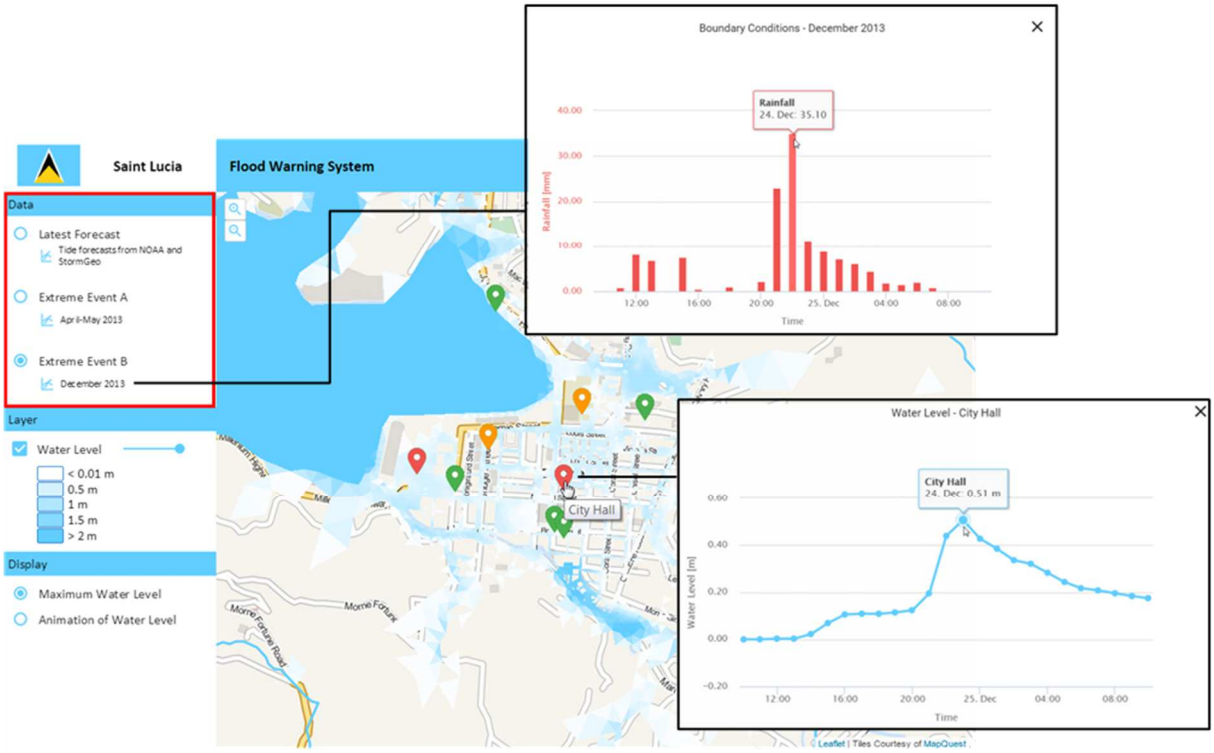

Figure 67 Latest flood forecasts as well as results from 2 historical event simulations could be viewed on the website (menu outlines in red). The boundary conditions data may be viewed through the menu on the left, and water depth time series results may be viewed by clicking on place markers on the map. The plot shows calculated flood depths for a rainfall event (i.e. Extreme Event B) in December 2013.

3.3.2 *Performance and evaluation*

The updated Saint Lucia Flood Warning System is relatively new, and was put into operation in November 2015 (see http://stlucia.dhigroup.com/ and Figure 57). To date, new 24-hour coastal flood forecasts are being issued regularly (i.e. every 4 hours) since the system was launched.

Data available for flood model verification are limited, as discussed in Rene et al. (2013b). Similar to earlier pluvial flood modelling efforts, available data for model calibration comprised of images for 2 flood events in Castries published online (Rene et al., 2013b; Rene et al., 2015). Examples are shown in Figure 68 for flooding on 1 May 2013. Comparison of observed and maximum simulated depths in Table 4 show flooding is calculated at the expected locations but that calculations overestimate depths compared to (estimated) observed values. However, although the exact times are uncertain, the images were most likely from after the event when floods have subsided, and not at the height of the flooding. Thus, more precise data are needed for verification, but nevertheless the current model gives a good indication of the location and magnitude of expected flooding for a real-time flood forecasting system.

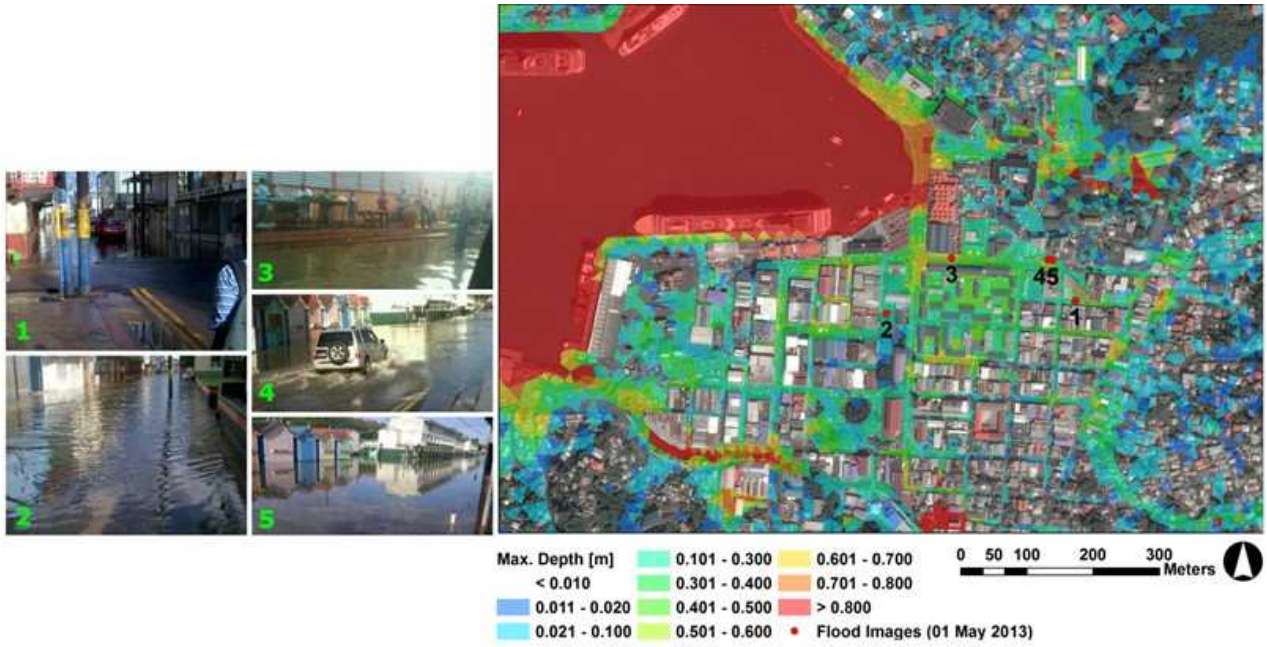

Figure 68 Images of flooding from during or after the 1 May 2013 flood event in Castries, Saint Lucia published online are shown on the left (Source: Rene et al., 2015). Maximum water depth results using the new Castries coastal flood model for the 1 May 2013 event are plotted on the right.

Table 4 Model verification based on estimated flood depths from images.

	1 May 2013 Event				
	Image 1	**Image 2**	**Image 3**	**Image 4**	**Image 5**
Observed estimated depth [m] (Source: Rene et al., 2015)	0.1	0.2	0.1	0.1	0.2
Simulated max depth [m] (Source: Rene et al., 2015)	0.4	0.2	0.3	0.3	0.2
Simulated max depth [m] (Current coastal flood model)	0.38	0.27	0.5	0.32	0.21

Collection of quantitative data on system performance, similar to that for the Greve Flood Warning System (Chapter 0) is underway. The system will continue to be monitored and improved within the course of the PEARL Project. And so far, several issues and points for improvement have been identified since its launch. These, include:

- **Collection of measured sea level data at Castries Harbour.** To be used for sea level and flood model verification.
- **Collection of operation (quantitative) performance statistics in MIKE Workbench**. Job statistics comprising of 'Duration' data could be recorded in MIKE Workbench. It is a time series of calculation times (in hours) for all forecast simulations, and thus provides not only information on how much time a forecast simulation took, but also whether the system is running at a point in time, as 'zero hours' simulation time is unlikely and probably indicates that the system is down. This type of data collection has been implemented for the Greve Flood Warning System (see Chapter 3.2), which was launched earlier than the Saint Lucia system.
- **Improving data presentation on the website**. The rainfall forecast boundary time series is not shown properly, and information on the current forecast period is not readily shown.
  Improving sea level forecast boundary data. Additional sources of forecasted sea level data used as boundary conditions for the coastal flood forecast model will be identified.

4 Summary and Conclusions

This report presents a review of modelling tools and techniques for urban coastal flood warning. In this assessment, state-of-the-art techniques and points for enhancement of existing methods for real-time coastal flood modelling and hazard mapping were identified. These techniques were then implemented in online real-time coastal flood warning systems in selected PEARL case studies, i.e. Greve, Denmark; Hamburg, The Elbe, Germany; Marbella, Spain and Castries, St. Lucia.

Coastal areas are under increasing risks from flooding. They are some of the most densely populated areas in the world, which are, at the same time, exposed to a multitude of water-related hazards such as storm surges, flash floods, and fluvial and pluvial flooding. Flood early warning systems are effective solutions for risk mitigation. They allow for damage reduction strategies before as well as during flood events. A flood warning system promotes preparedness, allowing communities to reduce direct interaction with the flood, and the authorities to prepare for the implementation of emergency plans, subsequently reducing overall damages.

The various modelling techniques that are used in establishing online real-time coastal flood warning systems were reviewed and evaluated. These techniques involve modelling and prediction of the main driving factors to coastal flooding, such as rainfall, sea levels and storm surges, and the inland flooding itself. The timely prediction and accuracy of these phenomena are important for early warning systems as they significantly influence warning lead times. Through the review, possibilities for improving their applicability in real-time warning systems were identified for each technique. The different merits and limitations of each technique were assessed with respect to real-time flood warning applications. It was found that…

Rainfall forecasting methods include Numerical Weather Prediction (NWP), radar-based forecasting, artificial neural network modelling, and knowledge-based nowcasting. NWP, which predicts global atmospheric circulation using numerical models of the atmosphere and oceans, is a widely-used method for rainfall prediction, and the use of nested NWP models allow for greater spatial and temporal detail in NWP outputs that are also appropriate for short-range and localized forecasting applications. Radar nowcasting, involving radar data extrapolation using a series of radar images to estimate future intensity and position of storms, is, on the other hand, one of the best short-period precipitation forecasting methods available, providing data with high spatial and temporal resolutions. However, radar nowcasting forecast skills decay quickly with time. But the combined use of radar extrapolation techniques with satellite and NWP modelling has been shown to significantly improve forecasts, e.g like in the case of Marbella, Spain. Moreover, the concept of probabilistic rainfall forecasting was also examined, as it enables the handling of uncertainties in atmospheric processes for flood forecasting and warning. Here, it should be noted at probabilistic rainfall forecasting for real-time flood forecast still is an emerging area, and at present the PEARL case in Marbella is the only one was found. Modelling techniques for the simulation of hydrodynamic driving factors to coastal flooding (e.g. sea levels) were examined. Two-dimensional (2D) models, especially those based on flexible calculation meshes, were shown to perform very well and much better than the Cartesian model in terms of simulating reality as well as calculation efficiency. Three-dimensional (3D) hydrodynamic models, are also used instead of 2D models for simulation of storm surges, in order to consider vertical stratification in the calculations and avoid the depth-averaging simplification with 2D models. Finally, inland flood modelling methods were reviewed, focusing on physically-based hydrodynamic models simulating water depths and discharges. Two-dimensional (2D) models are widely used for coastal flood analysis. However, they do not represent underground drainage networks that factor significantly in flooding in urbanized coasts. In which case, coupled 1D-2D models are used, wherein a 2D surface model is dynamically linked to a 1D model of the drainage network. Flows and water levels along drainage

networks and over the land surface, and flow exchanges between the two systems are simulated. Coupled 1D-2D models consider the role of underground sewers or channels in conveying water from the sea to inland areas, which is an improvement over 2D models for coastal flood modelling. But besides model accuracy, short computation times are important considerations in selecting models for real-time flood warning. Various techniques are now available for improving computational efficiency, especially for the 2D modelling parts of the flood simulations. These include the use of mesh elements instead of Cartesian grids for calculations, or the use of multiple-resolution grids that combine coarse and fine grids for computations and result presentation. Moreover, strategies involving parallel processing and hardware modifications, such as the use of Graphics Processing Units (GPUs) for model computations, afford further significant improvements in computational efficiency.

In this study, online real-time coastal flood modelling systems were implemented in selected case studies. Modelling techniques for coastal flood warning were applied and tested through online real-time coastal flood warning systems in the PEARL case study cities of Greve in Denmark, Hamburg in Germany, and Castries in Saint Lucia. In the following section the outcome from the PEARL cases are described:

The Elbe, Hamburg, Germany
An early warning system was developed for the Elbe river using water level forecast data provided by the BSH. Water level forecasts are available for several gauge locations along the tidal Elbe, which are updated every 15 min. These water level time series are automatically downloaded to a local server, stored into a database and prepared for the application as boundary conditions of the numerical model. The basic numerical model was divided into three sub-models in order to implement the BSH Model Output Statistics-forecast data. The prepared water level time series are applied at each sub-model boundary as hydrodynamic boundary conditions. In addition, discharge boundary conditions are applied to the upstream boundary of each sub-model. The sub-models are run sequentially. Within the implemented Elbe river early warning system, model results are analysed with respect to the water level distribution along the Elbe. The simulation results will be made available via a web platform. The results of the forecast are the input for the assessment of the failure of flood protection and the analysis of the consequences in the PEARL work packages WP3 and WP4. In accordance to the PEARL DoW (T4.1) it was shown how the Kalypso model chain is used to implement an early warning system for the tidally influenced section of the Elbe river, using externally provided time series as a boundary condition for the numerical model of the Elbe, which is set-up automatically. Additionally, it was shown that the accuracy of the applied numerical model, consisting of three sub-models, is extremely good.

Greve, Denmark
The coastal flood warning system for Greve employs a hydrodynamic flood model that calculates flooding using forecasted rainfall and sea water levels around the area. The system employs a coupled 1D-2D (flexible mesh) hydrodynamic model for flood forecasting. It makes use of NWP rainfall forecasts, which are the most readily-accessible types of precipitation forecast data for the area, and water level forecasts from a 3D hydrodynamic model, as boundary conditions. Data collection and processing of flood forecasts are done through a desktop client, and flood forecasts are published on a website. Since its launch, system reliability has been 94%. Continuous evaluation and improvement of the system are being conducted, focusing on enhancement of the accuracy and performance of the flood model, and improvement of dissemination and presentation of warning information.

Castries, St. Lucia
The Saint Lucia Flood Warning System uses a flexible mesh 2D flood model to forecast coastal flooding in Castries. The model is driven by NWP rainfall, and sea water level forecasts, and modelling results as well as various information about the system are published on a website in

real-time. Compared to the system in Greve, the Saint Lucia system is relatively new and still lacks a component for recording system reliability statistics. Nevertheless, continuous improvement of the system is being conducted, starting with enhancement of the flood model through a collection of additional sea level measurements at Castries Harbour, improved sea level forecast boundary data, a collection of operational performance statistics for the system, and improved data presentation on the website.

Implementation of the modelling techniques in the various PEARL case studies has shown that the choice of tools and methods depends not only on the flood type and dominant processes involved, but also on data availability and desired forecast times for the system. The use of state-of-the-art tools and methods is often challenged by the availability and accessibility of data, and types of data collection infrastructure that exist in the study area. The implementation of the new and updated tools demonstrates a step forward for establishing flood forecast systems which are accurate and fast enough for practical real life purposes.

References

Abebe, A., & Price, R. (2005). Decision support system for urban flood management. Journal of Hydroinformatics, 7, 3-15.

Alfieri, L., Salamon, P., Pappenberger, F., Wetterhall, F., & Thielen, J. (2012). Operational early warning systems for water-related hazards in Europe. Environmental Science & Policy, 21, 35-49.

Berbel Roman, S. (2014). Modelling flooding from the sea interacting with the drainage system under the influence of combined flood hazards to develop risk management strategies for the coastal region of Greve, Denmark (Master's thesis). University of Nice Sophia Antipolis, Nice, France.

Berenguer, M., Corral, C., Sánchez-Diezma, R., & Sempere-Torres, D. (2005). Hydrological validation of a radar-based nowcasting technique. Journal of Hydrometeorology, 6(4), 532-549.

Berenguer, M., Sempere-Torres, D., & Pegram, G. G. (2011). SBMcast–An ensemble nowcasting technique to assess the uncertainty in rainfall forecasts by Lagrangian extrapolation. Journal of Hydrology, 404(3), 226-240.

Bode, L., & Hardy, T. A. (1997). Progress and recent developments in storm surge modeling. Journal of Hydraulic Engineering, 123(4), 315-331.

Booij, N., Ris, R. C., & Holthuijsen, L. H. (1999). A third-generation wave model for coastal regions: 1. Model description and validation. Journal of Geophysical Research: Oceans (1978-2012), 104(C4), 7649-7666.

Bowler, N. E., Pierce, C. E., & Seed, A. W. (2006). STEPS: A probabilistic precipitation forecasting scheme which merges an extrapolation nowcast with downscaled NWP. Quarterly Journal of the Royal Meteorological Society, 132(620), 2127-2156.

Brown, S., Nicholls, R. J., Woodroffe, C. D., Hanson, S., Hinkel, J., Kebede, A. S., ... & Vafeidis, A. T. (2013). Sea-level rise impacts and responses: a global perspective. In Coastal Hazards [C.W. Finkl (Ed.)]. Springer Netherlands, Netherlands.

Butler, D., & Davies, J. (2011). Urban drainage (3rd ed.). CRCPress, Abingdon, Oxon, UK.

Carr, R. S. & Smith, G. P. (2006). Linking of 2D and pipe hydraulic models at fine spatial scales. Paper presented in 7th International Conference on Urban Drainage Modelling and 4th International Conference on Water Sensitive Urban Design, 2-7 April 2006, Melbourne, Australia.

Cavaleri, L., Alves, J. H., Ardhuin, F., Babanin, A., Banner, M., Belibassakis, K., ... & WISE Group. (2007). Wave modelling–the state of the art. Progress in Oceanography, 75(4), 603-674.

Chen, A. S., Evans, B., Djordjevic, S. & Savic, D. A. (2012). A coarse-grid approach to representing building blockage effects in 2D urban flood modelling. Journal of Hydrology 426-427, 1-16.

Christensen, B. B., Drønen, N., Klagenberg, P., Jensen, J., Deigaard, R., & Sørensen, P. (2013). Multiscale Modelling of Coastal Flooding. Paper presented in Coastal Dynamics 2013—7th International Conference on Coastal Dynamics, 24-28 June 2013, Bordeaux, France.

Collier, C.G. (1981). Objective rainfall forecasting using data from the United Kingdom weather radar network. In Proceedings of Int. Assoc. Meteorol. Atmos. Phys. (I.A.M.A.P.) Symposium on Nowcasting: Mesoscale Observations and Short-Range Prediction [Battrick and J. Mort (Eds.)], 25-28 August 1981, Hamburg, Germany.

COST (2005). EUR 21525 – COST Action 717 – Use of radar observation in hydrological and NWP models – Quantitative precipitation forecast (QPF) based on radar data for hydrological models [Mecklenburg, S., A. Jurczyk, J. Szturc, & K. Osrodka (Eds.)]. EU Publications Office (OPOCE), Luxembourg.

Danilov, S. (2013). Ocean modeling on unstructured meshes. Ocean Modelling, 69, 195-210.

DANVA (2007). En kogebog for analyser af klimaændringernes effekter på afløbssystemer.-Med fokus på oversvømmelser (A Cookbook for Analysis of Climate Change Effects on Floods in Cities). Retrieved from www.klimatilpasning.dk/media/5386/klimakogebog_juli_2007[1].pdf.

DHI (2011). Water Forecast for the Inner Danish Waters and the Baltic Sea. Setup and validation of flow and wave models. DHI: Hørsholm, Denmark.

DHI (2013). MIKE 21 & MIKE 3 Flow Model FM, Hydrodynamic and Transport Module, Scientific Documentation. DHI: Hørsholm, Denmark.

DHI (2013b). MIKE 21 Flow Model, Hydrodynamic Module, Scientific Documentation. DHI: Hørsholm, Denmark.

DHI (2013c). MIKE 21, Spectral Wave Module, Scientific Documentation. DHI: Hørsholm, Denmark.

DHI (2013d). MIKE FLOOD, ID-2D Modelling, User Manual. DHI: Hørsholm, Denmark.

DHI (n.d.). Water Forecast by DHI. Retrieved from http://www.waterforecast.com/.

Di Baldassarre, G., Schumann, G., Bates, P. D., Freer, J. E., & Beven, K. J. (2010). Flood-plain mapping: a critical discussion of deterministic and probabilistic approaches. Hydrological Sciences Journal–Journal des Sciences Hydrologiques, 55(3), 364-376.

Djordjevic, S., Butler, D., Gourbesville, P., Mark, O., & Pasche, E. (2011). New policies to deal with climate change and other drivers impacting on resilience to flooding in urban areas: the CORFU approach. Environmental Science & Policy, 14(7), 864-873.

ECMWF (2013). User guide to ECMWF forecast products (Version 1.1). Retrieved from http://www.ecmwf.int/sites/default/files/user_guide_0.pdf.

Einfalt, T., Arnbjerg-Nielsen, K., Golz, C., Jensen, N. E., Quirmbach, M., Vaes, G., & Vieux, B. (2004). Towards a roadmap for use of radar rainfall data in urban drainage. Journal of Hydrology, 299(3), 186-202.

Environment Agency (2010). Benchmarking of 2D hydraulic modelling packages. Environment Agency, Bristol, UK.

EU (2007). Directive 2007/60/EC of the European Parliament and of the Council of 23 October 2007 on the Assessment and Management of Flood Risks. Official Journal of the European Union, L288/27.

EXCIMAP (European exchange circle on flood mapping) (2007). Handbook on good practice on flood mapping in Europe [F. Martini & R. Loat (Eds.)]. Retrieved from http://ec.europa.eu/environment/water/flood_risk/flood_atlas/index.htm.

Fortes, C. J. E. M., Reis, M. T., Poseiro, P., Capitão, R., Santos, J. A., Pinheiro, L. V., ... & Silva, C. (2013). The HIDRALERTA project: Flood forecast and alert system in coastal and port areas. In Proceedings of the 8as jornadas portuguesas de engenharia costeira e portuária (In Portuguese).

Furuno (2015). Furuno Danmark. Retrieved from http://www.furuno.dk/.

Gallien, T. W., Sanders, B. F., & Flick, R. E. (2014). Urban coastal flood prediction: Integrating wave overtopping, flood defenses and drainage. Coastal Engineering, 91, 18-28.

Germann, U., Berenguer Ferrer, M., Sempere Torres, D., & Zappa, M. (2009). REAL-Ensemble radar precipitation estimation for hydrology in a mountainous region. Quarterly Journal of the Royal Meteorological Society, 135, 445-456.

Ghimire, B., Chen, A. S., Guidolin, M., Keedwell, E. C., Djordjevic, S., & Savic, D. a. (2013). Formulation of a fast 2D urban pluvial flood model using a cellular automata approach. Journal of Hydroinformatics, 15(3), 676.

Ghosh, S. N. (2014). Flood control and drainage engineering (4th ed.).CRC Press/Balkema, Leiden, The Netherlands.

Golding, B. W. (1998). Nimrod: A system for generating automated very short range forecasts. Meteorological Applications, 5(01), 1-16.

Golding, B. W. (2000). Quantitative precipitation forecasting in the UK. Journal of Hydrology, 239(1), 286-305.

Grasso, V. F., & Singh, A. (2011). Early warning systems: State-of-art analysis and future directions. Draft report, UNEP.

Greve Kommune (2007). Oversvømmelserne i Greve Kommune Juli 2007. Technical report. Retrieved from http://www.gsforsyning.dk/sites/default/files/oversvommelserne_i_greve_kommune_juli_2007.pdf.

Hankin, B., Waller, S., Astle, G. & Kellagher, R. (2008). Mapping space for water: screening for urban flash flooding. Journal of Flood Risk Management 1, 13-22.

Hartnack, J. N., Enggrob, H. G., & Rungø, M. (2009). 2D overland flow modelling using fine scale DEM with manageable runtimes. In: Flood Risk Management: Research and Practice [P. Samuels, S. Huntington, W. Allsop & J. Harrop (Eds.)]. Taylor & Francis Group, London, UK.

Henonin, J., Russo, B., Mark, O., & Gourbesville, P. (2013). Real-time urban flood forecasting and modelling–a state of the art. Journal of Hydroinformatics, 15(3), 717-736.

Higaki, M., Hayashibara, H., & Nozaki, F. (2009). Outline of the storm surge prediction model at the Japan Meteorological Agency. Japan Meteorological Agency, Tokyo, Japan.

IPCC (2012). Managing the Risks of Extreme Events and Disasters to Advance Climate Change Adaptation. A Special Report of Working Groups I and II of the Intergovernmental Panel on Climate Change [Field, C.B., V. Barros, T.F. Stocker, D. Qin, D.J. Dokken, K.L. Ebi, M.D. Mastrandrea, K.J. Mach, G.-K. Plattner, S.K. Allen, M. Tignor, and P.M. Midgley (Eds.)]. Cambridge University Press, USA.

IPCC (2014). Climate Change 2014: Synthesis Report. Contribution of Working Groups I, II and III to the Fifth Assessment Report of the Intergovernmental Panel on Climate Change [Core Writing Team, R.K. Pachauri and L.A. Meyer (eds.)]. IPCC, Geneva, Switzerland, 151 pp.

Jensen, D.M.R. (2015). Uncertainty assessment of an integrated storm surge model used for coastal flood forecasting in urban Greve, Denmark (Master's thesis). Technical University of Denmark, Lyngby, Denmark.

Jensen, N. E. & Pedersen, L. (2009). Unattended automatic real-time SMS flood warning using high-resolution X-band radar data and automatic real-time calibration of X-band radar data. Paper presented at World Meteorological Organization Symposium on Nowcasting and Very Short-term Forecasting, 31 August-4 September 2009, Whistler, British Columbia.

Jensen, N. E., & Pedersen, L. (2005). Automated short term forecast from LAWR x-band radar systems. Results from the first three month of operation. DHI, Aarhus, Denmark.

Jensen, N. E., & Pedersen, L. (2005b). Spatial variability of rainfall: Variations within a single radar pixel. Atmospheric Research, 77(1), 269-277.

Jha, A. K., Bloch, R., & Lamond, J. (2012). Cities and flooding: a guide to integrated urban flood risk management for the 21st century. World Bank Publications.

Kalyanapu, A. J., Shankar, S., Pardyjak, E. R., Judi, D. R., & Burian, S. J. (2011). Assessment of GPU computational enhancement to a 2D flood model. Environmental Modelling & Software, 26(8), 1009-1016.

Kerper, D., Larsen, L. C., Di Donato, M., & Cecconi, G. (2002). Storm Surge Forecasting and Flood Management System in Venice, Italy. Solutions to Coastal Disasters' 02. Proceedings for the Coastal Disasters Conference 2002 [L. Ewing & L. Wallendorf (Eds.)]. ASCE, San Diego, California, USA.

Kimura, R. (2002). Numerical weather prediction. Journal of Wind Engineering and Industrial Aerodynamics, 90(12), 1403-1414.

Komen, G. J., Cavaleri, L., Donelan, M., Hasselmann, K., Hasselmann, S., & Janssen, P. A. E. M. (1996). Dynamics and modelling of ocean waves. Cambridge University Press, New York, USA.

Kron, W. (2015). Flood disasters–a global perspective. Water Policy, 17(S1), 6-24.

Leandro, J., Chen, A. S., Djordjevic, S. & Savic, D. A. (2009). Comparison of 1D/1D and 1D/2D coupled (sewer/surface) hydraulic models for urban flood simulation. Journal of Hydraulic Engineering 135, 495-504.

Leitão, J. P., Almeida, M. D. C., Simões, N. E., & Martins, A. (2013). Methodology for qualitative urban flooding risk assessment. Water Science and Technology: A Journal of the International Association on Water Pollution Research, 68(4), 829-38.

Liguori, S., & Rico-Ramirez, M. A. (2014). A review of current approaches to radar-based quantitative precipitation forecasts. International Journal of River Basin Management, 12(4), 391-402.

Liguori, S., Rico-Ramirez, M. A., Schellart, A. N. A., & Saul, A. J. (2012). Using probabilistic radar rainfall nowcasts and NWP forecasts for flow prediction in urban catchments. Atmospheric Research, 103, 80-95.

Linsley, R. K. & Franzini, J. B. (1992). Water Resources Engineering. McGraw-Hill Series, London.

Liu, Y., Zhou, J., Song, L., Zou, Q., Liao, L., & Wang, Y. (2013). Numerical modelling of free-surface shallow flows over irregular topography with complex geometry. Applied Mathematical Modelling, 37(23), 9482-9498.

Llort, X., Sánchez-Diezma, R., Rodríguez, Á., Sancho, D., Berenguer, M., & Sempere Torres, D. (2014). FloodAlert: a simplified radar-based EWS for urban flood warning. Paper presented at HIC 2014 – 11th International Conference on Hydroinformatics, New York, USA.

Lynch, P. (2008). The origins of computer weather prediction and climate modeling. Journal of Computational Physics, 227(7), 3431-3444.

Maksimovic, C., & Prodanovic, D. (2001). Modelling of urban flooding-breakthrough or recycling of outdated concepts. In Urban Drainage Modeling: Proc., Specialty Symp. of the World Water and Environmental Resources Congress [R. Brashear & C. Maksimovic (Eds.)]. ASCE, Reston, Va., USA.

Mark, O., & Djordjevic, S. (2006). While waiting for the next flood in your city. Paper presented in 7th International Conference on Hydroinformatics, Nice, France.

Mark, O., Weesakul, S., Apirumanekul, C., Boonya-Aroonnet, S., & Djordjevic, S. (2004). Potential and limitations of 1D modelling of urban flooding. Journal of Hydrology, 299(3), 284-299.

Michalakes, J., J. Dudhia, D. Gill, T. Henderson, J. Klemp, W. Skamarock, and W. Wang, (2004). The Weather Research and Forecast Model: Software Architecture and Performance. Proceedings of the 11th ECMWF Workshop on the Use of High Performance Computing In Meteorology, 25-29 October 2004, Reading, UK.

Moel, H. d., Alphen, J. V., & Aerts, J. C. J. H. (2009). Flood maps in Europe–Methods, availability and use. Natural Hazards and Earth System Science, 9(2), 289-301.

Moore, R. J., Bell, V. A., & Jones, D. A. (2005). Forecasting for flood warning. Comptes Rendus Geoscience, 337(1), 203-217.

Müller-Navarra, S.H. & Bork, I. (2012). Entwicklung eines operationellen Tideelbemodels auf der Basis des hydrodynamischen-numerischen Modelverfahrens BSHcmod für die Nord- und Ostsee (OPTEL-A), In: Die Küste, Empfehlungen für Küstenschutzbauwerke (EAK 2002), Editor: Kuratorium für Forschung im Küsteningenieurwesen, Westholsteinische Verlagsanstalt Boysen & Co. Heide i. Holstein.

Müller-Navarra, S.H. & Knüpffer, K. (2010). Improvement of water level forecast for tidal harbours by means of model output statistics (MOS) Part I (Skew surge forecast), Bericht des BSH Nr. 47. Retrieved from: http://www.bsh.de/de/Produkte/Buecher/Berichte_/Bericht47/index.jsp.

Namin, M., Lin, B., & Falconer, R. A. (2004). Modelling estuarine and coastal flows using an unstructured triangular finite volume algorithm. Advances in Water Resources, 27(12), 1179-1197.

Neal, J. C., Fewtrell, T. J., Bates, P. D., & Wright, N. G. (2010). A comparison of three parallelisation methods for 2D flood inundation models. Environmental Modelling & Software, 25(4), 398-411.

Neumann, B., Vafeidis, A. T., Zimmermann, J., & Nicholls, R. J. (2015). Future Coastal Population Growth and Exposure to Sea-Level Rise and Coastal Flooding-A Global Assessment. PloS One, 10(6), e0131375.

Niemczynowicz, J. (1991). On storm movement and its applications. Atmospheric Research, 27(1), 109-127.

NIRAS (2014). Risikostyringsplan for Ishøj Kommune - Køge Bugt 2. Technical report. Retrieved from http://www.ishoj.dk/sites/default/files/files/Risikostyringsplan%20for%20Ish%C3%B8j.pdf.

NOAA National Ocean Service (2013). Castries, St. Lucia, TEC4775 Tidal Data Daily View. Retrieved from https://tidesandcurrents.noaa.gov/noaatidepredictions/NOAATidesFacade.jsp?Stationid=TEC4775.

NOAA NCEP (July 2015). GFS Europe. Retrieved from http://mag.ncep.noaa.gov/model-guidance-model-parameter.php?group=Model Guidance&model=gfs&area=europe&cycle=20151027 06 UTC&param=precip_p03&fourpan=no&imageSize=&ps=model.

OASIS (2015). OASIS Emergency Management TC. Retrieved from https://www.oasis-open.org/committees/tc_home.php?wg_abbrev=emergency.

Parkinson, J., & Mark, O. (2005). Urban stormwater management in developing countries. IWA publishing.

Polymer (2015). Feature Overview. Retrieved from https://www.polymer-project.org/1.0/docs/devguide/feature-overview.html.

Price, R. K. & Vojinovic, Z. (2008). Urban flood disaster management. Urban Water Journal, 5, 259-276.

Prodanovic, D., Djordjevic, S. & Maksimovic, Ć. (2008). GIS assisted model for dual drainage simulation. In: 3rd International Conference of Hydroinformatics, 24-26 August 1998, Copenhagen, Denmark, pp. 535-542.

Raposeiro, P. D., Fortes, C. J. E. M., Capitão, R., Reis, M. T., & Carlos, J. (2013). Preliminary phases of the HIDRALERTA system: Assessment of the flood levels at S. João da Caparica beach, Portugal. Journal of Coastal Research, SI65, 808-813.

Rene J.-R., Djordjevic S., Butler D., Madsen H. & Mark O (2013b). Getting started with urban flood modelling for real-time pluvial flood forecasting: a case study with sparse data. Proceedings for the International Conference on Flood Resilience: Experience in Asia and Europe [D. Butler, A. S. Chen, S. Djordjevic & J.M. Hammond (Eds.)]. Centre for Water Systems, University of Exeter, Exeter, UK.

Rene, J. R., Djordjevic, S., Butler, D., Madsen, H., & Mark, O. (2014). Assessing the potential for real-time urban flood forecasting based on a worldwide survey on data availability. Urban Water Journal, 11(7), 573-583.

Rene, J. R., Djordjevic, S., Butler, D., Mark, O., Henonin, J., Eisum, N., & Madsen, H. (2015). A real-time pluvial flood forecasting system for Castries, St. Lucia. Journal of Flood Risk Management.

Rene, J. R., Madsen, H., & Mark, O. (2013). A methodology for probabilistic real-time forecasting--an urban case study. Journal of Hydroinformatics, 15(3).

Rodríguez, A., Llort, X., Sancho, D., Sánchez-Diezma, R., Gomez, V., & Bella, R. (2014). Hidromet: A Cloud-Based EWS Platform for Real Time Urban Flood Warning. Paper presented at HIC 2014 – 11th International Conference on Hydroinformatics, New York, USA.

Schaake, J.C., Hamill, T.M., Buizza, R., & Clark, M. (2007). HEPEX: The Hydrological Ensemble Prediction Experiment. Bull. Amer. Meteor. Soc., 88, 1541-1547.

Schilling, W. (1991). Rainfall data for urban hydrology: what do we need?. Atmospheric Research, 27(1), 5-21.

Schmitt, T. G., Thomas, M. & Ettrich, N. (2004). Analysis and modelling of flooding in urban drainage systems. Journal of Hydrology 299, 300-311.

Shen, J., Zhang, K., Xiao, C., & Gong, W. (2006). Improved Prediction of Storm Surge Inundation with a High-Resolution Unstructured Grid Model. Journal of Coastal Research, 226(226), 1309-1319.

Sleigh, P., Gaskell, P., Berzins, M., & Wright, N. (1998). An unstructured finite-volume algorithm for predicting flow in rivers and estuaries. Computers & Fluids, 27(4), 479-508.

Smith, L. S., Liang, Q., & Quinn, P. F. (2014). Towards a hydrodynamic modelling framework appropriate for applications in urban flood assessment and mitigation using heterogeneous computing. Urban Water Journal, (August), 1-12.

Sto. Domingo, N. D., Paludan, B., Hansen, F., Madsen, H., Sunyer, M., and Mark, O. (2010). Modeling of sea level rise and subsequent urban flooding due to climate changes. Paper presented in SimHydro 2010: Hydraulic modeling and uncertainty, 2-4 June 2010, Sophia Antipolis, France.

StormGeo (n.d.). Metocean Forecasting. Retrieved from http://www.stormgeo.com/offshore/metocean-forecasting/.

Tablazon, J., Caro, C. V., Lagmay, A. M. F., Briones, J. B. L., Dasallas, L., Lapidez, J. P., ... & Mungcal, M. T. F. (2014). Developing an early warning system for storm surge inundation in the Philippines. Natural Hazards and Earth System Sciences Discussions, 2(10), 6241-6270.

Telemac (2014). Telemac Modeling System – User Manual. Retrieved from http://www.opentelemac.org/index.php/manuals/viewcategory/13-telemac-2d.

UNISDR (2007). Terminology. Retrieved from https://www.unisdr.org/we/inform/terminology.

Van Alphen, J., Martini, F., Loat, R., Slomp, R., & Passchier, R. (2009). Flood risk mapping in Europe, experiences and best practices. Journal of Flood Risk Management, 2(4), 285-292.

Vestergaard, L. F. (2011). *Analyse af oversvømmeslesmønstret ved havvandsstigning i Køge Bugt ud for Greve*. Note to agenda item for meeting in 'Teknik og Miljøudvalget', Copenhagen Municipality. Retrieved from http://www.gsforsyning.dk/sites/default/files/havstrategi_politiskvedtaegt_bilag.pdf.

Vojinovic, Z., & Tutulic, D. (2009). On the use of 1D and coupled 1D-2D modelling approaches for assessment of flood damage in urban areas. Urban Water Journal, 6(3), 183-199.

Vojinovic, Z., Abebe, Y., Sanchez, A., Pena, N.M., Nikolic, I., Manojlovic, N., Makroloulos, C., Pelling, M., & Abbot, M. (2014). Holistic Flood Risk Assessment in Coastal Areas—The PEARL Approach. Paper presented at HIC 2014 – 11th International Conference on Hydroinformatics, New York, USA.

Walters, R. A., Hanert, E., Pietrzak, J., & Le Roux, D. Y. (2009). Comparison of unstructured, staggered grid methods for the shallow water equations. Ocean Modelling, 28(1-3), 106-117.

Wamdi Group (1988). The WAM model-a third generation ocean wave prediction model. Journal of Physical Oceanography, 18(12), 1775-1810.

Wilson, J. W., Crook, N. A., Mueller, C. K., Sun, J., & Dixon, M. (1998). Nowcasting thunderstorms: A status report. Bulletin of the American Meteorological Society, 79(10), 2079-2099.

WMO (n.d.). Nowcasting. Retrieved from https://www.wmo.int/pages/prog/amp/pwsp/Nowcasting.htm.

WRF (n.d.). The Weather Research & Forecasting Model. Retrieved from http://wrf-model.org/index.php.

Wu, L., Seo, D. J., Demargne, J., Brown, J. D., Cong, S., & Schaake, J. (2011). Generation of ensemble precipitation forecast from single-valued quantitative precipitation forecast for hydrologic ensemble prediction. Journal of Hydrology, 399(3), 281-298.

Yu, D., & Lane, S. N. (2006). Urban fluvial flood modelling using a two-dimensional diffusion-wave treatment, part 1: mesh resolution effects. Hydrological Processes, 20(7), 1541-1565.

Yu, W., Nakakita, E., Kim, S., & Yamaguchi, K. (2015). Improvement of rainfall and flood forecasts by blending ensemble NWP rainfall with radar prediction considering orographic rainfall. Journal of Hydrology, 531(2), 494-507.